SYNTHESIS OF CELL-RESPONSIVE, BIODEGRADABLE POLYUREAS FOR LIGAMENT TISSUE ENGINEERING

A Thesis

by

HUGH ADAM BENHARDT

Submitted to the Office of Graduate Studies of
Texas A&M University
in partial fulfillment of the requirements for the degree of

MASTER OF SCIENCE

May 2010

Major Subject: Biomedical Engineering

SYNTHESIS OF CELL-RESPONSIVE, BIODEGRADABLE POLYUREAS FOR LIGAMENT TISSUE ENGINEERING

A Thesis

by

HUGH ADAM BENHARDT

Submitted to the Office of Graduate Studies of
Texas A&M University
in partial fulfillment of the requirements for the degree of

MASTER OF SCIENCE

Approved by:

Chair of Committee,	Elizabeth Cosgriff-Hernandez
Committee Members,	Melissa A. Grunlan
	Mariah Hahn
Head of Department,	Gerard L. Cote

May 2010

Major Subject: Biomedical Engineering

ABSTRACT

Synthesis of Cell-Responsive, Biodegradable Polyureas for Ligament Tissue Engineering. (May 2010)

Hugh Adam Benhardt, B.S., University of Missouri-Rolla

Chair of Advisory Committee: Dr. Elizabeth Cosgriff-Hernandez

An estimated 200,000 injuries to the anterior cruciate ligament (ACL) occur annually in the United States, with approximately 100,000 total ACL reconstructions performed each year. Due to inherent limitations with existing ACL reconstruction strategies, the development of tissue engineered ligaments is a key area of musculoskeletal research. Although great strides have been made in the scaffold design, current strategies are limited by the inability to replicate the mechanical behavior of native ligament tissue with synthetic polyesters or natural polymers. Poly(ester urethane)s have recently been investigated as possible scaffold materials because of their established biocompatibility, excellent mechanical properties, and exceptionally tunable structure. However, non-specific degradation makes it difficult to tailor polyurethane structure to complement ligament regeneration. In contrast, a biomaterial that features system-responsive degradation would integrate with native ligament remodeling and thus provide effective load transfer to newly formed tissue that is necessary to restore mechanical integrity.

In this study, enzyme-labile peptide sequences were conjugated to ether-based polyols to form collagen-mimetic soft segments that feature cell-responsive degradation. Synthetic routes were first developed to functionalize these polyols with favorable end groups for peptide coupling. Upon successful conjugation, biodegradable soft segments were then incorporated into the structure of linear polyurea elastomers. By varying soft segment chemistry, soft segment molecular weight, and the hard to soft segment ratio, a library of cell-responsive, biodegradable polyureas was developed. This library can then be used to elucidate key structure-property relationships necessary to complement neotissue formation. Overall, synthesis of a novel biomaterial that combines the strength and tunability of synthetic elastomers with cell-responsive degradation will assist in the development of an improved tissue engineered graft for ACL reconstruction.

TABLE OF CONTENTS

Page

ABSTRACT iii

TABLE OF CONTENTS v

LIST OF FIGURES vii

LIST OF TABLES ix

CHAPTER

I INTRODUCTION 1

1.1 Overview 1
1.2 Current Ligament Reconstruction 2
1.3 Anterior Cruciate Ligament Tissue Engineering 6
1.4 Current Biomaterial Scaffolds for Ligament Tissue Engineering 9
1.5 Segmented Polyurethane Elastomers 15
1.6 Polyurethanes in Biomedical Applications 18
1.7 System-Responsive Degradation 21

II END GROUP FUNCTIONALIZATION OF ETHER-BASED POLYOLS 25

2.1 Introduction 25
2.2 Carboxylic Acid Functionalization 26
2.3 NHS Activation of Carboxylic Acid Derivatives 32
2.4 Amine Functionalization 39
2.5 Conclusions 46

III SYNTHESIS OF CELL-RESPONSIVE, BIODEGRADABLE POLYUREAS 48

3.1 Introduction 48
3.2 Synthesis of Enzyme-Labile, Ether-Based Soft Segments …. 51

CHAPTER Page

3.3 Polyurea Synthesis 63
3.4 Conclusions 73

IV SUMMARY 75

REFERENCES 84

APPENDIX 100

VITA 106

LIST OF FIGURES

FIGURE		Page
1.1	Traditional tissue engineering paradigm	7
1.2	Effect of mechanical stretch on polyurethane deformation	17
1.3	Synthetic design of cell-responsive, biodegradable polyureas	24
2.1	Synthetic approach to create peptide-based soft segments	26
2.2	Synthesis of carboxylic acid functionalized PEG	28
2.3	FTIR spectra of PEG (1000) carboxylic acid functionalization	29
2.4	FTIR spectral comparison of PEG diacid syntheses	30
2.5	FTIR spectral comparison of PTMG diacid syntheses	32
2.6	NHS activation of PEG diacid in the presence of DCC	35
2.7	FTIR spectra of NHS activation of PEG (1000) diacid	36
2.8	FTIR spectral comparison of NHS ester derivatives of PEG diacids	37
2.9	FTIR spectral comparison of NHS ester derivatives of PTMG diacids	38
2.10	Functionalization of NHS-activated PEG diacid with EDA	42
2.11	Amine functionalization of PEG (6000) diacid	43
2.12	Amine functionalization of PEG (10000) diacid	44
2.13	Amine functionalization of PTMG (1000) diacid	45
2.14	FTIR spectra of PTMG (5600) diamine synthesis	46
3.1	Synthetic design of peptide-based, soft segment multiblocks	49
3.2	Synthetic design of cell-responsive, biodegradable polyureas	50

FIGURE Page

3.3 Synthesis of PEG triblocks in the presence of DMAp and Et_3N 54

3.4 Synthesis of amine-functionalized PEG multiblocks..... 55

3.5 FTIR spectra of PEG (1000) triblock synthesis 56

3.6 FTIR spectra of PEG (2000) triblock synthesis 57

3.7 FTIR spectra of PTMG (1000) triblock synthesis..... 59

3.8 FTIR spectra of amine-functionalized PEG (1000) multiblock synthesis 60

3.9 FTIR spectra of amine-functionalized PEG (2000) multiblock synthesis 61

3.10 FTIR spectra of amine-functionalized PTMG (1000) multiblock synthesis 62

3.11 Synthesis of ether-based polyureas using PEG diamine 66

3.12 FTIR spectral comparison of PEG (6000) control polyureas..... 67

3.13 FTIR spectral comparison of PEG (10000) control polyureas..... 68

3.14 FTIR spectral comparison of PTMG (5600) control polyureas 69

3.15 FTIR spectral comparison of PEG (1000) multiblock polyureas..... 70

3.16 FTIR spectral comparison of PEG (2000) multiblock polyureas..... 71

3.17 FTIR spectral comparison of PTMG (1000) multiblock polyureas 72

LIST OF TABLES

TABLE Page

3.1 Library of amine-functionalized, biodegradable soft segments 49

3.2 Library of collagen-mimetic polyureas 51

CHAPTER I

INTRODUCTION

1.1 Overview

Orthopaedic conditions have an enormous impact on quality of life and remain one of the leading reasons that patients seek medical care. In particular, musculoskeletal injuries comprise more than 14 percent of the health care dollar in the United States.[1] A significant portion of these injuries result from ligament and tendon damage. The anterior cruciate ligament (ACL) is the most commonly injured ligament of the knee with over 200,000 Americans requiring reconstructive surgery in 2002 at an associated medical cost exceeding five billion dollars.[2, 3]

The ACL is the major intra-articular ligament of the knee that connects the posterior-lateral part of the femur to the anterior-medial part of the tibia. It provides necessary joint stabilization for normal kinematics and prevents excessive anterior translation of the femur that could result in dislocation, bone fracture, or cartilage damage.[4] Damage to the ACL results in pain, loss of mobility, joint instability, and can eventually lead to injury of other tissues and the development of degenerative joint diseases, such as osteoarthritis.[5-7] After rupture, angiogenesis does not occur within the ACL for approximately 12 weeks.[8] As a result, damaged ACL tissue lacks significant vasculature and must depend on synovial fluid for nutrient and metabolic exchange,

---

This thesis follows the style of *Biomacromolecules*.

inhibiting its natural regeneration.[9-11] The intrinsic properties of ACL-derived cells also play a role in its inadequate healing capacity.[12-16] ACL fibroblasts exhibit inferior proliferation, migration, and responses to growth factors than fibroblast derived from the medial collateral ligament (MCL), and in response to injury, ACL fibroblasts demonstrate limited growth factor expression and lower upregulation of collagen type III, which has been shown to facilitate scar tissue formation.[12-17] The inability of damaged ACL tissue to heal post injury necessitates surgical intervention. Despite the large number of ligament reconstructions performed each year, an ideal grafting material has yet to be developed.[10, 11]

1.2 Current Ligament Reconstruction

1.2.1 Autografts

Current surgical techniques available for ACL reconstruction include transplantation of autografts, allografts, and synthetic grafts.[4, 10, 11, 18-22] Despite inherent limitations, the use of tendon autografts has been recognized as the "gold standard" of ACL repair.[18, 23, 24] During reconstructive surgery, the surgeon harvests a portion of the patient's patellar, hamstring, or quadriceps tendon to serve as a replacement ligament.[25, 26] The patellar tendon graft is explanted with a piece of bone from the patella and one from the insertion point at the tibia.[4] This "bone-patellar-bone" graft is then inserted through a tunnel drilled through the tibia, stretched across the knee, and attached through a tunnel drilled into the femur. The "bone-patellar-bone" graft has high initial graft strength, and because it has a bone plug on each end, it can incorporate quickly

with either fixation site. This allows for earlier motion of the knee and a shorter period of rehabilitation.[27]

Hamstring autografts are typically harvested from the semitendinosus and gracilis tendons, which are then braided and folded over to strengthen the graft. Advantages of a hamstring tendon graft include a smaller incision, less anterior knee pain, and a thicker tendinous portion within the knee joint.[18] Furthermore, despite removing two of the three medial muscular stabilizers of the knee, the hamstring retains most of its functionality.[18] The quadriceps tendon autograft is usually harvested from the central portion of the quadriceps with a bone plug from the proximal end of the patella to provide articular fixation. The major disadvantage of this technique is that the size and location of the donor-site scar can be problematic for the patient.

In general, autografts typically possess good initial mechanical strength and promote cell proliferation, and they are conducive to graft remodeling and integration into the joint.[24, 27-29] Despite these advantages, the use of autogenous grafts is limited. Their long-term success is dependent on revascularization of the transplanted tissue, which is progressively surrounded by the synovial membrane.[8, 30] The availability of autogenous grafts can be an issue, whether due to the need for multiple surgeries or age.[26, 31] Finally, donor site pain, muscle atrophy, and tendonitis can lead to prolonged rehabilitation periods and can restrict patients from achieving pre-injury levels of activity.[32]

1.2.2 Allografts

To circumvent problems associated with autogeneic tendon grafts, the use of allografts has been employed for ACL repair. Allografts are tissues harvested from a cadaver, such as the patellar, hamstring, and achilles tendon, which eliminates the need for an additional surgical site.[21, 33] This reduces surgical time and minimizes postoperative pain.[31] Like autografts, allografts provide good initial mechanical strength and promote cell proliferation and remodeling, with the added benefit of an unlimited graft supply.[24, 34] Nevertheless, there are still limitations to this therapy including disease transmission, bacterial infection, and unfavorable immunogenic responses.[23, 35] Although sterilization and preservation can minimize these risks, they also reduce the tensile properties of the graft, limiting its use for ACL reconstruction.[18, 31, 36-39]

1.2.3 Synthetic Grafts

Due to the limitations of biologic grafts, synthetic materials have been investigated for potential use in ACL reconstruction.[22, 40] These grafts do not require sacrifice of autogenous tissue and do not lose their strength due to tissue remodeling, which allows for much faster rehabilitation.[41] Prostheses of homogenous, non-degradable polymers evaluated for ACL repair include carbon fiber, the Gore-Tex ligament (polytetrafluoroethylene), the Stryker-Dacron and Leeds-Keio ligaments (polyethylene terephthalate), and the Kennedy Ligament Augmentation Device (polypropylene).[10, 11, 22, 23, 30, 42-44] The Gore-Tex ligament is composed of a single, continuous fiber of expanded polytetrafluoroethylene (ePTFE) that is wound into multiple loops and joined together to form a braid.[45] The Stryker-Dacron ligament

consists of a core of four tightly woven Dacron tapes encased by a sleeve of loosely woven Dacron velour, and it was designed to promote tissue ingrowth.[21, 46] Similar to the Stryker-Dacron ligament, the Leeds-Keio ligament is composed of polyethylene terephthalate (PET) with an open-weave tube to promote ingrowth of fibrous tissue.[47, 48] Finally, the Kennedy Ligament Augmentation Device (LAD) is a cylindrical prosthesis with a diamond-braided construction, and it was designed for simultaneous implantation with a biologic graft to augment the tissue and protect it during the early stages of healing.[49, 50] The Gore-Tex and Stryker-Dacron ligaments have each received general release from the Food and Drug Administration (FDA) as permanent ligament replacements, but only to salvage previously failed intra-articular reconstructions.[31, 48]

Although these devices typically provide immediate stabilization of the joint, they are unable to duplicate the mechanical behavior of the ACL and eventually fail due to material fatigue.[11, 31] Due to the high linear stiffness of synthetic implants, a majority of the physiological load is borne by the prosthesis, effectively stress shielding the surrounding tissue.[4, 11, 51, 52] Without proper mechanical cues to direct collagen alignment and tissue organization, the load-bearing capacity of the native tissue is reduced so that the synthetic graft is limited to its inherent fatigue properties. In addition to graft rupture, repeated elongation of these devices can lead to permanent deformation at points of stress, which results in a loosening of the ligament and a loss of joint stabilization.[53, 54] Contact with sharp edges of the bone tunnels can also cause abrasions that weaken the implant and create debris, which can elicit an unfavorable foreign body response.[11, 55] Woven prostheses face additional challenges such as axial splitting, low

extensibility, low tissue infiltration, and abrasive wear that can lead to synovitis in the joint.[4, 10, 11, 51, 52, 56] Long-term studies have also revealed a high incidence of osteoarthritis post implantation.[7, 54] Overall, the limitations of current ACL reconstruction strategies present a substantial margin for improvement in the escalating market for ACL repair.

1.3 Anterior Cruciate Ligament Tissue Engineering

Musculoskeletal tissue engineering has received growing interest throughout orthopedic medicine as a promising alternative to biologic and synthetic grafts.[4, 30, 57, 58] Tissue engineers attempt to harness the body's natural ability to repair and regenerate damaged tissue through the application of biological, chemical, and engineering principles. This strategy can potentially improve upon current clinical options by providing appropriate biological and mechanical properties to regenerate damaged ACL tissue without the aforementioned limitations of other grafts.[4, 10, 11, 19] ACL reconstruction utilizing a tissue-engineered ligament would eliminate donor site pain and morbidity, improve and accelerate rehabilitation, provide a limitless supply of graft tissue, eliminate the risk of disease transmission or unfavorable immunogenic responses, and increase the fatigue life of the graft.[10, 11]

The traditional tissue engineering paradigm combines isolated cells and bioactive factors on a biodegradable scaffold that sustains functionality during tissue regeneration and serves as a structural template for neotissue formation, **Figure 1.1**.[10, 11, 19, 59] In ligament constructs, scaffolds are seeded with fibroblasts or mesenchymal stem cells that are then provided with the necessary mechanical and biochemical cues to initiate

ligament regeneration. To facilitate this process, the biomaterial selected for these constructs must be biocompatible, biodegradable, and permit typical cell-material interactions necessary for cell proliferation, migration, and differentiation. The scaffold must also demonstrate interconnected porosity to enable nutrient transport, waste removal, and tissue infiltration. Finally, the tissue engineered construct must demonstrate appropriate mechanical behavior to maintain functionality throughout native tissue remodeling. The need to duplicate the complex function and unique mechanical properties of the ACL at all stages of remodeling is partly responsible for the difficulty encountered in developing a suitable surgical replacement. Therefore, advancement of ligament tissue engineering strategies is strongly dependent on the ability of tissue engineers to develop a biomaterial scaffold that reproduces both the mechanical and physiologic properties of native ACL tissue.

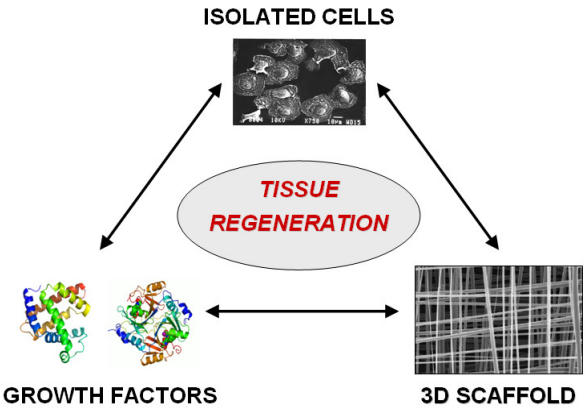

Figure 1.1. Traditional tissue engineering paradigm.

Knowledge of ligament structure and its components is extremely important in the development of a scaffold for ligament tissue engineering. Interactions among such

components and their arrangement in the tissue give ligaments their unique mechanical properties.[4] The ACL is predominantly composed of collagen, elastin, proteoglycans, glycoproteins, water, and fibroblasts.[4, 60] Fibroblasts not only synthesize fibrillar collagen but also enzymatically break down and remove old collagen as part of native tissue remodeling. Synthesis of collagen makes up roughly 80% of all protein synthesis in the ACL, with a ratio of type I collagen to type III collagen at approximately 88% to 12%, respectively.[61, 62] Type I collagen forms tough, nonelastic cross-linked fibers that contribute to the tensile strength of ligaments and tendons.[60, 62] Type III collagen forms loosely organized, thin fibrils that provide elasticity.[60, 62] Type I collagen molecules form a hierarchical structure of dense, highly organized, cable-like tissue in which fiber bundles orient parallel to the longitudinal axis in a helical formation.[4, 10, 11, 61, 63] Fibroblasts align between these collagen bundles and elongate in the direction of loading.[61] Fiber bundles form a periodic crimp pattern that permits 7 to 16% creep before permanent deformation or ligament damage can occur. Overall, it is this complex, hierarchical structure that dictates the bulk tensile properties of the ACL.

The mechanical and viscoelastic properties of the human ACL have been well-documented. The human ACL is regularly exposed to cyclic loads as high as 630N through all degrees of knee joint flexion/extension.[64] Its ultimate tensile strength of was found to be 1730 N, with a linear stiffness of 182 N/mm and 12.8 N-m for energy absorbed at failure, although such properties have been found to increase during development and diminish with age.[65-67] The maximum strain that a ligament can endure before failure is between 12 and 15%.[68] When exposed to strain, the ACL demonstrates

triphasic behavior, starting with a non-linear, toe region where the ligament exhibits low amount of stress per unit strain.[4] This results from a lateral contraction of fibrils, the release of water, and straightening of the crimp pattern. Once the crimp pattern has fully straightened, force is directly applied to the collagen triple helix and interfibrillar slippage occurs between crosslinks, forming a linear region in which stress increases per unit strain.[69-71] Eventually, collagen fibers begin to defibrillate, leading to a slight decrease in stress per unit strain and failure.[4, 69, 72] A biomaterial scaffold that can replicate this mechanical behavior and integrate with the native tissue is necessary for the development of a successful tissue engineered ligament.

1.4 Current Biomaterial Scaffolds for Ligament Tissue Engineering

1.4.1 Natural Polymers

Biocompatible and degradable biomaterials that have been investigated for ligament tissue engineering include natural polymers, such as collagen and silk, and synthetic materials. Type I collagen was selected for tissue engineering because, in addition to its abundance in ligament tissue, it is able to support the growth of fibrous tissue. Examples of tissue-engineered approaches using collagen fibers are presented extensively throughout the literature.[73, 74] Dunn et al. constructed fibroblast-seeded scaffolds composed of type I collagen fibers and found that such devices remain viable after implantation, showing excellent biocompatibility, enhanced cell attachment, proliferation, and extracellular matrix production.[74, 75] Nevertheless, these scaffolds are unable to maintain the mechanical integrity necessary to restore ligament function. Several strategies have been attempted to enhance the mechanical properties of

collagen-derived scaffolds, including cross-linking and copolymerization/blending with synthetic polymers.[11, 20, 31, 76-81]. Despite these efforts, relatively quick in vivo degradation and the resulting loss of mechanical strength are still major concerns with using collagen fibers for ligament tissue engineering.[73, 82] High cost, variability, complex handling properties, and potential disease transmission further limit the use of collagen, prompting the search for an improved biomaterial.[31, 83]

Due to its high tensile strength and linear stiffness, biocompatibility, and biodegradability, silk has received renewed interest as a potential biomaterial for tissue engineering.[84-88] The excellent mechanical properties of silk result from the high homogeneity of its secondary structure (β-sheet), extensive hydrogen bonding, and crystallinity. Silk is composed of a fibroin core and a glue-like sericin cover, and although sericin in silk has been shown to cause adverse problems with biocompatibility, there are several methods to remove it before usage. As a result, scaffolds constructed of silk fibroin demonstrate good biocompatibility and have been shown to support cell adhesion.[89] In addition, by coating the surface of these scaffolds with RGD sequences, increased cellular attachment, proliferation, and extracellular matrix production have been observed.[90] When organized into an appropriate wire-rope geometry, silk fibroin exhibits mechanical properties similar to the native ACL.[89] For example, Altman et al. constructed a tissue-engineered device consisting of a twisted fibrous matrix composed of silk fibers arranged into a hierarchical structure similar to the native ACL. Through modification of scaffold architecture, the stiffness of the scaffold can also be decreased to prevent stress shielding while maintaining tensile

strength. Silk undergoes proteolytic degradation at a rate that is dependent on its environment, but typically silk fibers lose their tensile strength within one year in vivo and degrade completely within two years. The slow rate of silk degradation allows for gradual load transfer from the polymer scaffold to newly formed tissue.[32] Even though silk has demonstrated much promise for ligament tissue engineering, its dependence on scaffold architecture to achieve mechanical properties limits independent control of mechanical strength and degradation necessary to promote effective load transfer.

Along with collagen and silk, other natural polymers have been investigated for potential use in ACL reconstructions. Funakoshi et al. constructed a tissue engineered scaffold from novel, chitosan-based hyaluronan hybrid polymer fibers, which were shown to exhibit enhanced mechanical properties and biological effects in vitro.[91] Majima et al. investigated the effect of alginate-based chitosan hybrid polymers on fibroblast adhesion, extracellular matrix synthesis, and mechanical properties.[92] Finally, Messenger et al. investigated the ability of enamel matrix derivative to enhance tissue induction around scaffolds used in ACL reconstruction.[93] These studies have considerable potential for ligament tissue engineering; however, they are still in preliminary stages of development and are far removed from clinical applications. Overall, despite the aforementioned advantages of natural polymers, concerns with mass production, variability, and the lack of independent control of degradation rate and mechanical properties limit their usefulness for ACL repair.

1.4.2 Synthetic Polymers

In addition to natural polymers, biodegradable, synthetic polymers have been investigated for ACL repair, including poly (glycolic acid) (PGA), poly (L-lactic acid) (PLLA), poly (lactic-co-glycolic acid) (PLGA), polydioxanone (PDS), and poly (desamino-tyrosyl-tyrosine ethyl carbonate) (poly (DTE carbonate)).[4, 19, 94-101] Similar to nondegradable synthetic polymers used to construct permanent prosthesis, there is no limit to graft supply and no risk of disease transmission. Unlike natural polymers, such as silk, which rely on modification of scaffold architecture to alter mechanical properties, the performance properties of synthetic polymers can also be controlled with polymer chemistry. For instance, the mechanical properties of a device may be controlled by altering the degree of polymer crystallinity or changing its molecular weight.

PGA and PLLA are excellent candidates for ligament tissue engineering because they are biocompatible, do not elicit unfavorable foreign body responses, and naturally degrade into non-toxic byproducts (glycolic acid, lactic acid). Additionally, because tissue engineered scaffolds are eventually replaced with neotissue, the fatigue properties of PGA and PLLA are not a concern. As a result, PGA, PLLA, and PLGA have been extensively studied for potential use in ACL reconstruction. [4, 19, 96-101] In particular, Laurencin et al. developed a series of cell-seeded, three-dimensional scaffolds from PGA, PLLA, and PLGA using a novel braiding technique designed to enhance mechanical properties and promote tissue infiltration, with PLLA proving to be the best option for ACL repair.[102, 103] Similar to native ligament tissue, these braided scaffolds

have a hierarchical structure composed of fibers arranged into bundles and wound throughout the thickness of the scaffold. This braiding technique was developed to create scaffolds with controlled pore size, integrated pores, resistance to wear and rupture, and mechanical properties comparable to the ACL. In in vitro studies, ACL fibroblasts were found to conform to the geometry of the scaffolds, exhibit spindle-like morphologies, and demonstrate extracellular matrix production. Additionally, cellular proliferation, tissue growth, and long-term extracellular matrix production were enhanced in the presence of fibronectin, an adhesion protein found in the extracellular matrix of native ligament tissue. These results suggest that braided scaffolds constructed of PLLA may become a viable option for ACL repair.[102-104]

Other synthetic polymers explored for potential use in ligament tissue engineering include PDS and poly (DTE carbonate). Buma et al. studied autogenous reconstruction of the ACL in goats in the presence of a degradable augmentation device composed of PDS and found that, after 6 weeks, a rapid decrease in strength was observed for augmented transplants.[95] In contrast, non-augmented transplants demonstrated a gradual increase in strength. These results suggest that PDS is a poor choice for ligament tissue engineering due to its rapid degradation. Bourke et al. fabricated ACL scaffolds from poly (DTE carbonate) fibers and found that these scaffolds have mechanical properties similar to the native ACL, and that they keep a much higher ultimate tensile strength (87% of original) after 30 weeks of degradation than PLLA (7% of original).[94] Despite these advantages, the parallel arrangement of

poly (DTE carbonate) fibers in these scaffolds leaves them susceptible to long-term failure due to fatigue and creep.

Overall, current research has shown that synthetic, biodegradable polymers can be viable options for ACL reconstruction; however, these materials are still limited in their ability to serve as ligament replacements. This is because the majority of these polymers lack the inherent material properties necessary to restore the mechanical strength and elasticity of the ACL. To overcome these mechanical limitations, a number of scaffolds derive their properties from their geometry and method of fabrication; however, this requires an understanding of how each structure behaves mechanically relative to one another. Changes in the mechanics of scaffold architecture due to degradation or repeated loading then increase the complexity of the graft, making it difficult to optimize scaffold design to promote effective load transfer. In addition to scaffold fabrication, polymer chemistry can be tailored to modulate these performance properties; however, a number of these structure-property relationships have overlapping components that complicate material design. For example, it is widely accepted that polymer crystallinity can be used to predict polymer modulus, yet highly crystalline polymers have also been shown to demonstrate slower hydrolytic degradation than amorphous polymers.[105] Without mechanisms to isolate specific structure-property relationships, these polymers are unable to balance the dual impact of tensile properties and the rate of degradation on the regeneration of ligament tissue. Additionally, the degradation mechanism for the majority of these polymers is non-specific hydrolysis, which makes it difficult to tailor scaffold degradation to complement neotissue

formation. Because current synthetic polymers are unable to either match the mechanical behavior of the ACL or integrate with native tissue remodeling, an improved material is needed to develop a successful tissue engineered ligament.

1.5 Segmented Polyurethane Elastomers

Due to the aforementioned limitations of current synthetic polymers, polyurethane elastomers have received growing interest for ligament tissue engineering.[106-109] Polyurethanes were first developed by Otto Bayer of I. G. Farbenindustrie, Leverkusen, Germany, in 1937.[106] Since then, polyurethanes have been used in a wide range of industrial applications, including machinery, textiles, packaging, adhesives, and sealants.[110, 111] Because of their outstanding mechanical properties and established biocompatibility, polyurethanes have also been used in a variety of biomedical applications over the past 40 years.[106, 112-114] Polyurethane chemistry dictates the physical, biological, and mechanical properties of these polymers and can be tailored to provide a variety of materials, such as soft elastomers, rigid thermosets, and foams.[106, 110, 111, 115] Therefore, understanding the hierarchical structure of polyurethanes and related materials, along with relevant structure-property relationships, is essential for effective biomaterial design.

Polyurethanes are a class of polymers that consist of urethane (-NH-CO-O-) linkages, typically generated by the reaction of isocyanates with hydroxyl-functional molecules by addition to the carbon-nitrogen bond.[115-117] Similarly, polyureas contain urea linkages (-NH-CO-NH-) and are generated by the addition of isocyanates and primary amine groups. Polyurethane and polyurea elastomers used for biomedical

applications are typically linear alternating block copolymers that consist of relatively high molecular weight soft segments linked with urethane/urea containing hard segments.[106-108] Common soft segments include hydroxyl-terminated polyethers, polyesters, and polycarbonates, all of which have relatively low glass transition temperatures. In contrast, hard segments usually have high glass transition temperatures and are characterized by semicrystalline, aromatic or aliphatic diisocyanates linked with a low molecular weight chain extender.[106] Thermodynamic incompatibility between these segments drives microphase separation in which hard segments form glassy, semicrystalline domains that, in polymers of lower hard segment content, are dispersed within an amorphous, rubbery matrix.[106-108, 118, 119] These hard domains are stabilized by hydrogen bonds between urea and urethane groups and serve as physical crosslinks and structural reinforcement for the soft segment matrix.[106, 118, 119] It is this microphase-separated morphology that dictates the ease of processing of polyurethane elastomers. This is because, unlike traditional elastomers, which derive their elasticity from an amorphous network interconnected with chemical crosslinks, the physical crosslinks of polyurethane elastomers are thermo-reversible and so breakup upon heating or dissolution.

Along with this ease of processing, the mechanical properties of segmented block copolymers are strongly dependent on this microphase-separated morphology. Deformation of segmented block copolymers begins with elastomeric stretching of the soft segment matrix, as indicated by a low initial modulus in the stress-strain curve, **Figure 1.2**.[120] Hard domains then breakup at flaws and begin to rotate into the strain

direction, causing a plateau of almost constant stress. This eventually results in the formation of microfibrils consisting of small, semi-crystalline hard domains separated by strain-crystallized soft segment chains that undergo strain hardening at higher strains.[120] Ultimately, these hard domains shear yield at a critical strain and the material fails.[120]. Because of this deformation profile, polyurethanes and polyureas have excellent mechanical properties, including high tensile strength, elongation to failure, fatigue life, and wear resistance, without additional processing. In addition to mechanical behavior, microphase separation has also been shown to directly influence the rate and extent of biodegradation.[121, 122] Factors that influence the degree of phase separation include soft segment molecular weight, hard and soft segment chemistries, and the hard to soft segment ratio.[123-127] Therefore, these variables can be adjusted to modulate the performance properties of polyurethanes and polyureas. For example, increased hard segment content puts greater constraint on the soft segment matrix, which leads to a higher initial modulus and strain hardening at a lower strain.[120, 128]

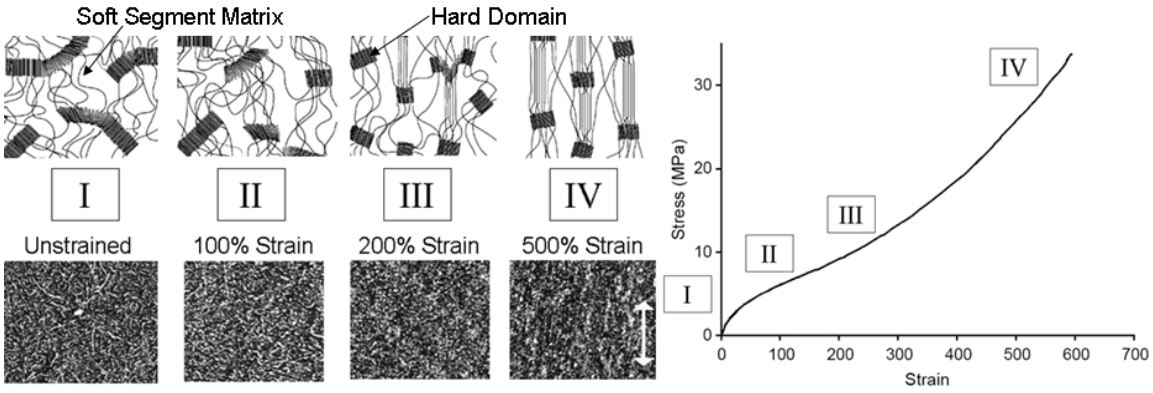

Figure 1.2. Effect of mechanical stretch on polyurethane deformation.[120]

Overall, the correlation between polyurethane chemistry and microphase separation, and thus performance properties, provides a means to elucidate key structure-property relationships. As with homogenous, biodegradable polymers, a number of these relationships have overlapping components that complicate material design for tissue engineering applications. A key challenge then is to isolate structure-property relationships that are essential to the development of engineered tissue. A polymer system with several mechanisms to modulate physical properties would provide the tools necessary to observe such phenomena. Due to the exceptional tunability of polyurethanes and polyureas, segmental modification of these polymers can be used to generate a library of polymers with broad structural diversity and a myriad of performance properties to better probe specific tissue-biomaterial interactions. Greater understanding of such structure-property relationships would then allow for rational design of a tissue engineered scaffold that promotes effective load transfer.

1.6 Polyurethanes in Biomedical Applications

As stated previously, in addition to the aforementioned mechanical requirements, tissue engineered scaffolds must be biocompatible and biodegradable. Polyurethanes used for biomedical applications have traditionally been intended for biostable, long-term use, such as cardiovascular applications and as artificial organs.[106, 114] Aromatic diisocyanates were often chosen for these materials due to their enhanced mechanical properties; however, concerns that the degradation of these diisocyanates (i.e., 4, 4'-methylenediphenyl diisocyanate (MDI), 2, 4-toluene diisocyanate (TDI)) can generate potentially carcinogenic byproducts (i.e., 4, 4'-methylenedianiline (MDA), 2,

4-toluene diamine (TDA)) have limited their transition to biodegradable polymers.[109, 129-131] As a result, aliphatic diisocyanates, such as hexamethylene diisocyanate (HDI) and L-lysine diisocyanate (LDI), have received interest for tissue engineering.[126, 132-143] Unlike aromatic diisocyanates, polyurethanes prepared from aliphatic diisocyanates have been reported to degrade to non-cytotoxic compounds in vitro and in vivo.[144, 145] LDI and HDI-based biodegradable polyurethanes have also demonstrated excellent mechanical properties and good biocompatibility, as well as promoted cell-material interactions necessary for tissue formation.[146-148] In addition to biocompatible diisocyanates, biodegradable hard segments composed of enzyme-labile chain extenders have been used to synthesize polyurethanes for tissue engineering.[136, 145, 149] Degradation of these linkages is dependent on hard segment crystallinity; however, crystallinity is a well-established barrier to degradation. Additionally, enhanced hard segment crystallinity leads to an increase in supramolecular interactions (i.e., hydrogen bonding) that dictate the mechanical properties of polyurethane elastomers. Due to the interactions among crystallinity, degradation rate, and mechanical strength, biodegradable hard segments limit the inherent tunability of polyurethane elastomers by inhibiting independent control of these structure-property relationships.

In contrast, the use of biodegradable soft segments can potentially decouple the effects on polyurethane structure on degradation rate and mechanical properties. Polyurethanes have been synthesized from a number of biodegradable soft segments, including poly (lactic acid), poly (glycolic acid), and poly (ε-caprolactone) (PCL).[133-137, 143, 150-156] These polyols were selected based on their established hydrolytic degradation

in vitro and in vivo. As a result, polyurethane degradation is dependent on soft segment content, chemistry, and molecular weight. Several polyurethanes composed of these polyols have demonstrated biocompatibility and excellent mechanical properties, as well as promoted tissue remodeling.[145, 153] Indeed, Gisselfalt et al. developed a series of PCL-based poly(urethane urea) fibers for ligament tissue engineering that displayed high tensile strength, modulus, and fatigue resistance, as well as supported ingrowth of connective tissue.[128, 157] Nonetheless, as with biodegradable polyesters previously used for ligament tissue engineering, degradation of these soft segments is dictated by non-specific hydrolysis, which makes it difficult to tailor polyurethane degradation to complement tissue regeneration.

Furthermore, the semi-crystalline nature of some of these soft segments can contribute to the performance properties of these materials. For example, PCL of higher molecular weight can lead to increased crystallinity of the soft segment, and thus a corollary increase in the modulus and tensile strength, along with a decreased rate of degradation.[126, 136] Therefore, soft segment crystallinity further compounds the complexity of polyurethane morphology and derived properties, which makes independent control of polyurethane structure-property relationships through segmental modifications difficult. In order to disrupt the crystallinity of PCL and achieve a greater range of degradation profiles, PCL and poly (ethylene glycol) (PEG) copolymers have been investigated; however, the hydrophilicity of PEG increases water uptake of the resulting polyurethane, which increases the rate of hydrolytic degradation.[144, 150, 153, 158-160] Overall, although segmented block copolymers possess the tools necessary to tailor

biomaterial chemistry and thus provide independent control of degradation and mechanical properties, non-specific degradation of current polyurethane elastomers makes it difficult to complement scaffold degradation with ligament regeneration.

1.7 System-Responsive Degradation

In general, the design of biomaterial scaffolds for tissue engineering is currently limited by the lack of independent control over mechanical properties and degradation and the difficulty of matching non-specific degradation with neotissue formation. This is because, without appropriate mechanical cues, neotissue cannot successfully regenerate the hierarchical structure of ACL tissue. Current research has established that mechanical stimulation increases fibroblast proliferation, and that this effect is dependent on the type, magnitude and duration of loading.[19, 161-164] In addition, cyclic stretch causes cells to adopt an elongated, spindle-like morphology consistent with the ligament phenotype.[161, 165-168] Mechanical loading is also needed to induce cellular alignment via restructuring of the actin cytoskeleton.[165, 169, 170] The orientation of fibroblasts with respect to mechanical loading is of particular interest because of its influence on *de novo* tissue formation.[166, 171-174] Fibroblasts oriented parallel to the direction of stretch demonstrate greater protein synthesis than cells aligned perpendicular to the direction of stretch, as well as generate an oriented collagen matrix.[166, 171] These effects have clear relevance to the mechanical properties of the resulting tissue. Finally, physical loading has been shown to increase protein synthesis, specifically type I collagen, which is of particular importance in the ACL due its role in establishing tensile properties.[161, 165-167, 170, 175-177] Overall, these studies establish the

need for mechanical stimulation to develop highly organized, cable-like tissue, indicative of the native ACL.

Because of this dependency on mechanical loading, a key challenge in the design of a successful tissue engineered ligament is to facilitate load transfer from the biodegradable scaffold to newly formed tissue. Initially, the biodegradable scaffold should exhibit sufficient mechanical properties to provide immediate restoration of ligament function. Isolated cells should then generate neotissue at a rate complementary to scaffold degradation so that the mechanical integrity of the ligament is sustained throughout the remodeling process up until the injured tissue is completely replaced.[4, 11, 178] Because the level of load borne unto *de novo* tissue dictates remodeling and thus, collagen alignment, a degradation rate that does not match new tissue formation can lead to either graft rupture (too fast) or stress shielding (too slow).[4, 19, 89] With stress shielding, the lack of collagen alignment can shift the dynamics of ligament remodeling toward degradation, which reduces the load-bearing capacity of the newly formed tissue. In order to integrate with native ligament remodeling and maintain mechanical functionality, new structure-property models are needed to elucidate the mechanisms of load transfer. A polymeric system with control over degradation rate and mechanical properties would provide insight into these mechanisms and allow for rational design of tissue engineered constructs. Biodegradable polyurethanes can be tailored to isolate the effects of polymer structure on specific performance properties; however, non-specific degradation remains problematic.

System-responsive degradation would eliminate this limitation by integrating polyurethane biodegradation with native ligament remodeling. As stated previously, during tissue regeneration, fibroblasts produce enzymes that systematically break down and remove the existing extra cellular matrix.[179] In particular, matrix metalloproteinase (MMP) production, including MMP-1 and MMP-2, is upregulated in response to ligament rupture and mechanical stimulation, with MMP-2 serving as the most efficient enzyme associated with type I collagen degradation.[180-182] The specificity of these enzymes has been extensively investigated with cleavage localized to the (Gly_{775}-Ile_{776}) site of the triple-helical collagen.[183-185] By incorporating this collagen oligopeptide sequence into the design of a novel biomaterial, guided scaffold degradation can be achieved. Moreover, integration of this enzyme-labile peptide sequence into the soft segment of a polyurethane elastomer would provide a means to decouple specific effects of polyurethane structure on performance properties.

For this study, an enzyme-labile peptide sequence with established specificity to MMP-2 was conjugated to ether-based polyols to form collagen-mimetic soft segments, **Figure 1.3.** Synthetic routes were first developed to generate reactive end groups necessary for peptide coupling. Upon successful conjugation, biodegradable soft segments were then incorporated into the structure of linear polyurea elastomers. By varying soft segment chemistry, soft segment molecular weight, and the hard to soft segment ratio, a series of cell-responsive, biodegradable polyureas was developed to elucidate key structure-property relationships necessary to complement neotissue formation. Overall, a novel biomaterial that combines the strength and tunability of

synthetic elastomers with cell-responsive degradation will assist in the development of an improved tissue engineered graft for ACL reconstruction.

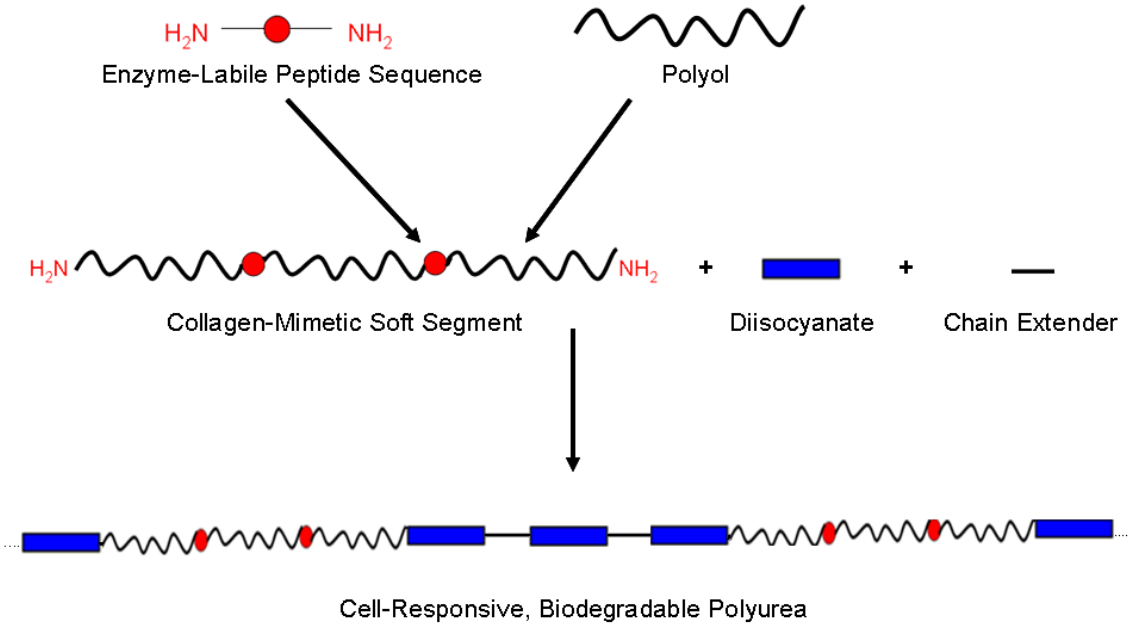

Figure 1.3. Synthetic design of cell-responsive, biodegradable polyureas.

CHAPTER II

END GROUP FUNCTIONALIZATION OF ETHER-BASED POLYOLS

2.1 Introduction

In this study, ether-based soft segments were functionalized to enable facile coupling to collagen-derived peptide sequences. By varying soft segment chemistry (PEG; poly (tetramethylene ether glycol) (PTMG)) and molecular weight (PEG: 1000, 2000 g/mol; PTMG: 1000 g/mol), a series of biodegradable soft segments that feature cell-responsive degradation can be developed. This library of soft segments will be used to elucidate the effects of polyol chemistry and molecular weight on the performance properties of polyureas. To this end, synthetic strategies were first developed to functionalize polyols with carboxylic acid end groups required to covalently bond with peptide sequences. Such end groups were then activated with N-hydroxysuccinimide (NHS) ester derivatives to serve as more favorable leaving groups for peptide coupling. In addition, carboxylic acid derivatives of higher molecular weight polyethers (PEG: 6000, 10000 g/mol; PTMG: 2900 g/mol) were functionalized with terminal amine groups to serve as control soft segments for subsequent polyurea syntheses, **Figure 2.1**.

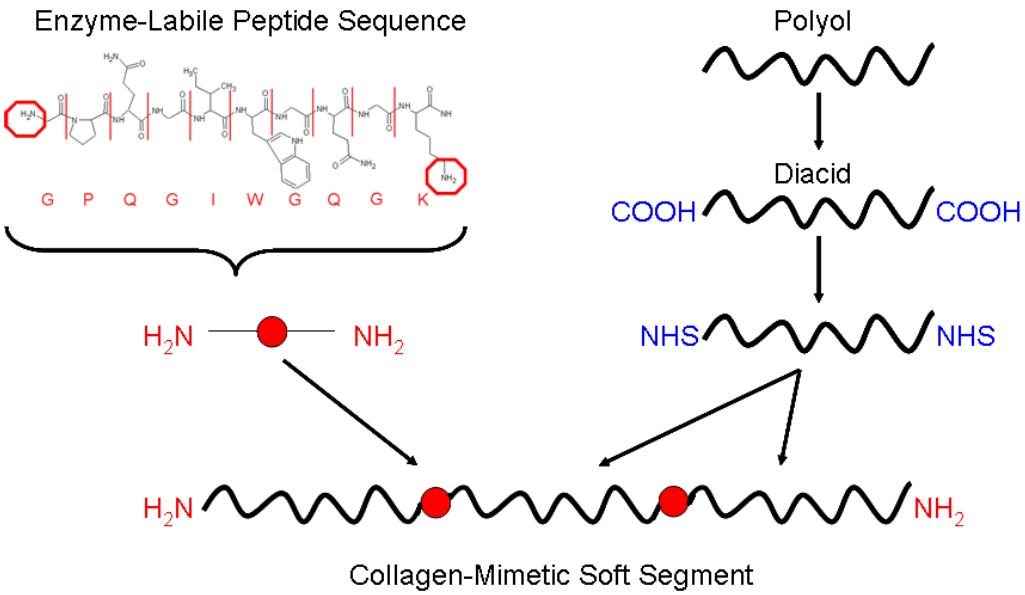

Figure 2.1. Synthetic approach to create peptide-based soft segments.

2.2 Carboxylic Acid Functionalization

In their native state, polyethers, such as PEG and PTMG, contain hydroxyl groups that often require activation or modification before conjugation to other molecules can occur. Functionalization of these polyols can be achieved through acylation with an anhydride to yield stable ester derivatives terminating in free carboxylate groups.[186] For example, modification of PEG with succinic anhydride in the presence of 4-(Dimethylamino) pyridine (DMAp) and triethylamine (Et_3N) yields *bis*-modified products equipped with carboxylates at either end.[187-191] Succinic anhydride has a five-atom cyclic structure that is highly reactive toward nucleophiles, including hydroxyl and amine groups. Nucleophilic attack at one of the carbonyl groups opens the anhydride ring, forming a covalent bond with that carbonyl and releasing the other to create a free carboxylic acid group.[192] The currently accepted mechanism for

such acylation involves the pre-equilibrium formation of an acylpyridinium cation generated from the reaction of succinic anhydride and DMAp.[193] DMAp is a commonly used catalyst used to accelerate the acylation of alcohols and amines. Hydroxyl groups react with the acylated catalyst in the rate-determining second step to form an ester linkage, along with the deactivated catalyst. The auxiliary base Et_3N is then utilized to recover the deactivated catalyst. In the current study, PEG and PTMG soft segments of varying molecular weight were reacted with an excess of succinic anhydride in the presence of DMAp and Et_3N to generate carboxylic acid derivatives.

2.2.1 Materials

Poly (ethylene glycol) (PEG; M_n ~1000, 2000, 6000, 10000 g/mol) was obtained from Fluka Chemical. Poly (tetramethylene ether glycol) (PTMG; M_n ~1000, 2900 g/mol) was obtained from Polysciences, Inc. Succinic anhydride, 4-(Dimethylamino) pyridine (DMAp), triethylamine (Et_3N), 1,4-dioxane, dimethylformamide (DMF), diethyl ether, and deuterated chloroform ($CDCl_3$) were obtained from Sigma Aldrich and used as received. Dichloromethane (DCM) was also obtained from Sigma-Aldrich but dried over 4Å molecular sieves.

2.2.2 Methods

PEG and PTMG diacids were prepared by esterification of each polyol with excess succinic anhydride in the presence of DMAp and Et_3N, **Figure 2.2**. Succinic anhydride, DMAp, and Et_3N were dissolved in 1, 4-dioxane and then added to a solution of PEG or PTMG in 1, 4-dioxane. The mixture was then stirred for 12 hours at 90°C under nitrogen. After cooling to room temperature, 1, 4-dioxane was removed by rotary

evaporation, and the condensed solution was filtered to remove excess succinic acid. PEG derivatives were re-dissolved with DMF and precipitated for ten minutes from excess diethyl ether (10:1) that had cooled in a salt ice bath. Following vacuum filtration, the final polymer was dried under vacuum at room temperature overnight. PTMG derivatives were re-dissolved with DCM and washed twice with distilled water (1:1). DCM was then removed by rotary evaporation and vacuum-dried to remove residual solvent. Fourier transform infrared (FTIR) spectroscopic analysis was performed on a Bruker TENSOR 27 spectrometer to confirm end group functionalization. Percent functionalization was quantified with proton nuclear magnetic resonance (^{1}H-NMR) spectroscopy using a Mercury 300 MHz spectrometer.

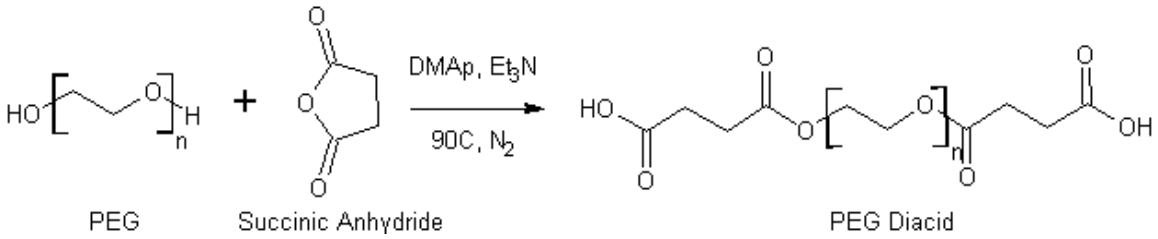

Figure 2.2. Synthesis of carboxylic acid functionalized PEG.

2.2.3 Results

Synthesis of PEG (1000) diacid

PEG (1000) (10.00 g, 0.01 mol), succinic anhydride (4.00 g, 0.04 mol), DMAp (2.44 g, 0.02 mol), and Et_3N (3.06 mL, 0.022 mol) were reacted as previously described. In this way, PEG (1000) diacid was obtained as a white, waxy solid (9.12 g, 76% yield). Carboxylic acid functionalization and ester formation (1732 cm^{-1}, C=O) were confirmed

with FTIR spectroscopy, **Figure 2.3**. Percent functionalization was calculated to be ~93% using NMR spectroscopy. ^{1}H-NMR (δ, ppm): 2.64 (m, 8H, -C*H*$_2$COO-), 3.64 (m, 85H, -C*H*$_2$O-), 4.25 (t, 4H, -C*H*$_2$OCO-).

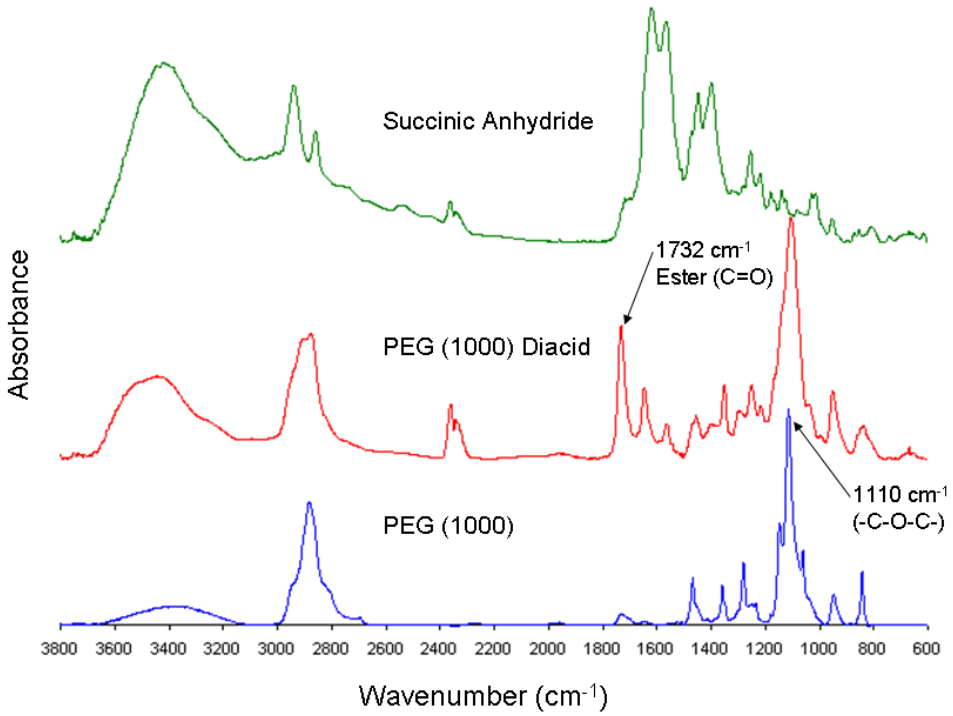

Figure 2.3. FTIR spectra of PEG (1000) carboxylic acid functionalization.

Synthesis of PEG (2000) diacid

PEG (2000) (10.00 g, 0.005 mol), succinic anhydride (2.00 g, 0.02 mol), DMAp (1.22 g, 0.01 mol), and Et_3N (1.53 mL, 0.011 mol) were reacted as previously described. In this way, PEG (2000) diacid was obtained as a white, waxy solid (9.57 g, 87% yield). Carboxylic acid functionalization and ester formation (1732 cm^{-1}, C=O) were confirmed with FTIR spectroscopy, **Figure 2.4**. Percent functionalization was calculated to be

~91% using NMR spectroscopy. ^{1}H-NMR (δ, ppm): 2.64 (m, 8H, -C*H*$_2$COO-), 3.64 (m, 176H, -C*H*$_2$O-), 4.25 (t, 4H, - C*H*$_2$OCO-).

Synthesis of PEG (6000) diacid

PEG (6000) (10.00 g, 1.67 mmol), succinic anhydride (0.67 g, 6.67 mmol), DMAp (0.41 g, 3.33 mmol), and Et_3N (0.51 mL, 3.67 mmol) were reacted as previously described. In this way, PEG (6000) diacid was obtained as a white, brittle solid (8.13 g, 79% yield). Carboxylic acid functionalization and ester formation (1730 cm^{-1}, C=O) were confirmed with FTIR spectroscopy, **Figure 2.4**. Percent functionalization was calculated to be ~93% using NMR spectroscopy. ^{1}H-NMR (δ, ppm): 2.64 (m, 8H, -C*H*$_2$COO-), 3.64 (m, 540H, -C*H*$_2$O-), 4.25 (t, 4H, - C*H*$_2$OCO-).

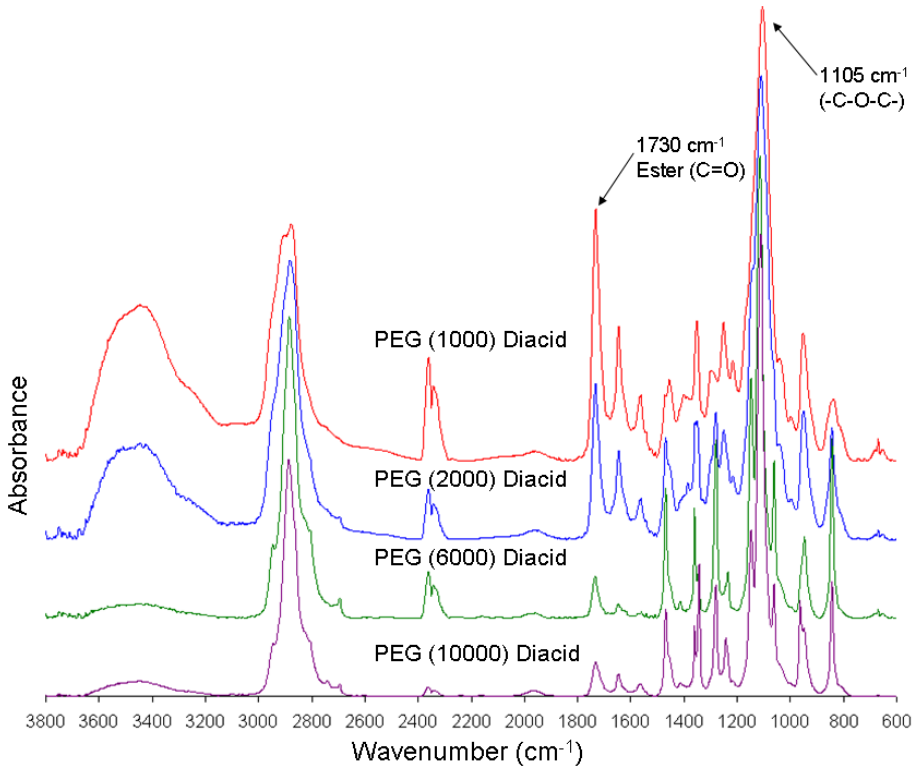

Figure 2.4. FTIR spectral comparison of PEG diacid syntheses.

Synthesis of PEG (10000) diacid

PEG (10000) (10.00 g, 0.001 mol), succinic anhydride (0.60 g, 0.006 mol), DMAp (0.49 g, 0.004 mol), and Et_3N (0.613 mL, 0.0044 mol) were reacted as previously described. In this way, PEG (10000) diacid was obtained as a white, brittle solid (8.13 g, 80% yield). Carboxylic acid functionalization and ester formation (1726 cm^{-1}, C=O) were confirmed with FTIR spectroscopy, **Figure 2.4**. Percent functionalization was calculated to be ~91% using NMR spectroscopy. ^{1}H-NMR (δ, ppm): 2.64 (m, 8H, -C*H*$_2$COO-), 3.64 (m, 904H, -C*H*$_2$O-), 4.25 (t, 4H, -C*H*$_2$OCO-).

Synthesis of PTMG (1000) diacid

PTMG (1000) (7.14 g, 7.14 mmol), succinic anhydride (2.86 g, 28.56 mmol), DMAp (1.75 g, 14.28 mmol), and Et_3N (2.19 mL, 15.71 mmol) were reacted as previously described. In this way, PTMG (1000) diacid was obtained as a clear, viscous liquid (7.20 g, 84% yield). Carboxylic acid functionalization and ester formation (1736 cm^{-1}, C=O) were confirmed with FTIR spectroscopy, **Figure 2.5**. Percent functionalization was calculated to be ~92% using NMR spectroscopy. ^{1}H-NMR (δ, ppm): 1.62 (m, 55H, -C*H*$_2$-), 2.63 (m, 8H, -C*H*$_2$COO-), 3.41 (m, 51H, -C*H*$_2$O-), 4.12 (t, 4H, - C*H*$_2$OCO-).

Synthesis of PTMG (2900) diacid

PTMG (2900) (10.00 g, 3.45 mmol), succinic anhydride (1.38 g, 13.79 mmol), DMAp (0.84 g, 6.90 mmol), and Et_3N (1.06 mL, 7.59 mmol) were reacted as previously described. In this way, PTMG (2900) diacid was obtained as a clear, viscous liquid (9.19 g, 86% yield). Carboxylic acid functionalization and ester formation (1736 cm^{-1}, C=O)

were confirmed with FTIR spectroscopy, **Figure 2.5**. Percent functionalization was calculated to be ~95% using NMR spectroscopy. ^{1}H-NMR (δ, ppm): 1.62 (m, 160H, -C*H*$_2$-), 2.63 (m, 8H, -C*H*$_2$COO-), 3.41 (m, 156H, -C*H*$_2$O-), 4.12 (t, 4H, - C*H*$_2$OCO-).

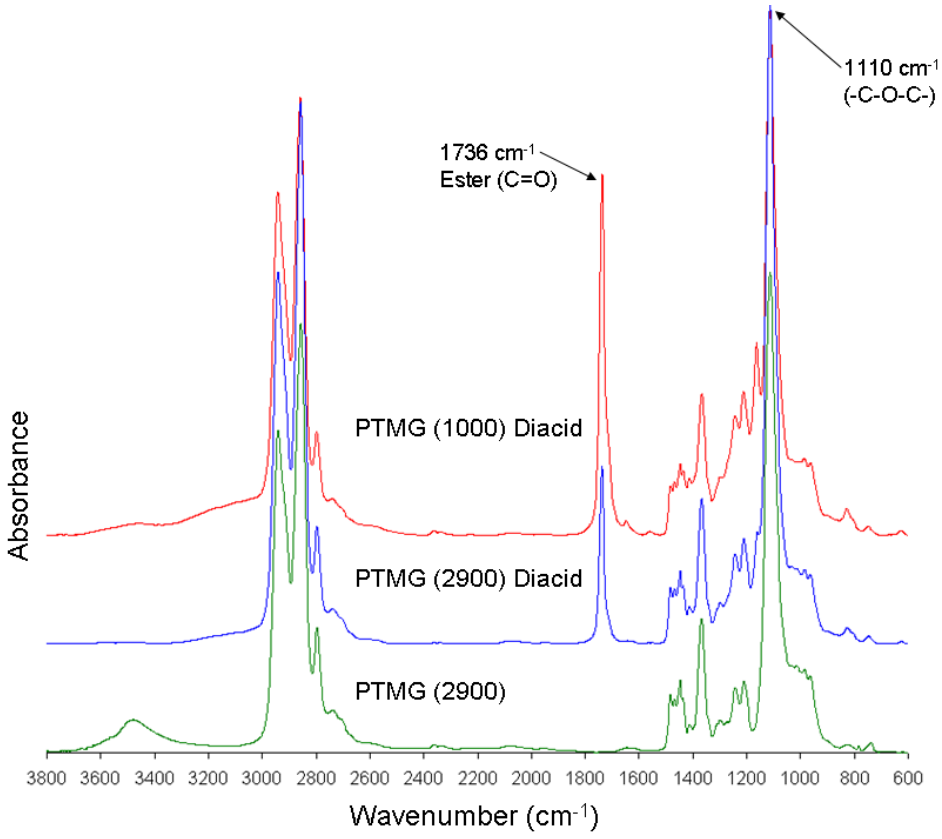

Figure 2.5. FTIR spectral comparison of PTMG diacid syntheses.

2.3 NHS Activation of Carboxylic Acid Derivatives

Once successful functionalization has been verified, carboxylic acid derivatives of PEG and PTMG can be used to react with other molecules via nucleophilic acyl substitution; however, due to the relatively poor reactivity of carboxylic acid end groups, activation with a superior leaving group is often necessary to ensure optimal

conjugation. The use of NHS ester derivatives is one of the more common strategies to activate such acylating agents.[194-200] An NHS ester is often formed by the reaction of a carboxylate with NHS in the presence of a carbodiimide, such as dicyclohexylcarbodiimide (DCC), in a non-aqueous medium.[191, 197, 201-203] Carbodiimides are cross-linking agents used to mediate the formation of amide or ester linkages between a carboxylate and an amine or hydroxyl group, respectively.[204] N-substituted carbodiimides react with carboxylic acids to form highly reactive, O-acylisourea derivatives, which then react with a nucleophile to form a bond, generating an isourea byproduct.[205] In the present study, the O-acylisourea intermediate reacts with the hydroxyl group of free NHS, forming an ester linkage and essentially upgrading to a better leaving group. A potential limitation to DCC coupling reactions is the spontaneous rearrangement of the O-acylisourea to an inactive N-acylisourea, which is enhanced in aprotic solvents such as DMF.[186] To minimize this effect on NHS activation of carboxylate groups, a large excess of DCC and NHS is typically used.[191, 197] In the current study, carboxylic acid functionalized polyethers from the previous step were reacted with excess NHS and DCC to form NHS ester derivatives.

2.3.1 Materials

PEG and PTMG diacids were prepared as previously described. Dicyclohexylcarbodiimide (DCC) was purchased from Fluka Chemical. Ethyl acetate was obtained from Fisher Scientific. N-hydroxysuccinimide (NHS), hexane, diethyl ether, and deuterated chloroform ($CDCl_3$) were obtained from Sigma Aldrich and used

as received. Dichloromethane (DCM) was obtained from Sigma-Aldrich and dried over 4Å molecular sieves.

2.3.2 Methods

Activated NHS ester derivatives of PEG and PTMG diacids were prepared in the presence of excess NHS and DCC, **Figure 2.6**. PEG or PTMG diacid and NHS were first dissolved in DCM, and then excess DCC was added. After stirring for 12 hours at room temperature, precipitated dicyclohexylurea was removed with vacuum filtration. For PEG diacid derivatives, the filtered solution was condensed by rotary evaporation and re-dissolved in ethyl acetate. Additional urea byproduct was removed and the filtered solution was then precipitated for 10 minutes from excess diethyl ether (10:1) that had cooled in a salt ice bath. PEG derivatives of higher molecular weight (2000, 6000, and 10000 g/mol) were retrieved using vacuum filtration and dried under vacuum at room temperature overnight. Because NHS-activated PEG (1000) diacid was a viscous liquid, diethyl ether was decanted and the polymer residue was re-dissolved with DCM. DCM was then removed by rotary evaporation and the polymer residue was dried under high vacuum to remove residual solvent. After filtration, PTMG diacid derivatives were washed once with distilled water (1:1) and then precipitated from excess hexane (10:1) that had been cooled in a salt ice bath. After ten minutes, hexane was decanted, and the polymer residue was re-dissolved with DCM. DCM was removed by rotary evaporation and the polymer residue was vacuum-dried to remove residual DCM. Infrared spectroscopic analysis was performed on a Bruker TENSOR 27 spectrometer to

confirm end group functionalization. Percent functionalization was quantified with ^{1}H-NMR spectroscopy using a Mercury 300 MHz spectrometer.

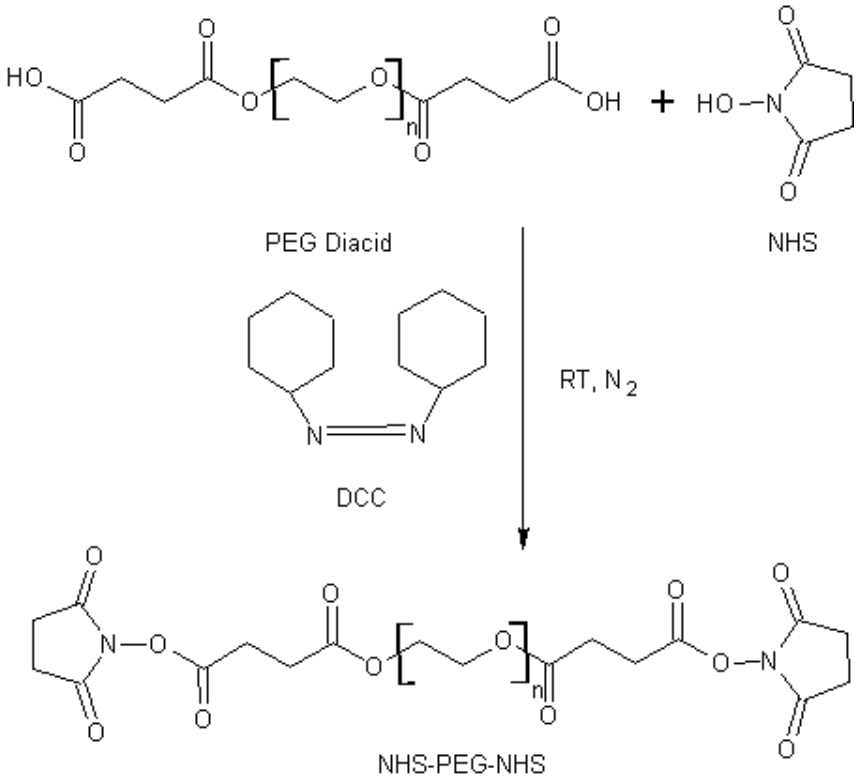

Figure 2.6. NHS activation of PEG diacid in the presence of DCC.

2.3.3 Results

NHS activation of PEG (1000) diacid

PEG (1000) diacid (3.09 g, 2.575 mmol), NHS (2.96 g, 25.75 mmol), and DCC (6.91 g, 33.47 mmol) were reacted as previously described. In this way, NHS- PEG (1000)-NHS was obtained as a yellow, viscous liquid (2.53 g, 70% yield). Formation of activated NHS ester derivatives (1738, 1778, 1811 cm^{-1}, C=O) was confirmed with FTIR spectroscopy, **Figure 2.7**. ^{1}H-NMR (δ, ppm): 2.71 (s, free NHS), 2.78 (t, 4H,

-CH_2COO-), 2.84 (m, 8H, NHS ester), 2.96 (t, 4H, -CH_2COON-), 3.64 (m, 85H, -CH_2O-), 4.27 (t, 4H, -CH_2OCO-).

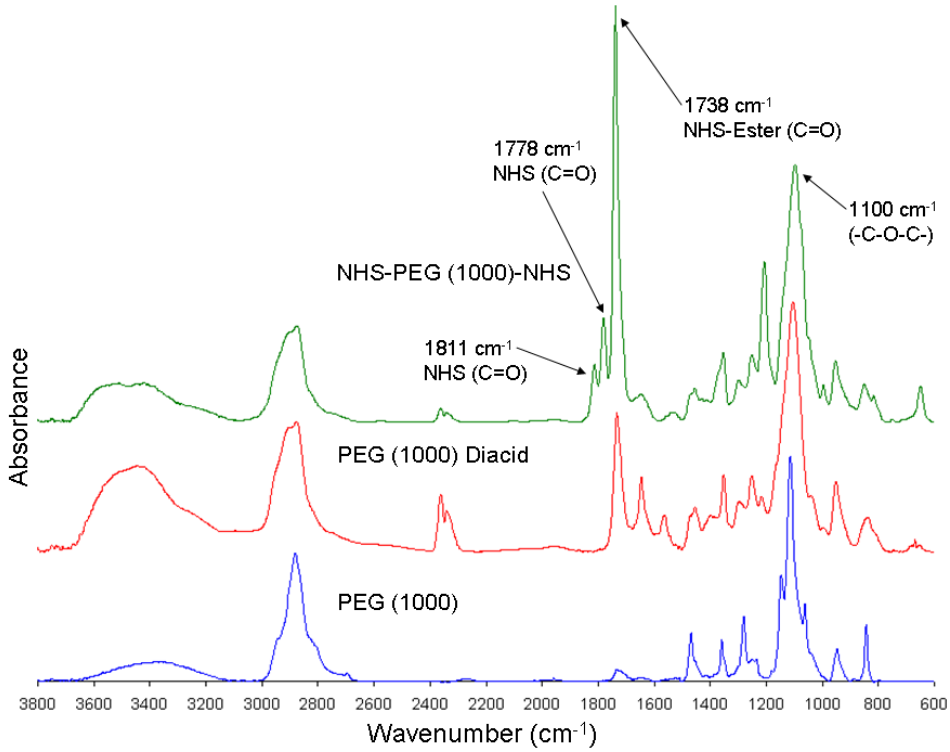

Figure 2.7. FTIR spectra of NHS activation of PEG (1000) diacid.

NHS activation of PEG (2000) diacid

PEG (2000) diacid (3.04 g, 1.38 mmol), NHS (1.59 g, 13.8 mmol), and DCC (3.71 g, 17.96 mmol) were reacted as previously described. In this way, NHS-PEG (2000)-NHS was obtained as a white, waxy solid (2.92 g, 88% yield). Formation of activated NHS ester derivatives (1738, 1778, 1811 cm^{-1}, C=O) was confirmed with FTIR spectroscopy, **Figure 2.8**. ^{1}H-NMR (δ, ppm): 2.71 (s, free NHS), 2.78 (t, 4H, -CH_2COO-), 2.84 (m, 8H, NHS ester), 2.96 (t, 4H, -CH_2COON-), 3.64 (m, 176H, -CH_2O-), 4.27 (t, 4H, -CH_2OCO-).

NHS activation of PEG (6000) diacid

PEG (6000) diacid (8.00 g, 1.29 mmol), NHS (1.49 g, 12.9 mmol), and DCC (3.46 g, 16.77 mmol) were reacted as previously described. In this way, NHS-PEG (6000)-NHS was obtained as a white powder (6.43 g, 78% yield). Formation of activated NHS ester derivatives (1738, 1776, 1807 cm^{-1}, C=O) was confirmed with FTIR spectroscopy, **Figure 2.8**. ^{1}H-NMR (δ, ppm): 2.71 (s, free NHS), 2.78 (t, 4H, -CH_2COO-), 2.84 (m, 8H, NHS ester), 2.96 (t, 4H, -CH_2COON-), 3.64 (m, 540H, -CH_2O-), 4.27 (t, 4H, -CH_2OCO-).

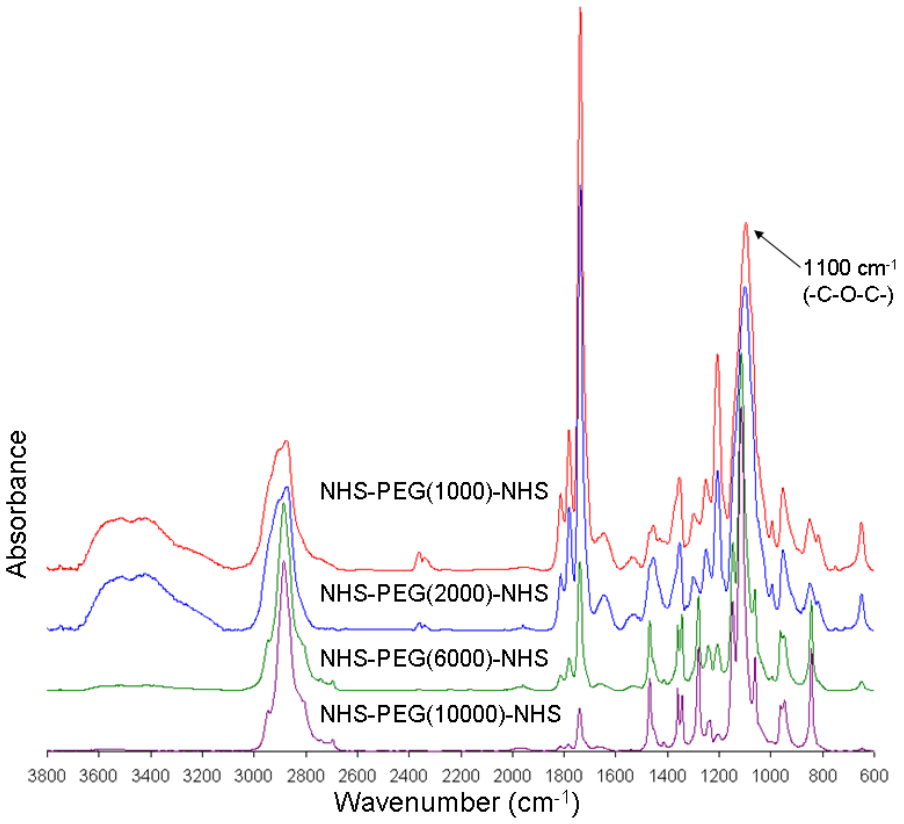

Figure 2.8. FTIR spectral comparison of NHS ester derivatives of PEG diacids.

NHS activation of PEG (10000) diacid

PEG (10000) diacid (3.06 g, 0.299 mmol), NHS (0.35 g, 2.999 mmol), and DCC (0.81 g, 3.899 mmol) were reacted as previously described. In this way, NHS-PEG (10000)-NHS was obtained as a white, brittle solid (2.80 g, 90% yield). Formation of activated NHS ester derivatives (1738, 1774, 1800 cm^{-1}, C=O) was confirmed with FTIR spectroscopy, **Figure 2.8**. ^{1}H-NMR (δ, ppm): 2.71 (s, free NHS), 2.78 (t, 4H, -CH_2COO-), 2.84 (m, 8H, NHS ester), 2.96 (t, 4H, -CH_2COON-), 3.64 (m, 904H, -CH_2O-), 4.27 (t, 4H, -CH_2OCO-).

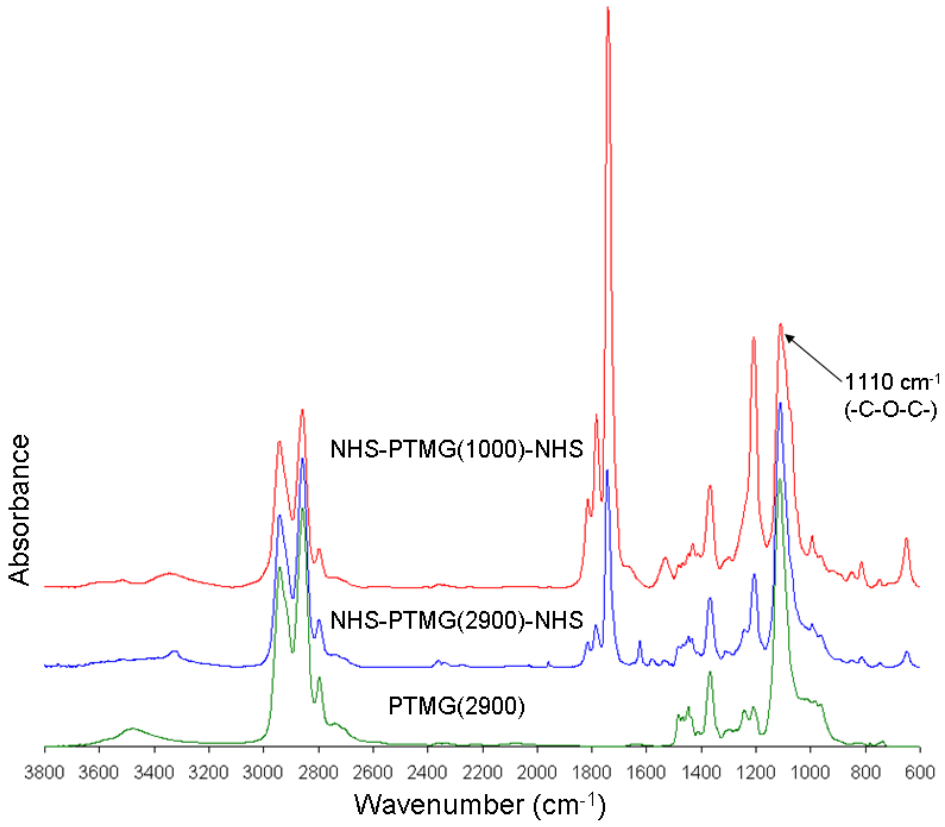

Figure 2.9. FTIR spectral comparison of NHS ester derivatives of PTMG diacids.

NHS activation of PTMG (1000) diacid

PTMG (1000) diacid (3.22 g, 2.68 mmol), NHS (3.09 g, 26.83 mmol), and DCC (7.19 g, 34.88 mmol) were reacted as previously described. In this way, NHS-PTMG (1000)-NHS was obtained as a yellow, waxy solid (2.90 g, 78% yield). Formation of activated NHS ester derivatives (1739, 1782, 1811 cm^{-1}, C=O) was confirmed with FTIR spectroscopy, **Figure 2.9**. ^{1}H-NMR (δ, ppm): 1.62 (m, 55H, -CH_2-), 2.74 (t, 4H, -CH_2COO-), 2.84 (m, 8H, NHS ester), 2.95 (t, 4H, -CH_2COON-), 3.41 (m, 51H, -CH_2O-), 4.14 (t, 4H, -CH_2OCO-).

NHS activation of PTMG (2900) diacid

PTMG (2900) diacid (7.99 g, 2.57 mmol), NHS (2.97 g, 25.8 mmol), and DCC (6.91 g, 33.5 mmol) were reacted as previously described. In this way, NHS-PTMG (1000)-NHS was obtained as a white, waxy solid (7.72 g, 91% yield). Formation of activated NHS ester derivatives (1743, 1780, 1811 cm^{-1}, C=O) was confirmed with FTIR spectroscopy, **Figure 2.9**. ^{1}H-NMR (δ, ppm): 1.62 (m, 160H, -CH_2-), 2.74 (t, 4H, -CH_2COO-), 2.84 (m, 8H, NHS ester), 2.95 (t, 4H, -CH_2COON-), 3.41 (m, 156H, -CH_2O-), 4.14 (t, 4H, -CH_2OCO-).

2.4 Amine Functionalization

Activation of acylated PEG and PTMG compounds with NHS ester groups produces a highly reactive polymer that can be covalently modified with various molecules to alter end group functionality.[186] NHS ester-containing reagents react with nucleophiles with release of the NHS leaving group to form an acylated product. For example, active NHS ester derivatives can react with short compounds that contain

primary amine groups on either end to form an amide bond, which blocks the carboxylate group and generates terminal amino groups.[206-208] Ethylene diamine (EDA) is a popular choice for amine functionalization because its short chain length ensures minimal steric effects and virtually no hydrophobic interactions.[209, 210] An excess of diamine is typically used to ensure both ends of the target molecule react with free amine-terminated compounds instead of cross-linking.[209] Modification of carboxylate groups with diamines can be done in organic solvents, provided the target molecule is soluble and stable in such environments.[186, 208, 210, 211] For such reactions, an organic base is typically added, such as Et_3N or DMAp.[186] In the current study, NHS-activated, PEG-based diacids of higher molecular weight (6000, 10000 g/mol) were end capped with excess EDA in the presence of DMAp and Et_3N to form amine-terminated soft segments for polyurea syntheses. To generate a PTMG-based soft segment of comparable molecular weight to PEG, a carboxylic acid derivative of low molecular weight was first terminated with amine groups and then subsequently used to end cap a higher molecular weight molecule.

2.4.1 Materials

NHS-activated PEG and PTMG diacids were prepared as previously described. Ethylene diamine (EDA), 4-(Dimethylamino) pyridine (DMAp), triethylamine (Et_3N), dimethylformamide (DMF), diethyl ether, and deuterated chloroform ($CDCl_3$) were obtained from Sigma-Aldrich and used as received. Dichloromethane (DCM) was obtained from Sigma-Aldrich and dried over 4Å molecular sieves. The Kaiser test kit was obtained from Fluka Chemical.

2.4.2 Methods

PEG and PTMG diamines were prepared by nucleophilic substitution of NHS-activated diacids with excess EDA in the presence of DMAp and Et_3N, **Figure 2.10.** NHS-activated PEG and PTMG diacids were dissolved in DMF and then added drop wise to a solution of EDA, DMAp, and Et_3N while stirring. After addition, the mixture was stirred at room temperature overnight under nitrogen. Free NHS byproducts were removed with vacuum filtration and PEG-based solutions were precipitated for ten minutes from excess diethyl ether (10:1) that had been cooled in a salt ice bath. PEG diamine was then retrieved with vacuum aspiration and subsequently dried under vacuum overnight. After filtration, PTMG solutions were washed with DCM and brine (1:1) and then condensed by rotary evaporation. PTMG diamine was finally dried under high vacuum to remove residual solvent. Upon successful functionalization, the resulting PTMG diamine was used to end cap NHS-activated PTMG 2900 diacid in place of EDA to form a PTMG-based control soft segment for polyurea syntheses. Formation of this PTMG-based control soft segment followed the same synthetic strategy as EDA-based functionalization; however, ultrafiltration was used in place of washing to remove excess PTMG 1000 diamine and other contaminants. Infrared spectroscopic analysis was performed on a Bruker TENSOR 27 spectrometer to confirm end group functionalization. A Kaiser test kit was used to verify the presence of free primary amine groups, as indicated by a color shift from yellow to a dark blue/purple hue. Due to hydrogen bonding among functional groups, ^{1}H-NMR spectroscopy could not be used to quantify end group functionalization.

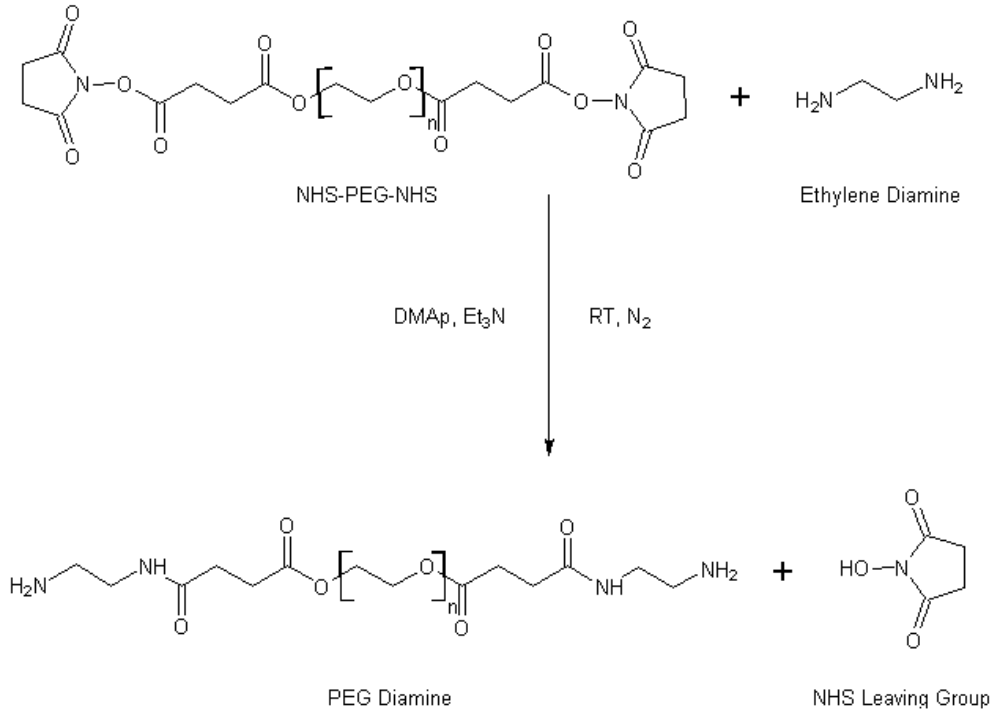

Figure 2.10. Functionalization of NHS-activated PEG diacid with EDA.

2.4.3 Results

Synthesis of PEG (6000) diamine

NHS-PEG (6000)-NHS (1.00 g, 0.156 mmol), EDA (62.9 µL, 0.938 mmol), DMAp (38.214 mg, 0.313 mmol), and Et_3N (47.9 µL, 0.344 mmol) were reacted as previously described. In this way, PEG (6000) diamine was obtained as a white, brittle solid (0.72 g, 73% yield). Amide formation (1640 cm^{-1}, C=O) was confirmed with FTIR spectroscopy, **Figure 2.11**. In addition, the carbonyl peak at 1730 cm^{-1} attenuated due to the loss of carboxylic acid groups and shifted to 1684 cm^{-1} because of hydrogen bonding among ester linkages. The Ninhydrin assay turned dark blue, indicating free amine groups are present.

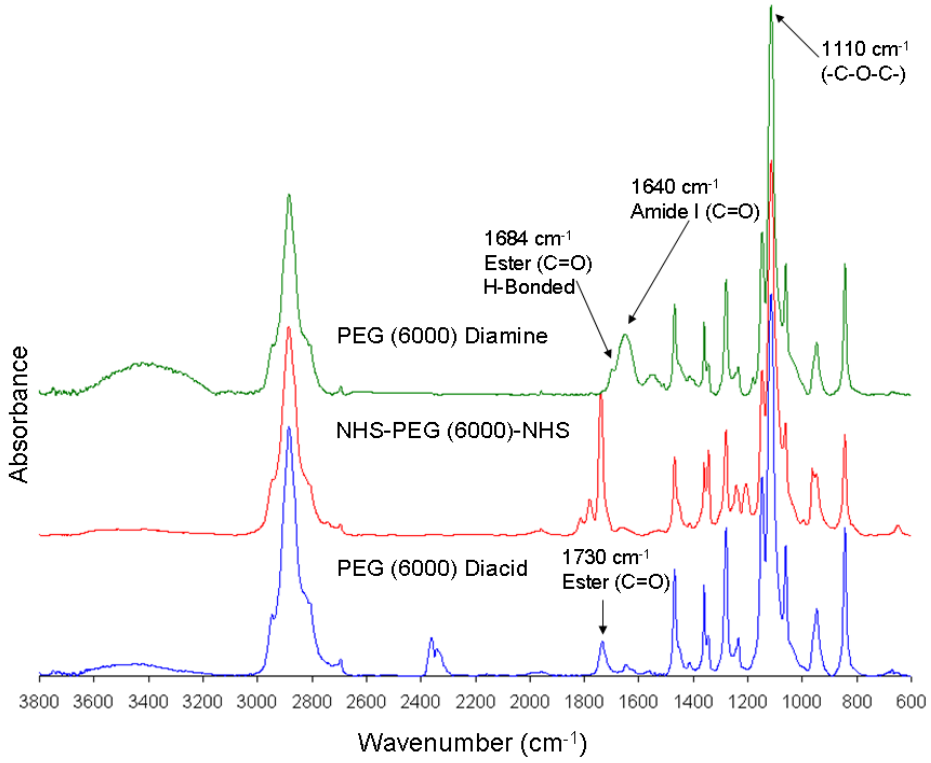

Figure 2.11. Amine functionalization of PEG (6000) diacid.

Synthesis of PEG (10000) diamine

NHS-PEG (10000)-NHS (1.00 g, 0.096 mmol), EDA (38.7 µL, 0.577 mmol), DMAp (23.51 mg, 0.192 mmol), and Et_3N (29.47 µL, 0.212 mmol) were reacted as previously described. In this way, PEG (10000) diamine was obtained as a white, brittle solid (0.72 g, 54% yield). Amide formation (1629 cm^{-1}, C=O) was confirmed with FTIR spectroscopy, **Figure 2.12**. In addition, the carbonyl peak at 1726 cm^{-1} attenuated due to the loss of carboxylic acid groups and shifted to 1684 cm^{-1} because of hydrogen bonding among ester linkages. The Ninhydrin assay turned dark blue to indicate that free amine groups are present.

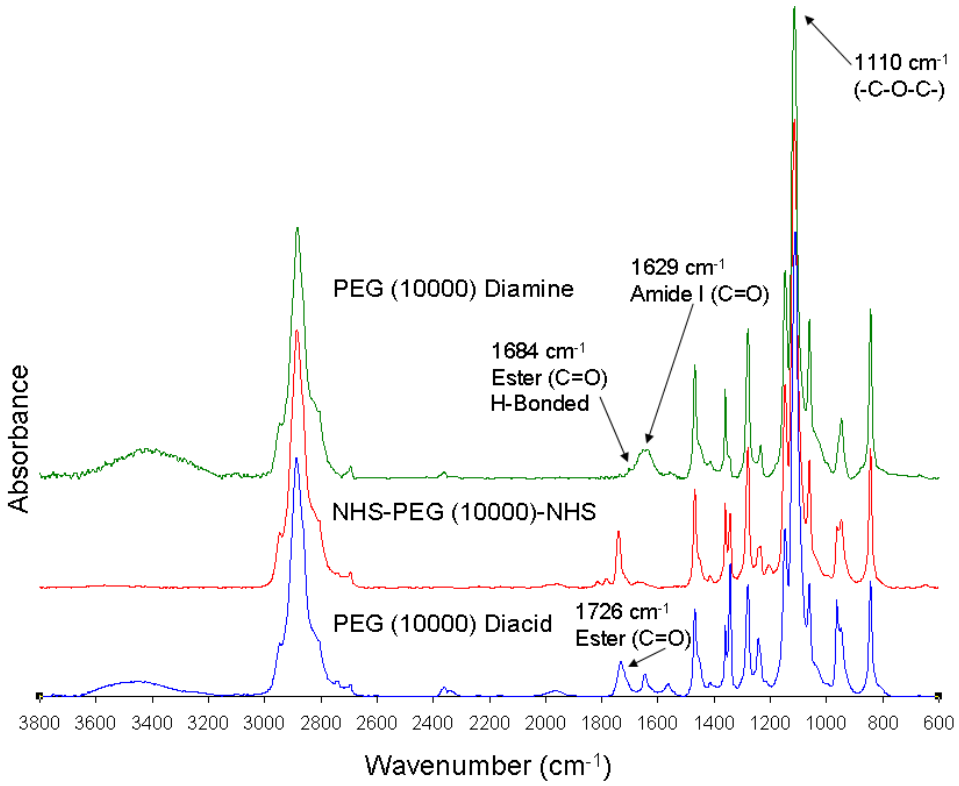

Figure 2.12. Amine functionalization of PEG (10000) diacid.

Synthesis of PTMG (1000) diamine

NHS-PTMG (1000)-NHS (0.62 g, 0.448 mmol), EDA (180 µL, 2.69 mmol), DMAp (109.4 mg, 0.896 mmol), and Et_3N (137.2 µL, 0.985 mmol) were reacted as previously described. In this way, PTMG (1000) diamine was obtained as a yellow, waxy solid (0.53 g, 92% yield). Amide formation (1658 cm^{-1}, C=O) was confirmed with FTIR spectroscopy, **Figure 2.13**. In addition, the carbonyl peak at 1730 cm^{-1} attenuated due to the loss of carboxylic acid groups. The Ninhydrin assay turned dark blue to indicate that free amine groups are present.

Synthesis of PTMG-based control soft segment (PTMG (5600) diamine)

NHS-PTMG (2900)-NHS (0.34 g, 0.103 mmol), PTMG (1000) Diamine (0.53 g, 0.412 mmol), DMAp (25.2 mg, 0.206 mmol), and Et_3N (31.6 µL, 0.227 mmol) were reacted as previously described. In this way, PTMG (5600) diamine was obtained as a yellow, waxy solid (0.37 g, 64% yield). As expected, carbonyl peaks of ester (1735 cm^{-1}, C=O) and amide (1655 cm^{-1}, C=O) linkages were reduced in the FTIR spectra of the control soft segment with respect to the internal reference ether peak, **Figure 2.14**. This is because, as the molecular weight of the base polymer increased, the relative ratio of all functional groups decreased. The Ninhydrin assay turned dark blue to indicate that free amine groups are present.

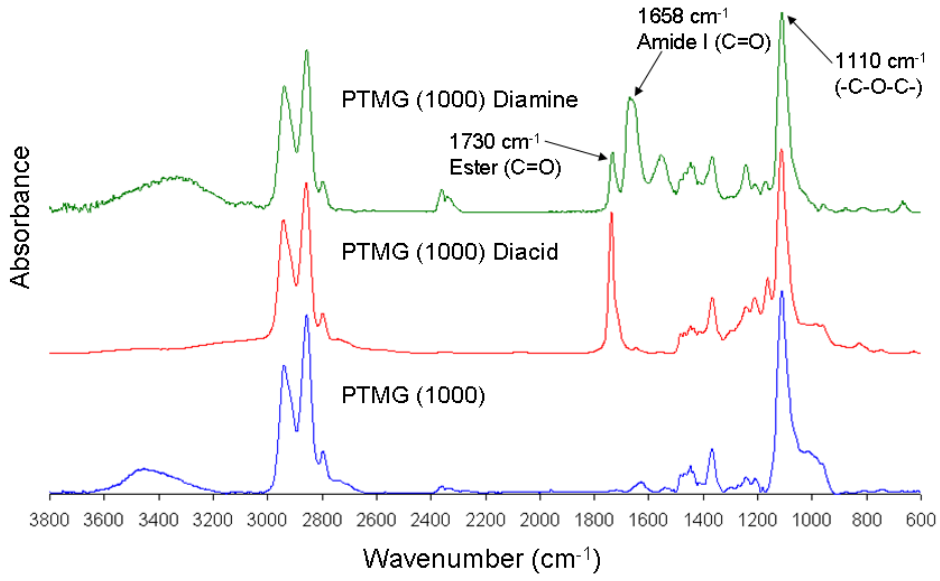

Figure 2.13. Amine functionalization of PTMG (1000) diacid.

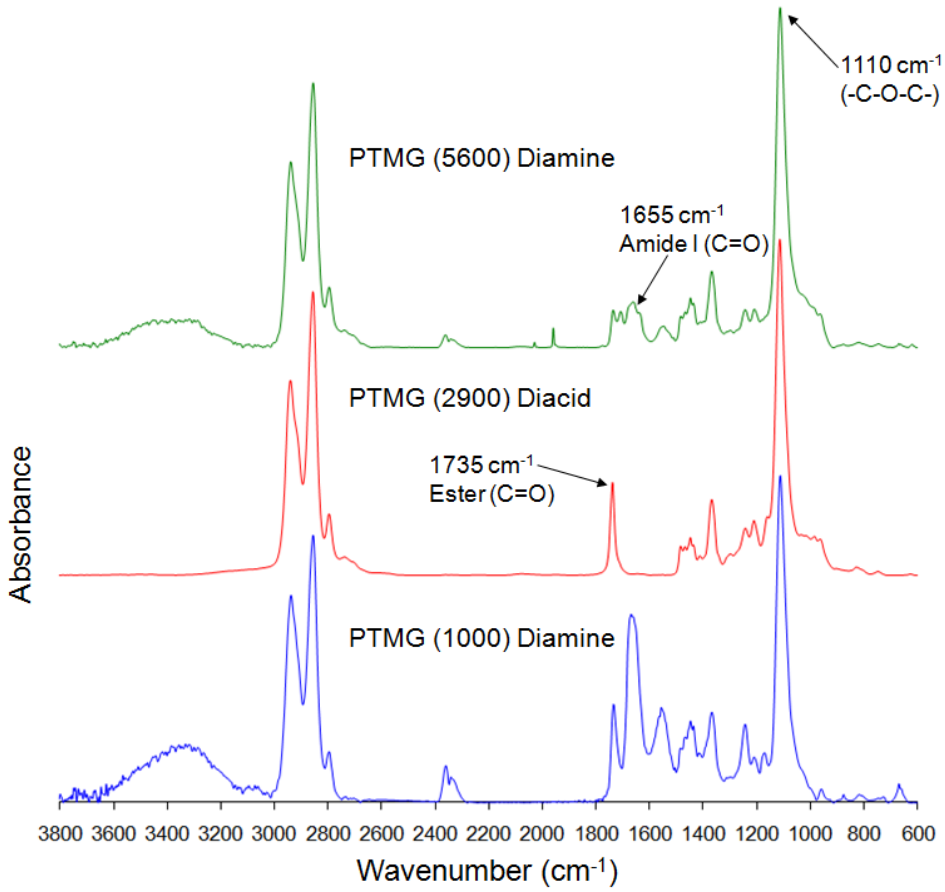

Figure 2.14. FTIR spectra of PTMG (5600) diamine synthesis.

2.5 Conclusions

End group functionalization is a useful means to tailor polymer chemistry for various applications. In the current study, synthetic routes were developed to modify ether-based polyols over a range of molecular weights with carboxylic acid end groups necessary for peptide coupling and amine functionalization. Successful functionalization of all target polyols was confirmed with FTIR and NMR analysis. As expected, FTIR spectra of all carboxylic acid derivatives demonstrated ester formation at 1730 cm^{-1}, with relative heights of absorbance with respect to the internal reference ether peak

decreasing with increased molecular weight. A similar correlation was observed in the FTIR spectra for all NHS-activated compounds. These samples also showed comparable increases in the absorbance at 1730 cm^{-1} due to the generation of NHS esters. ^{1}H-NMR analysis verified at least 90% functionalization of all polyols with carboxylic acid end groups, with succinate groups demonstrating appropriate chemical shifts upon activation with NHS. Amine functionalization of ether-based carboxylic acid derivatives was also confirmed with FTIR spectroscopy and a Ninhydrin assay; however, the lack of quantitative analysis is a concern as these polymers are used for subsequent syntheses.

Due to the versatility of these synthetic routes, a broad polymer toolbox was generated to enable segmental modification of polyurethane chemistry. Additionally, synthesis of highly reactive polyethers provides the means to conjugate such polymers with enzyme-labile peptide sequences necessary for system-responsive degradation. In the following chapter, functionalized polyols will be utilized to synthesize collagen-mimetic soft segments that will then be incorporated into cell-responsive, biodegradable polyureas. Because of the structural diversity of these polyols, a library of polyureas will be generated to gain a better understanding of intrinsic structure-property relationships and their relation to tissue remodeling. This will assist in the development of an optimal tissue engineered replacement for ACL reconstruction.

CHAPTER III

SYNTHESIS OF CELL-RESPONSIVE, BIODEGRADABLE POLYUREAS

3.1 Introduction

Throughout the literature, tissue engineers have modified biomaterial chemistry with targeted peptide sequences to modulate cell behavior.[194, 197, 212-216] In particular, collagenase-sensitive materials, including hydrogels and polyurethane elastomers, have been investigated for tissue engineering applications to provide system-responsive degradation; however, an enzyme-labile material suitable for ACL repair has yet to be developed.[145, 196, 217-230] In the previous section, synthetic routes were developed to functionalize ether-based polyols with favorable end groups for peptide coupling. This chapter will focus on the use of these functionalized, ether-based polyols to synthesize peptide-based soft segments, and subsequently, cell-responsive, biodegradable polyureas for potential use in ligament tissue engineering.

NHS-activated carboxylic acid derivatives from the previous step were first coupled to collagen-derived peptide sequences to form peptide-polyol-peptide triblocks, **Figure 3.1**. These triblocks were then end capped with NHS-activated carboxylic acid derivatives of the same polyol chemistry to form biodegradable multiblocks. By varying the chemistry and molecular weight of these polyols, a library of peptide-based soft segments was developed, **Table 3.1**.

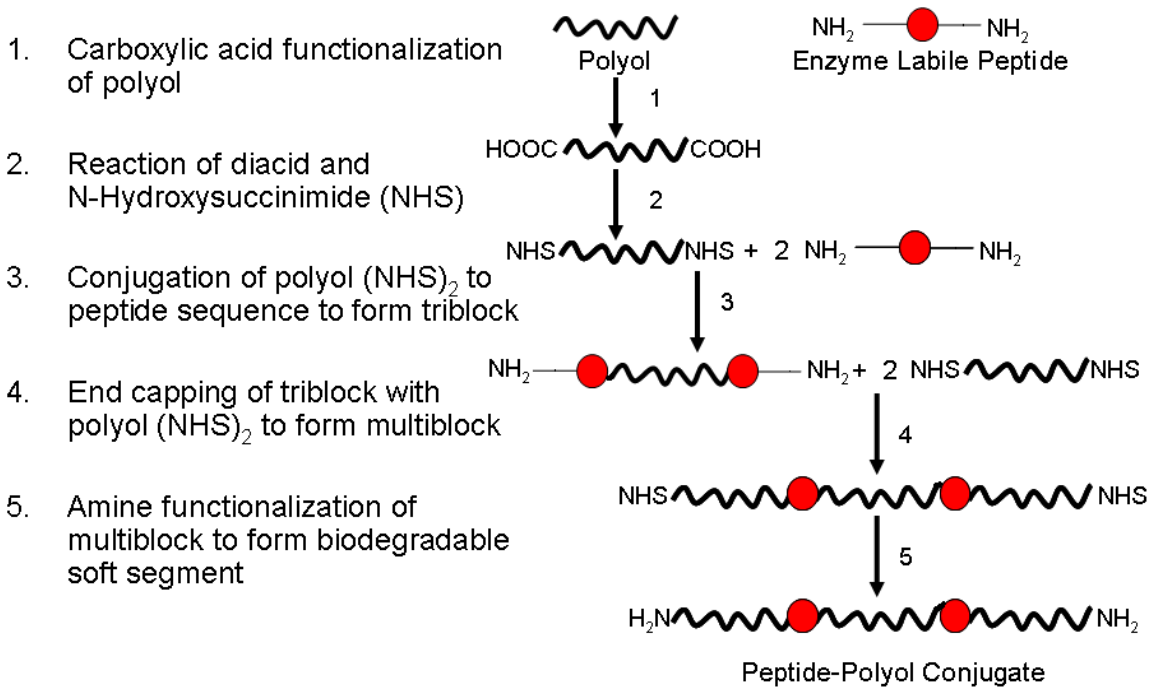

Figure 3.1. Synthetic design of peptide-based, soft segment multiblocks.

Table 3.1. Library of amine-functionalized, biodegradable soft segments

Polyol	Variable Polyurea Soft Segment
PTMG (1000)	H_2N ~~~ NH_2 H_2N ~~~ NH_2*
PEG (1000)	H_2N ~~~ NH_2 H_2N ~~~ NH_2*
PEG (2000)	H_2N ~~~ NH_2 H_2N ~~~ NH_2*

*** Polyol controls**

Following amine functionalization, multiblocks were reacted with aliphatic diisocyanates (HDI) and diamine chain extenders (EDA) to form linear polyurea elastomers, **Figure 3.2**. Amine-functionalized polyethers of similar molecular weight and chemistry as the peptide-polyol multiblocks were also implemented into polyurea design to serve as control soft segments. Along with soft segment chemistry and molecular weight, the hard to soft segment ratio was varied to produce a library of cell-responsive, biodegradable polyureas, **Table 3.2.** Two ratios of diisocyanate to soft segment to chain extender (3:1:2; 5:1:4) were selected to create hard segment weight fractions that range from 6-17%. Including polyol controls, the final library of polyureas consisted of twelve linear polyurea elastomers. This library should provide the necessary comparisons to isolate the effects of hard segment content, polyol chemistry, and soft segment molecular weight on performance properties. Understanding these structure-property relationships will enable rational design of an improved biomaterial scaffold for ligament tissue engineering.

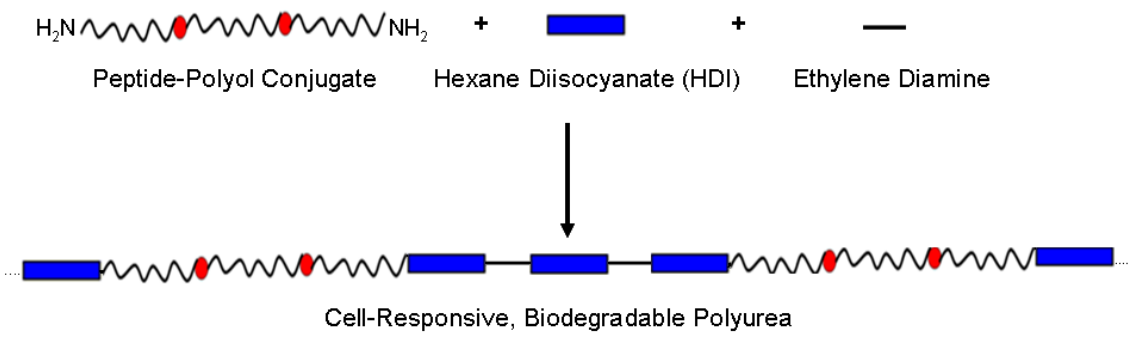

Figure 3.2. Synthetic design of cell-responsive, biodegradable polyureas.

Table 3.2. Library of collagen-mimetic polyureas

Soft Segment	DI:SS:CE	Cell-Responsive Biodegradable Polyurea
PTMG (1000) Multiblock	3 : 1 : 2	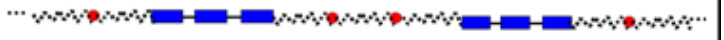
	5 : 1 : 4	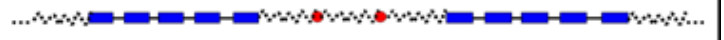
PEG (1000) Multiblock	3 : 1 : 2	
	5 : 1 : 4	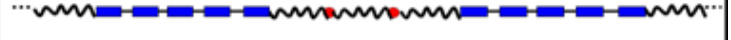
PEG (2000) Multiblock	3 : 1 : 2	
	5 : 1 : 4	

3.2 Synthesis of Enzyme-Labile, Ether-Based Soft Segments

In order to synthesize cell-responsive, biodegradable polyureas, a collagenase-sensitive peptide sequence (GPQGIWGQGK) with specificity to MMP-2 was coupled to NHS-activated carboxylic acid derivatives of PEG and PTMG to form peptide-polyol conjugates. Similar to amine functionalization, NHS ester reagents react with α-amines at the N-terminals of protein molecules, as well as ε-amines of lysine (K) side chains, to form stable amide bonds.[186] Reaction of NHS esters with protein molecules occurs at physiological pH, or under slightly basic conditions to accelerate coupling with primary amines, and so peptide-polyol conjugation is typically performed in buffered solution.[191, 196, 197, 199, 219, 226] Even so, the use of buffered media is limited by the potential for hydrolysis of NHS esters, which results in a loss of reactivity.

In this study, enzyme-labile peptide sequences were used to end cap NHS-activated PEG and PTMG diacids to form peptide-polyol-peptide triblocks. The

sequence GPQGIWGQG was selected because it is degraded by several MMPs, including MMP-2, and it has been reported to be the most rapidly degradable sequence among GPQGIXGQG (X = arbitrary amino acid) motifs.[219, 231] Preliminary studies revealed that the hydrolytic rate of degradation of NHS ester groups linked to PEG and PTMG diacids was too rapid for effective peptide coupling. As a result, peptide conjugation was conducted in an organic solvent in the presence of DMAp and Et_3N. For such a reaction, an excess of peptide is typically used to ensure both ends of the target molecule react with free amine-terminated compounds; however, the high cost of synthesizing the biodegradable peptide sequence limits its availability.[209] Instead, lysine was incorporated into the peptide sequence, GPQGIWGQGK, to create a bifunctional polymer. This enables polymer stoichiometry to dictate peptide-polyol conjugation, which promotes effective end capping. Following triblock synthesis, terminal amine groups generated from conjugation to the peptide sequence were further coupled to NHS-activated, ether-based carboxylic acid derivatives to form peptide-polyol multiblocks. These multiblocks were then reacted with EDA to form amine-functionalized, biodegradable soft segments.

3.2.1 Materials

NHS-activated PEG and PTMG diacids were prepared as previously described. 4-(Dimethylamino) pyridine (DMAp), triethylamine (Et_3N), ethylene diamine (EDA), dimethylformamide (DMF), and deuterated dimethyl sulfoxide (d_6-DMSO) were obtained from Sigma-Aldrich and used as received. The biodegradable peptide sequence (GPQGIWGQGK) was synthesized at the Baylor Protein Chemistry Core Laboratory

where it was generated on an ABI 433A solid-phase synthesizer and analyzed by reverse phase HPLC and mass spectroscopy. Once received, peptide sequences were stored at -80°C and then lyophilized prior to use. The Kaiser test kit was obtained from Fluka Chemical.

3.2.2 Methods

PEG and PTMG triblocks were prepared by nucleophilic substitution of NHS-activated diacids with primary amine groups of bifunctional peptide sequences in the presence of DMAp and Et_3N, **Figure 3.3.** NHS-activated PEG or PTMG diacids were dissolved in DMF and then added drop wise to a solution of DMAp, Et_3N, and the biodegradable peptide sequence while stirring. After addition, the mixture was stirred at room temperature under nitrogen until NHS ester groups were no longer reactive (FTIR samples were taken periodically to monitor absorption peaks indicative of NHS activation). Solutions were then diluted with distilled water and peptide-polyol conjugates were retrieved with ultrafiltration through a solvent-resistant stirred cell. Molecular weight retention of ultrafiltration membranes was ~1000 g/mol. PEG and PTMG-based triblocks were then re-dissolved with distilled water, stored at -80°C, and subsequently lyophilized for characterization.

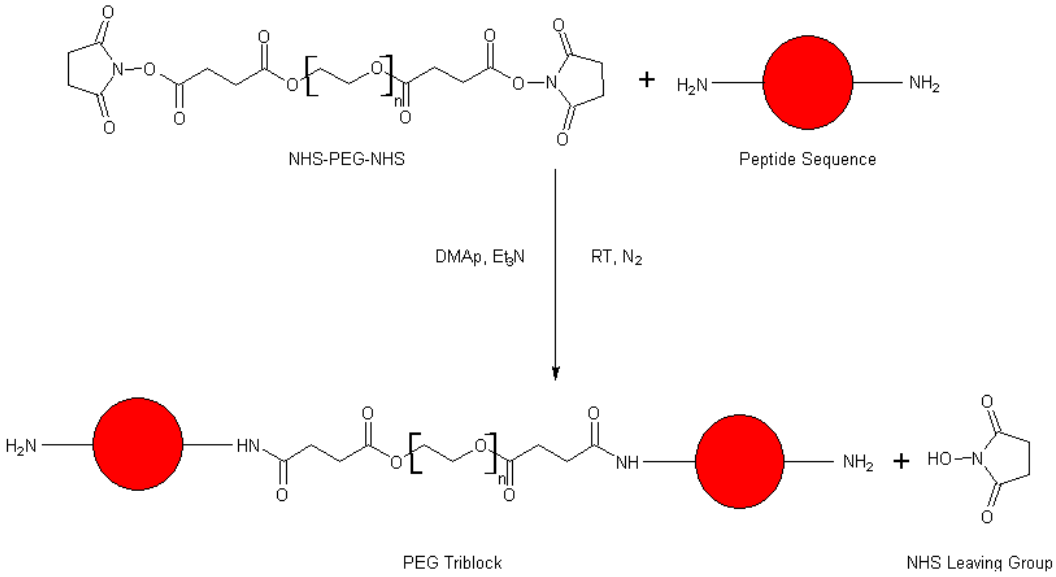

Figure 3.3. Synthesis of PEG triblocks in the presence of DMAp and Et_3N.

Upon successful conjugation, terminal amine groups of PEG and PTMG-based triblocks were reacted with NHS-activated carboxylic acid derivatives to form peptide-polyol multiblocks. PEG or PTMG triblocks were first dissolved in DMF and then added drop wise to a solution of DMAp, Et_3N, and their respective NHS-activated carboxylic acid derivative while stirring. After addition, the mixture was stirred at room temperature under nitrogen until NHS ester groups remained stable (FTIR samples were taken periodically to monitor absorption peaks indicative of NHS activation). Excess EDA was then added to the solution to functionalize multiblocks with primary amine end groups, **Figure 3.4**. Solutions were then diluted with distilled water and peptide-polyol conjugates were retrieved with ultrafiltration through a solvent-resistant stirred cell. PEG and PTMG-based multiblocks were then re-dissolved with distilled water, stored at -80°C, and subsequently lyophilized for characterization. Infrared

spectroscopic analysis was performed on a Bruker TENSOR 27 spectrometer to confirm peptide conjugation. A Kaiser test kit was used to verify the presence of free primary amine groups, as indicated by a color shift from yellow to a dark blue/purple hue. ^{1}H-NMR spectroscopy was also used to verify peptide conjugation, but due to low concentrations of peptide-polyol conjugates, it could not be used to quantify conjugation.

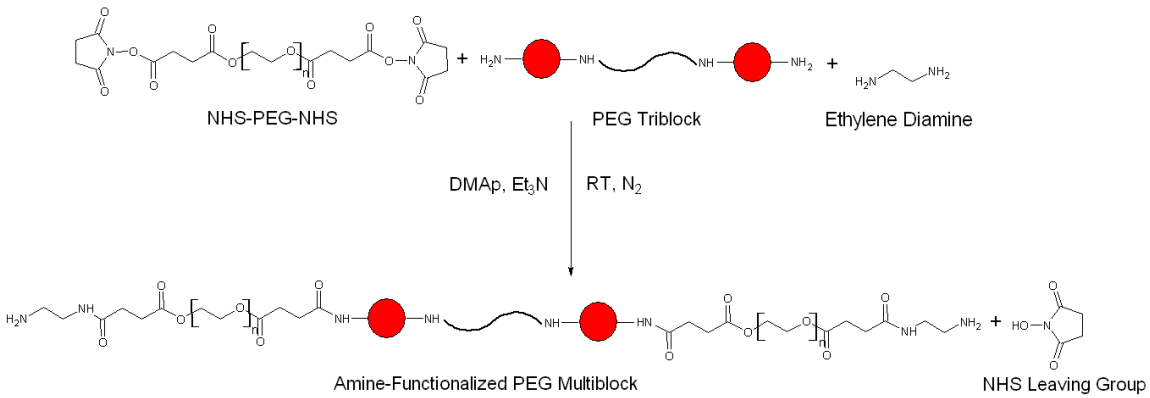

Figure 3.4. Synthesis of amine-functionalized PEG multiblocks.

3.2.3 Results

Synthesis of PEG (1000) triblock

NHS-PEG (1000)-NHS (7.76 mg, 0.0056 mmol), peptide (11.5 mg, 0.0117 mmol), DMAp (2.72 mg, 0.0223 mmol), and Et_3N (3.41 µL, 0.0245 mmol) were reacted as previously described. In this way, PEG (1000) triblock was obtained as a white powder (2.32 mg, 13% yield). Successful conjugation was confirmed with FTIR spectroscopy based on the generation of a significant amide peak (1660 cm^{-1}, C=O) indicative of the peptide backbone, **Figure 3.5.** In addition, the carbonyl peak at 1730

cm^{-1} attenuated due to the loss of carboxylic acid groups. The Ninhydrin assay turned purple, indicating free amine groups are present. ^{1}H-NMR (δ, ppm): 0.6-0.9 (12H, -CH_3), 1.5-2.1 (12H, -CH_2-), 1.7-1.9 (2H, -CH-), 1.7-2.3 (24H, -CH_2CH-), 2.1-2.7 (16H, -CH_2CO-), 2.9-3.1 (4H, -CH_2NHCO-), 3.64 (m, 85H, -CH_2O-), 3.6-3.9 (16H, -NHCH_2CO-), 4.1-4.3 (4H, -NCH_2-), 4.1-4.6 (10H, -NHCH-), 4.2-4.4 (4H, -CH_2OCO-), 4.4-4.6 (2H, -NCH-), 6.7-6.9 (8H, NH_2CO-), 6.9-7.4 (10H, =CH-), 7.1-8.5 (18H, -NHCO-), 9.3-9.5 (2H, -NH-).

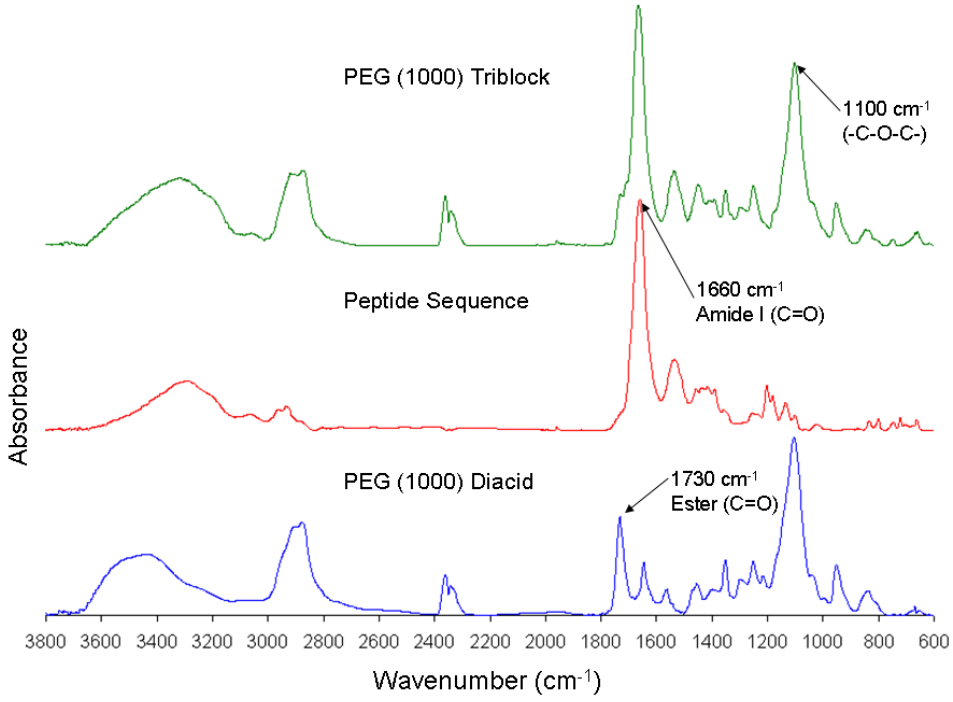

Figure 3.5. FTIR spectra of PEG (1000) triblock synthesis.

Synthesis of PEG (2000) triblock

NHS-PEG (2000)-NHS (13.32 mg, 0.0056 mmol), peptide (11.5 mg, 0.0117 mmol), DMAp (1.36 mg, 0.0111 mmol), and Et_3N (1.71 µL, 0.0122 mmol) were reacted

as previously described. In this way, PEG (2000) triblock was obtained as a yellow powder (11.25 mg, 49% yield). Successful conjugation was confirmed with FTIR spectroscopy based on the generation of a significant amide peak (1662 cm^{-1}, C=O) indicative of the peptide backbone, **Figure 3.6.** In addition, the carbonyl peak at 1730 cm^{-1} attenuated due to the loss of carboxylic acid groups. The Ninhydrin assay turned purple, indicating free amine groups are present. ^{1}H-NMR (δ, ppm): 0.6-0.9 (12H, -C*H*$_3$), 1.5-2.1 (12H, -C*H*$_2$-), 1.7-1.9 (2H, -C*H*-), 1.7-2.3 (24H, -C*H*$_2$CH-), 2.1-2.7 (16H, -C*H*$_2$CO-), 2.9-3.1 (4H, -C*H*$_2$NHCO-), 3.64 (m, 176H, -C*H*$_2$O-), 3.6-3.9 (16H, -NHC*H*$_2$CO-), 4.1-4.3 (4H, -NC*H*$_2$-), 4.1-4.6 (10H, -NHC*H*-), 4.2-4.4 (4H, -C*H*$_2$OCO-), 4.4-4.6 (2H, -NC*H*-), 6.7-6.9 (8H, N*H*$_2$CO-), 6.9-7.4 (10H, =C*H*-), 7.1-8.5 (18H, -N*H*CO-), 9.3-9.5 (2H, -N*H*-).

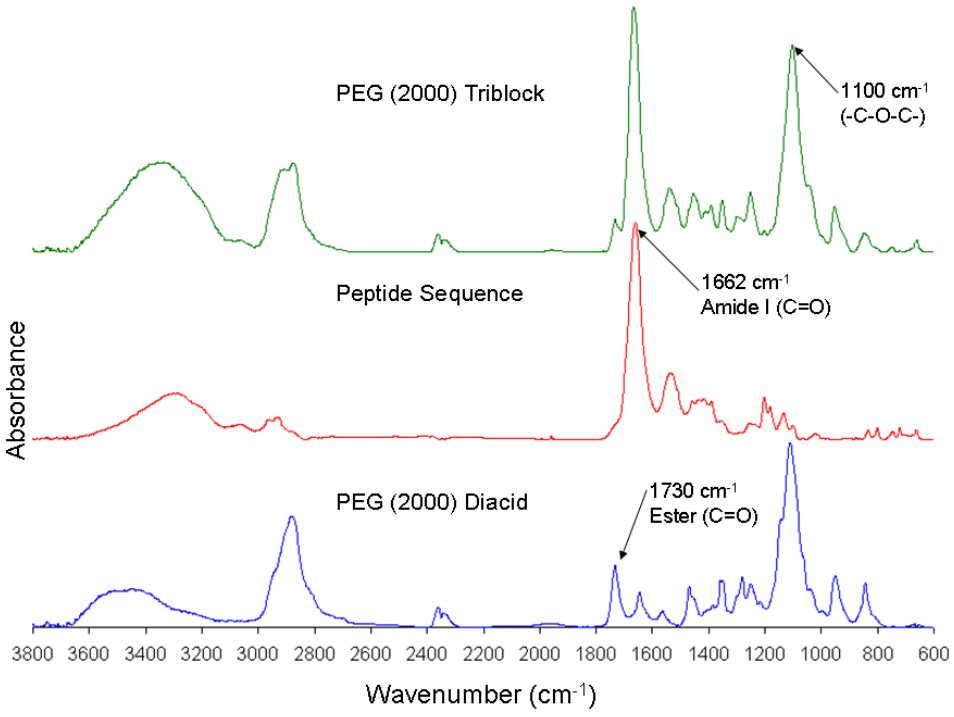

Figure 3.6. FTIR spectra of PEG (2000) triblock synthesis.

Synthesis of PTMG (1000) triblock

NHS-PTMG (1000)-NHS (7.76 mg, 0.0056 mmol), peptide (11.5 mg, 0.0117 mmol), DMAp (5.44 mg, 0.0445 mmol), and Et_3N (6.82 µL, 0.0490 mmol) were reacted as previously described. In this way, PTMG (1000) triblock was obtained as a white powder (2.22 mg, 13% yield). Successful conjugation was confirmed with FTIR spectroscopy based on the generation of a significant amide peak (1658 cm^{-1}, C=O) indicative of the peptide backbone, **Figure 3.7.** In addition, the carbonyl peak at 1735 cm^{-1} attenuated due to the loss of carboxylic acid groups. The Ninhydrin assay turned purple, indicating free amine groups are present. ^{1}H-NMR (δ, ppm): 0.6-0.9 (12H, -C*H*$_3$), 1.5-2.1 (67H, -C*H*$_2$-), 1.7-1.9 (2H, -C*H*-), 1.7-2.3 (24H, -C*H*$_2$CH-), 2.1-2.7 (16H, -C*H*$_2$CO-), 2.9-3.1 (4H, -C*H*$_2$NHCO-), 3.41 (m, 51H, -C*H*$_2$O-), 3.6-3.9 (16H, -NHC*H*$_2$CO-), 4.0-4.2 (4H, -C*H*$_2$OCO-), 4.1-4.3 (4H, -NC*H*$_2$-), 4.1-4.6 (10H, -NHC*H*-), 4.4-4.6 (2H, -NC*H*-), 6.7-6.9 (8H, N*H*$_2$CO-), 6.9-7.4 (10H, =C*H*-), 7.1-8.5 (18H, -N*H*CO-), 9.3-9.5 (2H, -N*H*-).

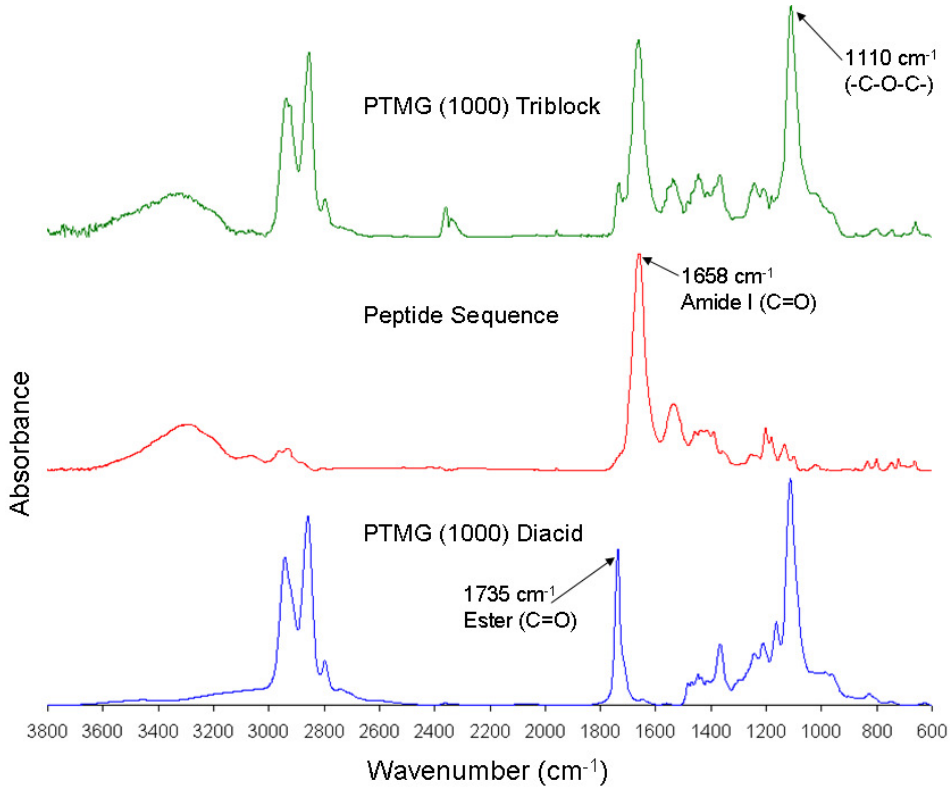

Figure 3.7. FTIR spectra of PTMG (1000) triblock synthesis.

Synthesis of PEG (1000) multiblock

PEG (1000) triblock (1.5 mg, 0.000479 mmol), NHS-PEG (1000)-NHS (1.4 mg, 0.001005 mmol), DMAp (0.47 mg, 0.00383 mmol), Et_3N (0.59 µL, 0.00421 mmol), and EDA (0.19 µL, 0.00287 mmol) were reacted as previously described. In this way, PEG (1000) multiblock was obtained as a clear solid (0.51 mg, 19% yield). Successful conjugation was confirmed with FTIR spectroscopy based on the shift in the relative heights of amide (1531 cm^{-1}, C-N) and ether (1100 cm^{-1}, -C-O-C-) peaks, **Figure 3.8** The Ninhydrin assay turned blue, indicating free amine groups are present.

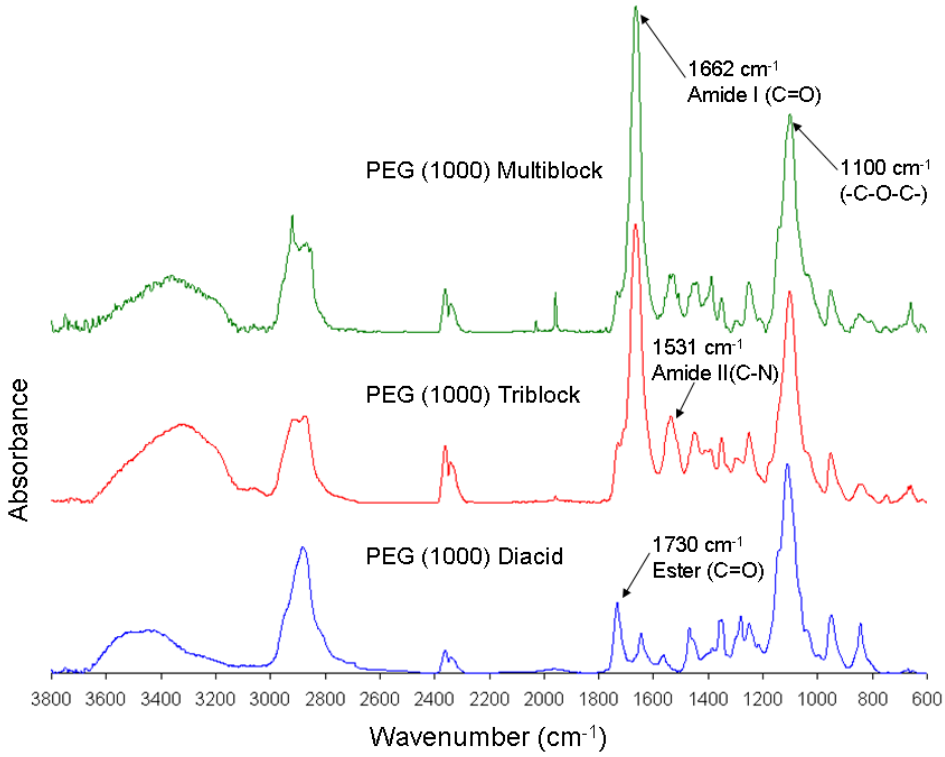

Figure 3.8. FTIR spectra of amine-functionalized PEG (1000) multiblock synthesis.

Synthesis of PEG (2000) multiblock

PEG (2000) triblock (5.8 mg, 0.0014 mmol), NHS-PEG (2000)-NHS (7.05 mg, 0.0029 mmol), DMAp (1.37 mg, 0.0112 mmol), Et_3N (1.72 µL, 0.0123 mmol), and EDA (0.56 µL, 0.008 mmol) were reacted as previously described. In this way, PEG (2000) multiblock was obtained as a white powder (5.47 mg, 46% yield). Successful conjugation was confirmed with FTIR spectroscopy based on the shift in the relative heights of amide (1531 cm^{-1}, C-N) and ether (1100 cm^{-1}, -C-O-C-) peaks, **Figure 3.9.** The Ninhydrin assay turned blue, indicating free amine groups are present.

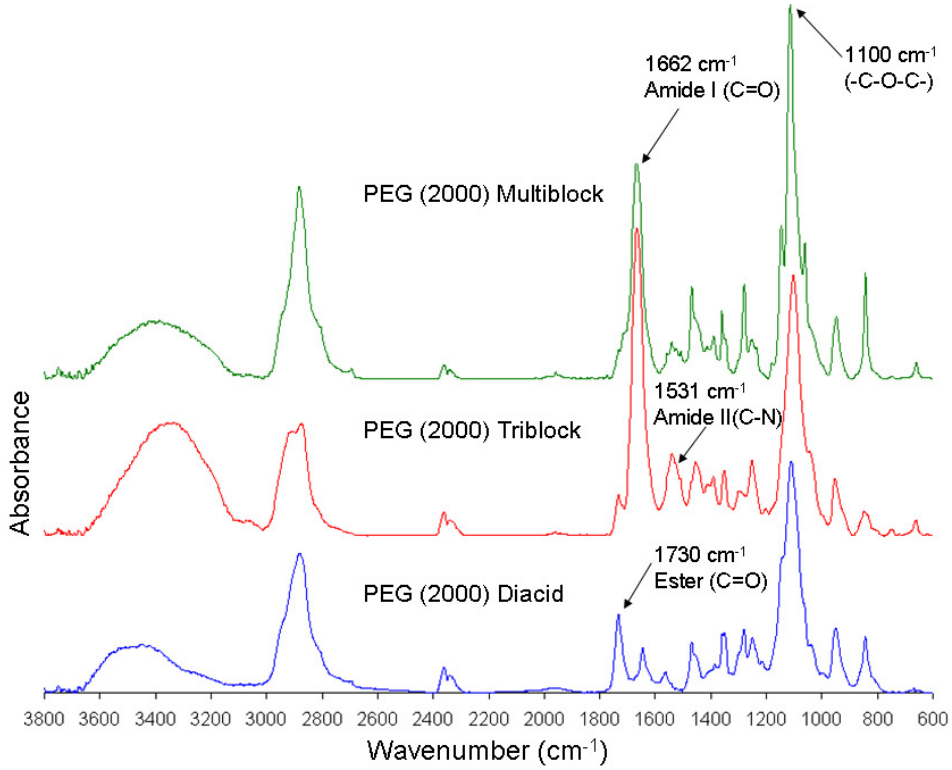

Figure 3.9. FTIR spectra of amine-functionalized PEG (2000) multiblock synthesis.

Synthesis of PTMG (1000) multiblock

PTMG (1000) triblock (0.85 mg, 0.00027 mmol), NHS-PTMG (1000)-NHS (0.79 mg, 0.00057 mmol), DMAp (0.27 mg, 0.00217 mmol), Et_3N (0.33 µL, 0.00239 mmol), and EDA (0.109 µL, 0.00163 mmol) were reacted as previously described. In this way, PTMG (1000) multiblock was obtained as a white powder (0.46 mg, 30% yield). Successful conjugation was confirmed with FTIR spectroscopy based on the shift in the relative heights of amide (1529 cm^{-1}, C-N) and ether (1110 cm^{-1}, -C-O-C-) peaks, **Figure 3.10** The Ninhydrin assay turned blue, indicating free amine groups are present.

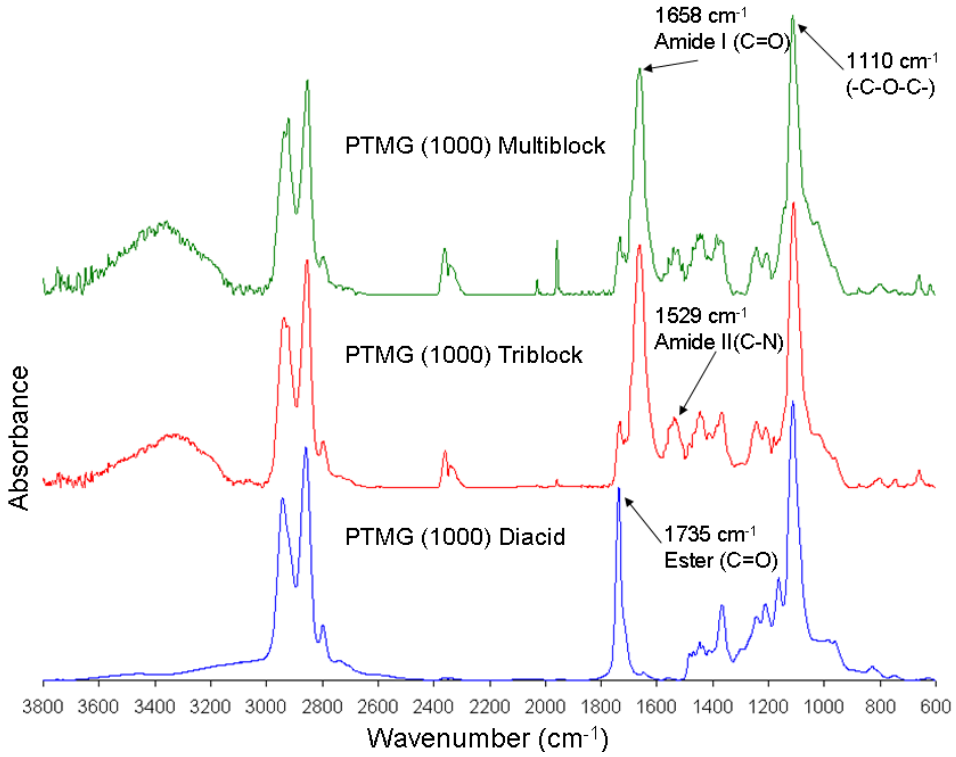

Figure 3.10. FTIR spectra of amine-functionalized PTMG (1000) multiblock synthesis.

The results of FTIR and NMR analysis revealed that all polyols were successfully conjugated to biodegradable peptide sequences, as indicated by the generation of significant amide peaks. Due to such low concentrations of peptide-polyol conjugates, as well as hydrogen bonding, quantitative analysis could not be performed with NMR spectroscopy; however, changes in the relative absorbance of specific peaks between FTIR spectra can be used to provide a qualitative measure of conjugation. For this study, the absorbance at 1730 cm^{-1} indicating the presence of carboxylic acid and ester groups was investigated for triblock syntheses. With limited conjugation, this absorbance peak should be of similar height to what it was in the spectrum for its respective diacid. As conjugation increases, this peak should attenuate until the

remaining contributions are solely from the presence of ester linkages. For all peptide-polyol-triblocks, this peak was reduced by approximately 50%, indicating significant conjugation. For multiblock syntheses, the relative ratio of amide peaks with respect to internal reference ether peaks was examined. A reduction in the relative height of the amide peak at 1531 cm^{-1} by roughly 50% was observed for all polymer samples, indicating successful multiblock formation.

3.3 Polyurea Synthesis

Following synthesis of ether-based soft segments, terminal amine groups generated by functionalization with EDA can react with free isocyanate groups to form stable urea linkages. Similar to polyurethanes, polyurea synthesis is a step-growth polymerization in which bifunctional molecules react to produce a linear chain of monomers.[106] Polyureas can be synthesized via a "one-step" process, in which all reagents are mixed at once, or a multistep synthesis. Segmented block copolymers are typically generated using a two step synthesis, referred to as the prepolymer method. In the first step, the soft segment is stirred with excess diisocyanate to form a prepolymer. The prepolymer is then chain extended with a low molecular weight diol or diamine to increase molecular weight and form a block copolymer. This method imparts greater control over the chemistry of the reaction, influencing the structure, physical properties, and processability of the final product.[106]

Because of these advantages, the two-step method is the favored strategy to synthesize segmented block copolymers for biomedical applications. For polyurethane syntheses, soft segment diols are typically added drop wise to excess diisocyanate in the

presence of an organo-tin catalyst and at elevated temperature.[136, 141, 232-238] Shortly thereafter, the chain extender is added to the mixture, and FTIR spectroscopy is used to monitor the presence of free isocyanate groups to verify full polymerization. Because of the relatively high NCO-reactivity of primary amines compared to secondary hydroxyl groups, polyurea formation can predominate at room temperature in non-catalyzed systems.[136, 234, 239, 240] The exceptionally high reactivity of primary amine groups also limits side reactions with water that affect the desired chemistry of the final product. A limitation of polyurea synthesis is the risk of biuret formation, in which secondary amine groups of urea linkages react with free isocyanate groups, effectively cross-linking the polymer. To prevent this, polyurea synthesis can be run at lower temperature to inhibit biuret formation. Overall, urea-based segmented block copolymers were selected for this application due to their relative ease of synthesis and because polyureas demonstrate higher mechanical properties than polyurethanes due to bidentate hydrogen bonding of urea linkages. This is especially important for the development of a biomaterial for ligament tissue engineering.[128]

3.3.1 Materials

Amine-functionalized soft segments were prepared as previously described and dried 24 hours at 80°C under vacuum prior to use. Hexamethylene diisocyanate (HDI) was obtained from Fluka Analytical and used as received. Ethylene diamine (EDA) and diethyl ether were obtained from Sigma-Aldrich and used as received. Dimethylacetamide (DMAc) was obtained from Sigma-Aldrich and dried over 4Å molecular sieves 24 hours prior to use.

3.3.2 Methods

In the current study, amine-functionalized multiblocks and ether-based control soft segments were reacted with excess HDI and EDA to develop a series of linear polyurea elastomers, **Figure 3.11**. All polymerizations were carried out in a Labconco Controlled Atmosphere glove box containing dry nitrogen gas. Soft segments were first dissolved in DMAc and then added drop wise to an HDI solution while stirring. After 30 minutes, EDA solution was added and the mixture was stirred at room temperature. The reaction was allowed to proceed until the NCO peak (~2270 cm^{-1}) disappeared in the IR spectrum. For PEG and PTMG control polyurea syntheses, final products were precipitated for ten minutes from excess diethyl ether or aqueous KCL solution (10:1) that had been cooled in a salt ice bath. PEG and PTMG-based polyureas were then retrieved with vacuum aspiration and subsequently dried in a vacuum oven overnight. Peptide-based polyurea solutions were diluted with distilled water and then retrieved via ultrafiltration through a solvent-resistant stirred cell. Resulting peptide-based polyureas were then re-dissolved with distilled water, stored at -80°C, and subsequently lyophilized for characterization. Infrared spectroscopic analysis was performed on a Bruker TENSOR 27 spectrometer to confirm urea formation.

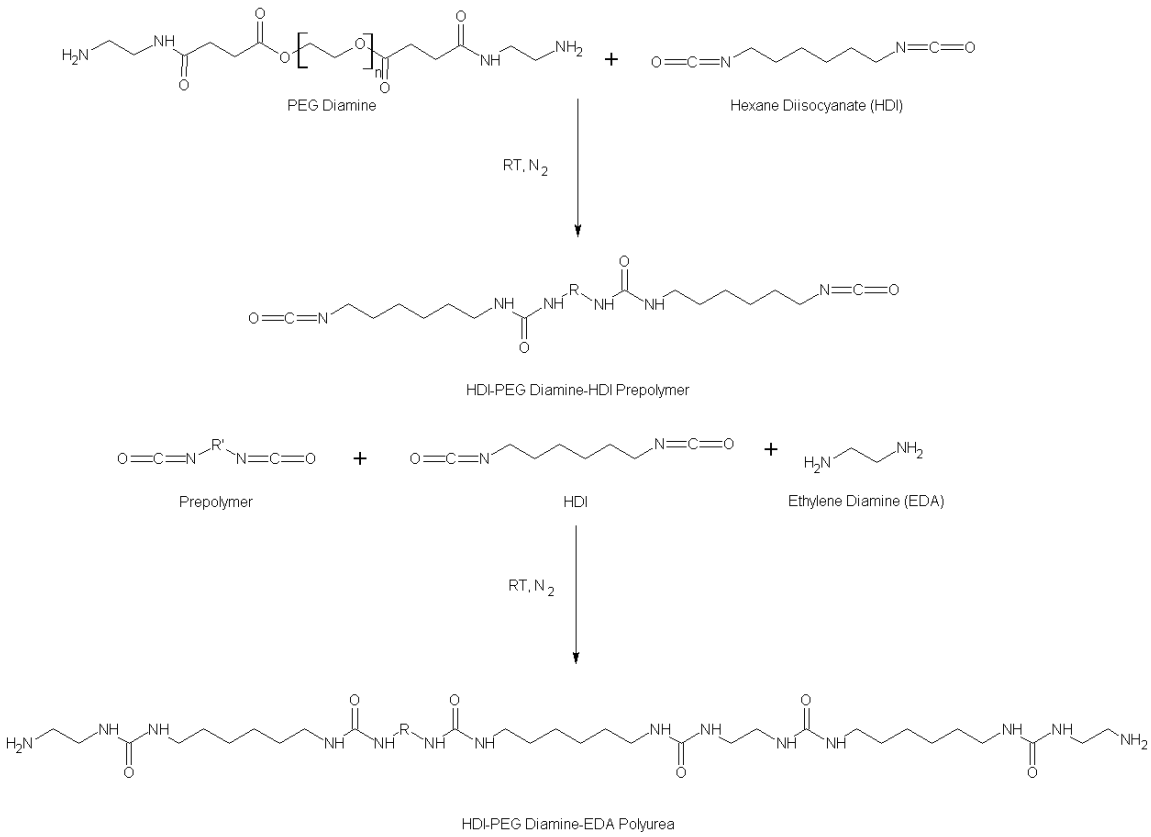

Figure 3.11. Synthesis of ether-based polyureas using PEG diamine.

3.3.3 Results

Synthesis of PEG (6000) control polyureas

3 – 1 – 2: PEG (6000) diamine (0.23 g, 0.0366 mmol), HDI (18.22 µL, 0.1134 mmol), and EDA (4.90 µL, 0.0732 mmol) were reacted as previously described. In this way, PEG (6000) polyurea (3-1-2) was obtained as a brittle, white solid (0.19 g, 76% yield). 5 – 1 – 4: PEG (6000) diamine (0.50 g, 0.0795 mmol), HDI (65.17 µL, 0.4056 mmol), and EDA (21.32 µL, 0.3182 mmol) were reacted as previously described. In this way, PEG (6000) polyurea (5-1-4) was obtained as a flaky, clear solid (0.48 g, 82%

yield). Urea formation (1632 cm^{-1}, hydrogen-bonded C=O; 3320 cm^{-1}, hydrogen-bonded N-H) was confirmed with FTIR spectroscopy, **Figure 3.12**.

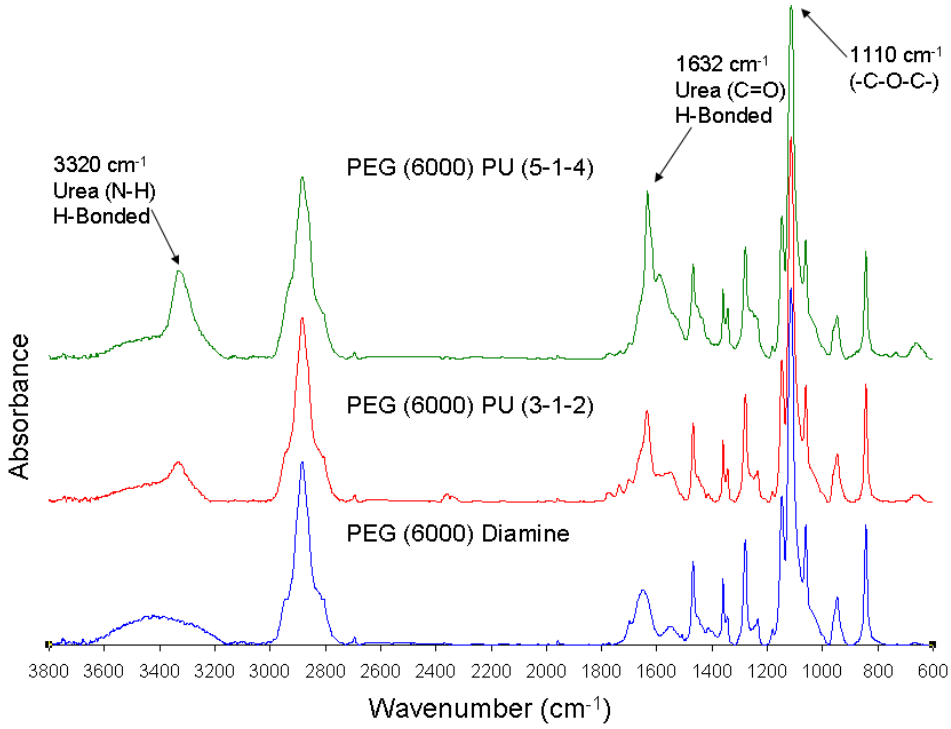

Figure 3.12. FTIR spectral comparison of PEG (6000) control polyureas.

Synthesis of PEG (10000) control polyureas

3 – 1 – 2: PEG (10000) diamine (0.10 g, 0.0097 mmol), HDI (4.84 µL, 0.0301 mmol), and EDA (1.303 µL, 0.0194 mmol) were reacted as previously described. In this way, PEG (10000) polyurea (3-1-2) was obtained as a white powder (57.4 mg, 54% yield). 5 – 1 – 4: PEG (10000) diamine (0.11 g, 0.0107 mmol), HDI (8.76 µL, 0.0545 mmol), and EDA (2.87 µL, 0.0428 mmol) were reacted as previously described. In this way, PEG (10000) polyurea (5-1-4) was obtained as a white powder (77.9 mg, 64%

yield). Urea formation (1632 cm^{-1}, hydrogen-bonded C=O; 3320 cm^{-1}, hydrogen-bonded N-H) was confirmed with FTIR spectroscopy, **Figure 3.13**.

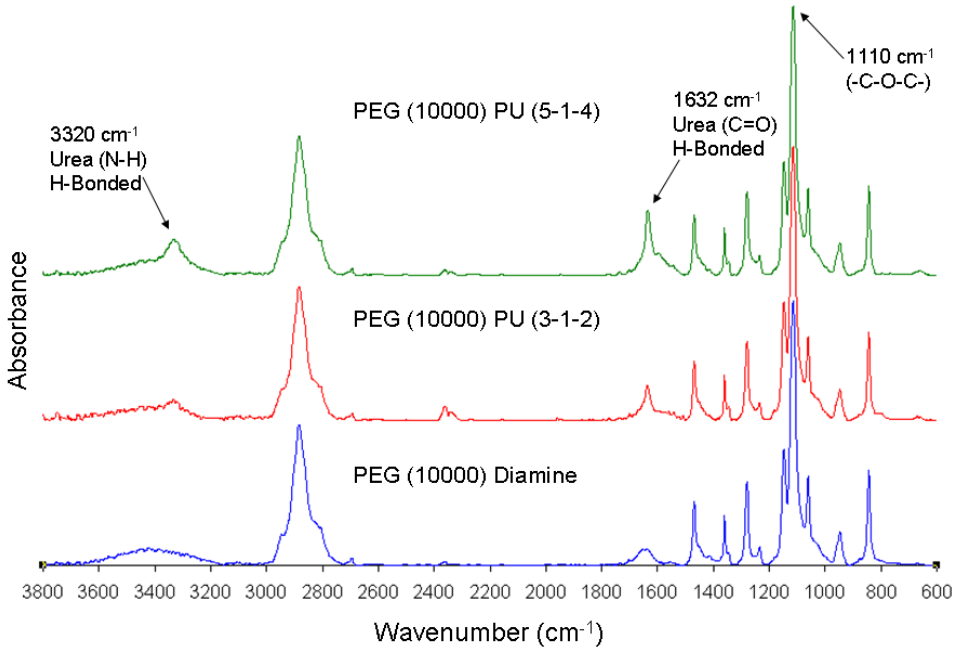

Figure 3.13. FTIR spectral comparison of PEG (10000) control polyureas.

Synthesis of PTMG (5600) control polyureas

3 – 1 – 2: PTMG (5600) diamine (0.10 g, 0.0177 mmol), HDI (8.83 µL, 0.055 mmol), and EDA (2.38 µL, 0.0355 mmol) were reacted as previously described. In this way, PTMG (5600) polyurea (3-1-2) was obtained as a yellow, waxy solid (74.6 mg, 67% yield). 5 – 1 – 4: PTMG (5600) diamine (0.10 g, 0.0177 mmol), HDI (14.53 µL, 0.0904 mmol), and EDA (4.75 µL, 0.071 mmol) were reacted as previously described. In this way, PTMG (5600) polyurea (5-1-4) was obtained as a yellow, waxy solid (88.4 mg, 74% yield). Urea formation (1701 cm^{-1}, free C=O; 1633 cm^{-1}, hydrogen-bonded

C=O; 3328 cm^{-1}, hydrogen-bonded N-H) was confirmed with FTIR spectroscopy, **Figure 3.14**.

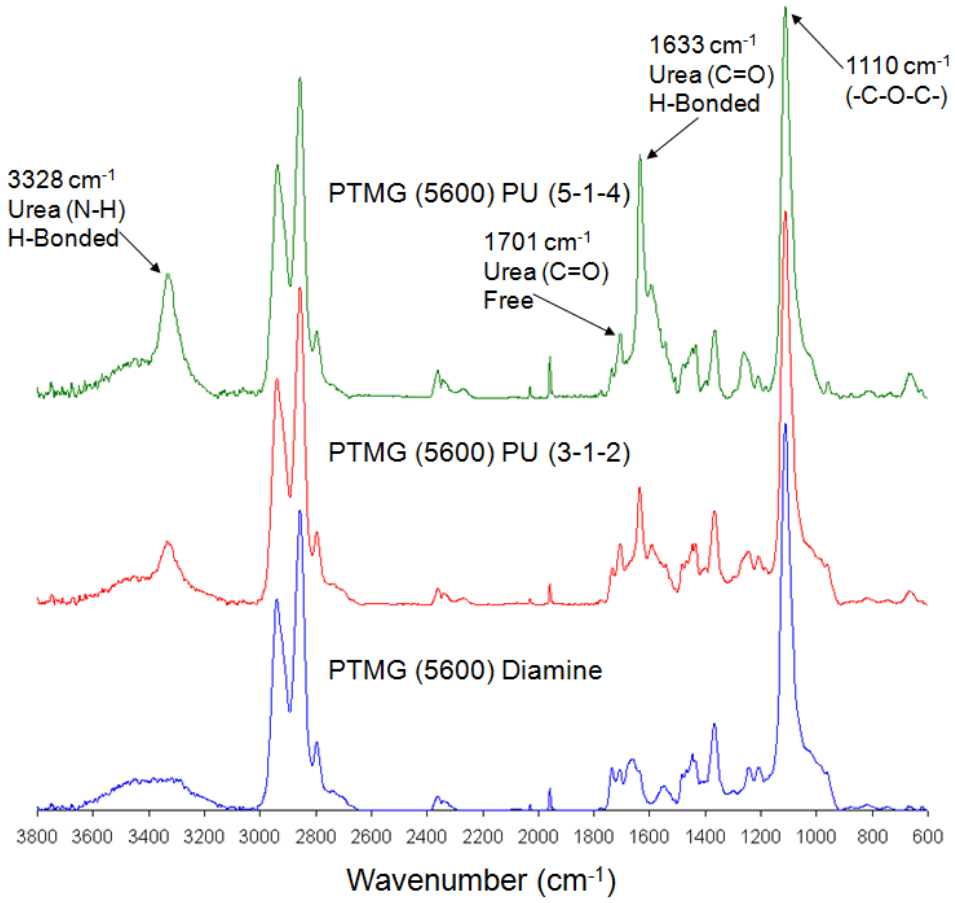

Figure 3.14. FTIR spectral comparison of PTMG (5600) control polyureas.

Synthesis of PEG (1000) multiblock polyureas

3 – 1 – 2: PEG (1000) multiblock (0.20 mg, 0.0358 µmol), HDI (0.0178 µL, 0.1109 µmol), and EDA (0.0048 µL, 0.0716 µmol) were reacted as previously described. 5 – 1 – 4: PEG (1000) multiblock (0.20 mg, 0.0358 µmol), HDI (0.0293 µL, 0.1825 µmol), and EDA (0.0096 µL, 0.1432 µmol) were reacted as previously

described. Urea formation (1691 cm^{-1}, free C=O; 1635 cm^{-1}, hydrogen-bonded C=O; 3328 cm^{-1}, hydrogen-bonded N-H) was confirmed with FTIR spectroscopy, **Figure 3.15**.

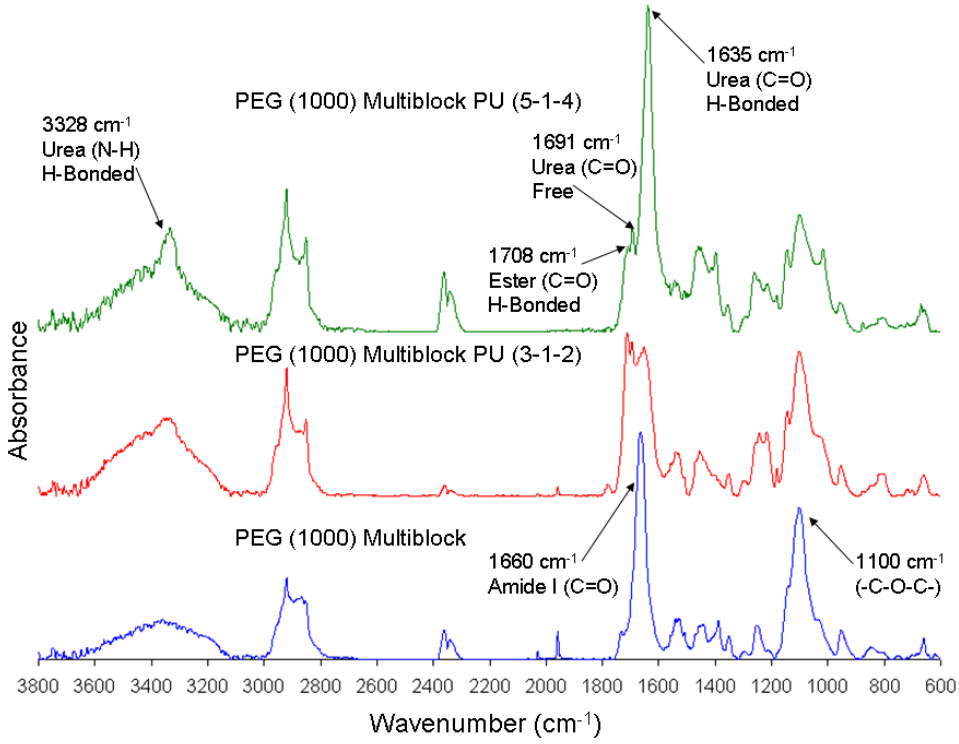

Figure 3.15. FTIR spectral comparison of PEG (1000) multiblock polyureas.

Synthesis of PEG (2000) multiblock polyureas

3 – 1 – 2: PEG (2000) multiblock (1.0 mg, 0.116 µmol), HDI (0.058 µL, 0.361 µmol), and EDA (0.0156 µL, 0.233 µmol) were reacted as previously described. 5 – 1 – 4: PEG (2000) multiblock (1.0 mg, 0.116 µmol), HDI (0.095 µL, 0.594 µmol), and EDA (0.0312 µL, 0.466 µmol) were reacted as previously described. Urea formation (1635 cm^{-1}, hydrogen-bonded C=O; 3327 cm^{-1}, hydrogen-bonded N-H) was confirmed with FTIR spectroscopy, **Figure 3.16**.

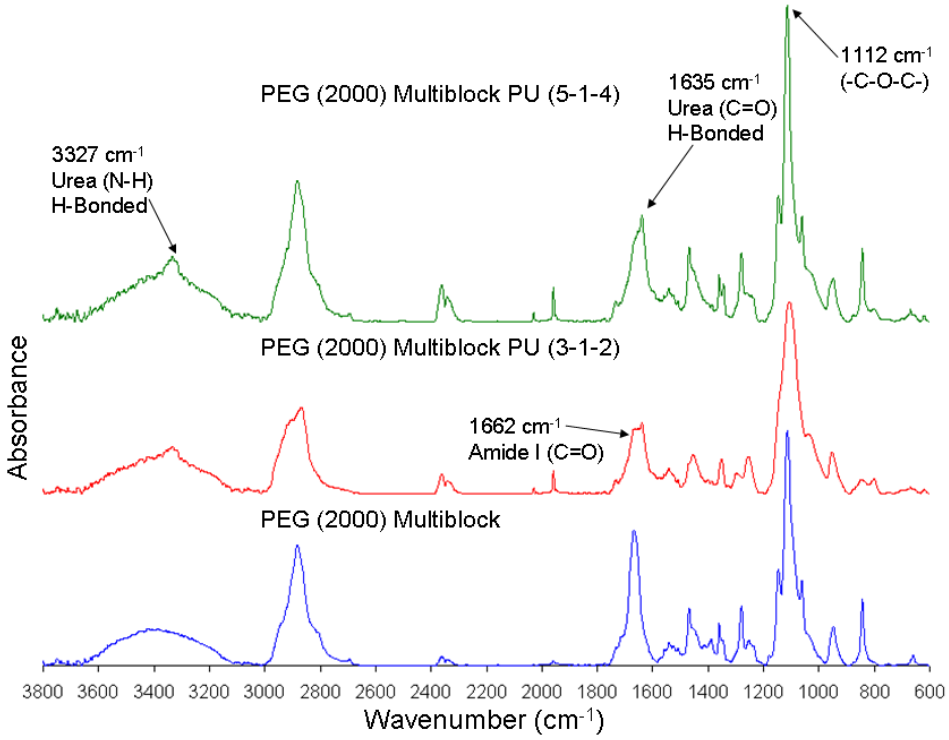

Figure 3.16. FTIR spectral comparison of PEG (2000) multiblock polyureas.

Synthesis of PTMG (1000) multiblock polyureas

3 – 1 – 2: PTMG (1000) multiblock (0.18 mg, 0.0322 µmol), HDI (0.016 µL, 0.1 µmol), and EDA (0.0043 µL, 0.0644 µmol) were reacted as previously described. 5 – 1 – 4: PTMG (1000) multiblock (0.18 mg, 0.0322 µmol), HDI (0.0264 µL, 0.164 µmol), and EDA (0.0086 µL, 0.129 µmol) were reacted as previously described. Urea formation (1689 cm^{-1}, free C=O; 1635 cm^{-1}, hydrogen-bonded C=O; 3328 cm^{-1}, hydrogen-bonded N-H) was confirmed with FTIR spectroscopy, **Figure 3.17**.

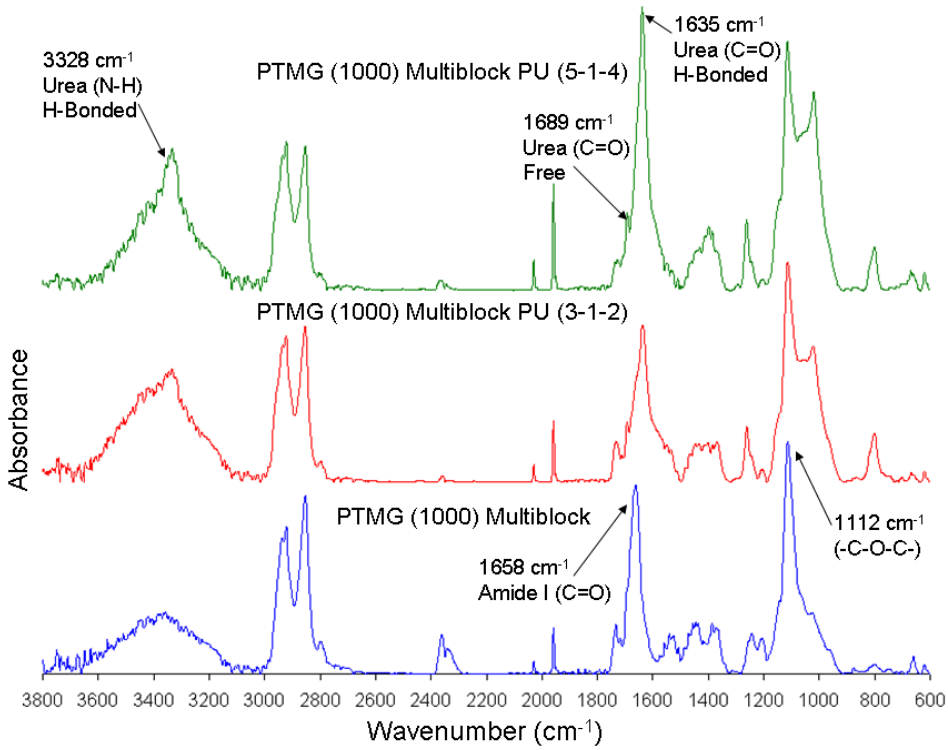

Figure 3.17. FTIR spectral comparison of PTMG (1000) multiblock polyureas.

FTIR spectral analysis revealed the presence of characteristic urea peaks (~1630 cm^{-1}, hydrogen-bonded C=O; ~1690 cm^{-1}, free C=O; ~3328 cm^{-1}, hydrogen-bonded N-H) among all polymer samples. FTIR spectra of PEG-based control polyureas predominantly consisted of hydrogen-bonded urea peaks, indicating a relatively high degree of phase separation. PTMG-based control polyureas also demonstrated a significant amount of hydrogen-bonded urea peaks, although free carbonyl peaks were also observed. The relative height of these peaks, with respect to the internal reference ether peak, is proportional to the hard segment content. Therefore, these peaks are elevated at higher hard to soft segment ratios. This trend was observed in the FTIR spectra for all control and multiblock polyureas. Similar to PEG-based control

polyureas, FTIR spectra of PEG (2000) multiblock polyureas revealed the presence of hydrogen-bonded urea peaks that were elevated at higher hard to soft segment ratios. The FTIR spectrum for PEG (1000) multiblock polyurea (5-1-4) also demonstrated considerable hydrogen-bonded urea formation, although free carbonyl peaks were detected. This free carbonyl peak was expressed more significantly in the FTIR spectrum for PEG (1000) multiblock polyurea (3-1-2), indicating a degree of phase mixing. Finally, similar to PTMG-based control polyureas, the FTIR spectra for PTMG (1000) multiblock polyureas predominantly consisted of hydrogen-bonded urea peaks**,** although free carbonyl peaks were also observed.

3.4 Conclusions

Integration of biomimetic peptide sequences into the design of novel biomaterials is a useful strategy to achieve desired cell behavior. In the current study, synthetic routes were developed to conjugate collagenase-sensitive peptide sequences to ether-based polyols to form biodegradable multiblocks. Successful protein conjugation of all desired NHS-activated carboxylic acid derivatives was confirmed with FTIR and NMR analysis. Changes in the relative absorbance of specific peaks between FTIR spectra were used as a qualitative measure of conjugation. Furthermore, the Ninhydrin assay verified the presence of free amine groups, which are needed for subsequent syntheses. Based on these results, ether-based triblocks were further reacted with NHS-activated carboxylic acid derivatives and then EDA to form amine-functionalized, biodegradable multiblocks. Again, FTIR analysis confirmed successful multiblock formation, and the Ninhydrin assay verified the presence of free amine groups.

Amine-functionalized, multiblock soft segments were then reacted with excess HDI and EDA to develop a series of linear polyurea elastomers. Successful urea formation was confirmed with FTIR analysis. As expected, relative absorbances of urea linkages with respect to internal reference ether peaks were elevated at higher hard to soft segment ratios. Synthesis of polyureas was also demonstrated by changes in the physical properties of all polymer samples, including an increase in viscosity as well as reduced solubility that results from hydrogen bonding. Further characterization is needed to verify molecular weight using size exclusion chromatography.

The results of the current study indicate successful synthesis of cell-responsive, biodegradable polyureas. By altering soft segment chemistry and polyol molecular weight, as well as the hard to soft segment content, a library of polyurea elastomers was developed. The next step will be to further characterize these polymers to elucidate key structure-property relationships. To do so, dynamic mechanical analysis (DMA) can be used in conjunction with FTIR spectroscopy to determine the effect of composition on microphase-separated morphology. The tensile properties of these polyureas can then be determined using an Instron testing machine. Finally, the effect of polymer chemistry on the rate of enzyme-mediated degradation must also be investigated. Ultimately, understanding such relationships will be critical for the development of an improved tissue engineered ligament for ACL reconstruction.

CHAPTER IV

SUMMARY

In this study, a library of cell-responsive, biodegradable polyureas was synthesized to elucidate key structure-property relationships for the development of a tissue engineered ligament. The first step was to functionalize ether-based polyols with reactive end groups necessary for facile coupling to collagen-derived peptide sequences. PEG and PTMG of varying molecular weights were reacted with succinic anhydride to modify these polyols with carboxylic acid end groups. Functionalization was confirmed with FTIR spectroscopy based on the generation of characteristic ester peaks within the carbonyl region at ~1730 cm^{-1}. The relative height of such ester peaks with respect to the internal reference ether (-C-O-C-) peak corresponded with the molecular weight of each polyol. In addition, the appearance of methylene (-CH_2OCO-) proton peaks at 4.25 ppm and succinate (-CH_2COO-) peaks at 2.64 ppm in all NMR spectra indicated successful syntheses. The peak areas for these chemical shifts showed that functionalization of all candidate polyols was greater than 90%.

Carboxylic acid derivatives of PEG and PTMG soft segments were then activated with NHS in the presence of DCC to generate superior leaving groups for peptide coupling. Successful NHS activation of all polymer samples was indicated by the appearance of typical NHS carbonyl peaks at ~1810 cm^{-1} and ~1780 cm^{-1} in FTIR spectra. Formation of NHS ester groups was further demonstrated by corollary increases in all ester peaks at 1730 cm^{-1}. Similar to carboxylic acid functionalized polyols, the

relative height of these NHS carbonyl peaks corresponded with the molecular weight of each polymer. NMR spectra of all PEG and PTMG-based NHS ester derivatives showed proton peaks of succinimide at 2.84 ppm. In addition, proton peaks at 2.64 ppm shifted to 2.78 ppm and 2.96 ppm upon activation with NHS due to changes in the electronegativity of succinate groups. A singlet at 2.71 ppm represented the presence of unreacted NHS that cannot be completely removed using typical purification methods.

Following activation with NHS, carboxylic acid derivatives of higher molecular weight (PEG: 6000, 10000 g/mol) were reacted with excess EDA in the presence of DMAp and Et_3N to form amine-functionalized, control soft segments for subsequent polyurea syntheses. Successful functionalization was determined by the generation of characteristic amide peaks among FTIR spectra between 1625 and 1640 cm^{-1}, which are also indicative of hydrogen bonding. Again, the relative height of these amide peaks with respect to the internal reference ether peak was dependent on the molecular weight of the polyol. Hydrogen bonding was also found to shift the ester carbonyl peak of PEG-based derivatives to ~1685 cm^{-1}. Because of hydrogen bonding, NMR spectroscopy could not be used as a quantitative measure of functionalization due to variations in the relaxation time of such proton peaks.

A higher molecular weight derivative of PTMG was not commercially available, and so PTMG (1000) was first functionalized with excess EDA, and then used to end cap PTMG (2900) diacid to form a PTMG-based control soft segment of comparable molecular weight. The FTIR spectrum for PTMG (1000) diamine showed an amide peak at ~1660 cm^{-1}; however, unlike PEG (6000) and PEG (10000) diamine, characteristic

amide and ester peaks were not significantly affected by hydrogen bonding. Upon successful functionalization with EDA, PTMG (1000) diamine was reacted with PTMG (2900) diacid in the presence of DMAp and Et_3N to form PTMG (5600) diamine. The FTIR spectrum for PTMG (5600) diamine showed a reduction in the relative heights of amide and ester peaks with respect to the internal reference ether peak, as compared to the FTIR spectra for PTMG (1000) diamine and PTMG (2900) diacid. This resulted from a decrease in the amount of functional end groups available after successful synthesis, as well as an overall reduction in the relative amount of particular functional groups due to increased molecular weight. Unlike PTMG (1000) diamine, the FTIR spectrum for PTMG (5600) diamine displayed characteristic peaks of both free and hydrogen bonded amide and ester peaks. This suggests that the low molecular weight of PTMG (1000) diamine inhibited hydrogen bonding, and not its polyol chemistry. Following FTIR analyses, Ninhydrin assays confirmed the presence of free amine groups in all PEG and PTMG-based control soft segments, which are necessary for subsequent polyurea syntheses.

Similar to amine-functionalized, control soft segments, NHS-activated carboxylic acid derivatives of lower molecular weight (PEG: 1000, 2000 g/mol; PTMG: 1000 g/mol) were reacted with collagen-derived peptide sequences in the presence of DMAp and Et_3N to form peptide-polyol conjugates. First, NHS ester derivatives were end capped with peptide sequences to form peptide-polyol-peptide triblocks. Successful conjugation was verified with FTIR and NMR spectroscopy, as indicated by the generation of significant amide peaks at ~1660 cm^{-1} and between 7.1 and 8.2 ppm,

respectively. Due to such low concentrations of peptide-polyol conjugates, as well as hydrogen bonding, NMR spectroscopy could not be used for quantitative analysis. Instead, changes in the relative absorbance at 1730 cm^{-1} were used as a qualitative measure of conjugation for all triblock syntheses. With limited conjugation, this absorbance peak should be similar to what it was in the spectrum for its respective diacid, with carboxylic acid and ester groups contributing to its effective height. As conjugation increases, this peak should attenuate until the remaining contributions are solely from the presence of ester linkages. For all peptide-polyol-triblocks, this peak was reduced by approximately 50%, indicating significant conjugation. Following FTIR analysis, Ninhydrin assays verified the presence of free amine groups among PEG and PTMG-based triblocks. For multiblock syntheses, the relative ratio of amide peaks with respect to internal reference ether peaks was examined. A significant reduction in the relative height of the amide peak at 1531 cm^{-1} was observed for all polymer samples, indicating successful multiblock formation. Again, Ninhydrin assays confirmed the presence of free amine groups of all amine-functionalized multiblocks that are necessary for polyurea synthesis.

Amine-functionalized control and multiblock soft segments were then reacted with HDI and EDA to form linear polyurea elastomers. Successful urea formation was determined based on the generation of characteristic urea peaks (~1630 cm^{-1}, hydrogen-bonded C=O; ~1690 cm^{-1}, free C=O; ~3328 cm^{-1}, hydrogen-bonded N-H) in the FTIR spectra of these polymers. The spectra for PEG-based control polyureas predominantly consisted of hydrogen-bonded urea peaks, indicating a relatively high

degree of phase separation. The relative height of these peaks, with respect to the internal reference ether peak, is proportional to the hard segment content. Therefore, these peaks are elevated at higher hard to soft segment ratios. This trend was observed in the FTIR spectra for all candidate polyureas.

PTMG-based control polyureas also demonstrated a significant amount of hydrogen-bonded urea peaks; however, free carbonyl peaks were present. Formation of these peaks indicates that not all urea linkages separated into semi-crystalline, hard domains, referred to as phase mixing. The degree of phase separation is dictated by the reduction of interfacial energy between hard and soft segments, and phase mixing is enhanced by decreases in this free surface energy.[241-243] PTMG is more hydrophobic than PEG, and so it has less surface energy.[244] Therefore, the presence of free carbonyl peaks in the FTIR spectra of PTMG-based polyureas resulted from their hydrophobic nature. Regardless, a relatively high degree of phase separation was still achieved. Furthermore, increased hard segment content was found to increase the relative ratio of hydrogen-bonded to free urea peaks, thus enhancing the degree of phase separation.

Unlike the control polyureas, the FTIR spectrum for PEG (1000) multiblock polyurea (3-1-2) displayed dominant free carbonyl peaks, indicating a relatively low degree of phase separation. In this instance, the use of such a low molecular weight polyol combined with the incorporation of bulky peptide sequences prevented the formation of semi-crystalline, hard domains.[245] However, by increasing the hard to soft segment ratio, formation of hard domains became more favorable due to the increased presence of symmetrical HDI and EDA-based segments.[246] This trend was demonstrated

in the FTIR spectrum for PEG (1000) multiblock polyurea (5-1-4), which showed a dominant hydrogen-bonded urea peak at 1635 cm^{-1}. FTIR spectra for PEG (2000) multiblock polyureas (3-1-2; 5-1-4) did not reveal a free carbonyl peak, but only significant hydrogen-bonded urea peaks. This is due to increased flexibility of the soft segment resulting from the use of a slightly higher molecular weight polyol.[247] Similar to the control polyureas, the relative height of these urea peaks increased at higher hard to soft segment ratios.

The FTIR spectra for PTMG (1000) multiblock polyureas also predominantly consisted of hydrogen-bonded urea peaks, although free carbonyl peaks were detected. As with PTMG-based control polyureas, the generation of these peaks was reflective of the soft segment chemistry of these polyureas, and the relative ratio of hydrogen-bonded to free urea peaks increased at higher hard to soft segment ratios. It is important to note that, unlike PEG (1000) multiblock polyurea (3-1-2), the FTIR spectrum for PTMG (1000) multiblock polyurea (3-1-2) did not show a significant free carbonyl peak. This suggests that, because of its hydrophobic nature, PTMG is more conducive to the formation of semi-crystalline, hard domains than PEG in the presence of such large peptide sequences at low hard segment contents. Still, additional experiments are necessary to further elucidate this structure-property relationship. Overall, a library of linear polyurea elastomers was successfully developed using the aforementioned synthetic strategies, and these polymers feature a relatively high degree of phase separation.

As stated previously, the microphase-separated morphology of polyurea elastomers dictates their unique deformation behavior. This behavior is the foundation for understanding key structure-property relationships. In addition to FTIR spectroscopy, DMA is needed to further monitor the effect of polymer composition on phase separation of all candidate polyureas. Instron testing can then be used to determine the tensile properties of these polymers. In addition to mechanical testing, enzyme-mediated degradation studies are needed to determine the effect of phase separation on the rate of degradation. Based on these results, polyurea chemistry can be tailored to alter the degree of phase separation, and thus obtain specific performance properties. Investigation of structure-property relationships will enable the rational design of an improved biomaterial for ligament tissue engineering.

The first step in the rational design of a biodegradable material for tissue engineering is to determine the effect of system-responsive degradation on its mechanical properties. To do this, mechanical testing of all candidate polyureas is needed at specific points of degradation. By utilizing elucidated structure-property relationships, polyurea chemistry can be tailored to synthesize control specimens with mechanical properties comparable to these stages of degradation. Cells may then be seeded onto control polyurea scaffolds to observe the effect of these mechanical properties on cell behavior.[248, 249] Based on these results, biodegradable polyurea elastomers can be designed so that scaffold degradation complements neotissue formation. Due to the versatility of the aforementioned synthetic routes, polyurea chemistry can be further modified as necessary to achieve this desired behavior. For

example, polyol molecular weight can be adjusted to modulate the relative concentration of enzyme-labile peptide sequences. PEG and PTMG-based derivatives can be utilized within the same system to modify the hydrophilicity of the soft segment, which would alter the degree of phase separation. Finally, additional peptide sequences, such as RGD, can be incorporated into enzyme-labile soft segments, which would not only provide cell-responsive degradation, but also increase cell adhesion.[250]

In order to conduct further experimentation, mass production of cell-responsive, biodegradable polyureas is needed. Currently, these polymers are developed in very small quantities, and as a result, the effective yields for these reactions are fairly low (~10-50%). Increasing the scale of production would improve these yields; however, due to the high cost to synthesize custom peptide sequences, this approach would not be cost effective. Recombinant strategies could be utilized instead of solid phase peptide synthesis, which would enable large-scale peptide synthesis at a reasonable cost.[251-253] Although synthesis of short peptide chains can be problematic with microbial systems, research is currently in progress to circumvent this issue. Fusion proteins are in development from which a short peptide sequence can be released and recovered.[254, 255] Through isolation and purification, a desired peptide sequence can thus be obtained.[256, 257] These sequences can then be implemented into the synthesis of cell-responsive, biodegradable polyureas, allowing large-scale production of these polymers.

In addition to the development of an improved biomaterial for ACL reconstruction, synthetic strategies used to generate a library of cell-responsive, biodegradable polyureas can be utilized for a variety of other biomedical applications as

well. Similar to the current approach, enzyme-labile poly (urethane urea)s can be developed to create new structure-property models for bone or cardiovascular tissue engineering. A polymeric system that combines the tunability of segmented block copolymers with system-responsive degradation can also be used to achieve effective drug delivery.[258, 259] Based on the versatility of the synthetic routes described above, enzyme-labile peptide sequences can be replaced with other sequences to produce an assortment of biomimetic materials. For instance, a peptide chromophore can be implemented into the design of a novel biomaterial and serve as an effective biosensor.[260, 261] Carboxylic acid and amine functionalization of PTMG is of particular importance because, unlike PEG, functionalization of PTMG has not been well-established throughout the literature.[186] As a result, the synthetic routes and purification techniques reported in this study can be adapted to utilize PTMG in various applications previously dominated by PEG. Overall, the synthesis of a library of cell-responsive, biodegradable polyureas will assist in the development of a tissue engineered ligament, as well as provide additional tools to advance biomaterial design.

REFERENCES

1. *Orthop. Res. Soc. Newsletter* **2005,** *18*, 1.

2. Albright, J. C.; Carpenter, J. E.; Graf, B. K.; Richmond, J. C. *Knee and Leg: Soft-Tissue Trauma*. American Academy of Orthopaedic Surgeons: Rosemont, 1999.

3. Pennisi, E. *Science* **2002,** *295*, 1011.

4. Laurencin, C. T.; Freeman, J. W. *Biomaterials* **2005,** *26*, 7530.

5. Segawa, H.; Omori, G.; Koga, Y. *Knee* **2001,** *8*, 5.

6. Woo, S. L.-Y.; Hildebrand, K.; Watanabe, N.; Fenwick, J. A.; Papageorgiou, C., D.; Wang, J. H.-C. *Clin. Orthop. Relat. Res.* **1999,** *367S*, S312.

7. Maletius, W.; Gillquist, J. *Am. J. Sports Med.* **1997,** *25*, 288.

8. Arnoczky, S. P.; Tarvin, G. B.; Marshall, J. L. *J. Bone Joint Surg.* **1982,** *64*, 217.

9. Lyon, R. M.; Akeson, W. H.; Amiel, D.; Kitabayashi, L. R.; Woo, S. L.-Y. *Clin. Orthop. Relat. Res.* **1991,** *272*, 279.

10. Altman, G. H.; Horan, R. L. In *An Introduction of Biomaterials*, Guelcher, S. A.; Hollinger, J. O., Eds.; CRC Press: Boca Raton, 2006; pp. 499-524.

11. Vunjak-Novakovic, G.; Altman, G. H.; Horan, R. L.; Kaplan, D. L. *Annu. Rev. Biomed. Eng.* **2004,** *6*, 131.

12. Nagineni, C. N.; Amiel, D.; Green, M. H.; Berchuck, M.; Akeson, W. H. *J. Orthop. Res.* **1992,** *10*, 465.

13. Yoshida, M.; Fujii, K. *J. Orthop. Sci.* **1999,** *4*, 293.

14. Wiig, M. E.; Ivarsson, M.; Nagineni, C. N.; Wallace, C. D.; Arfors, K.-E. *J. Orthop. Res.* **1991,** *9*, 374.

15. Lee, J.; Harwood, F. L.; Akeson, W. H.; Amiel, D. *Iowa Orthop. J.* **1998,** *18*, 19.

16. Lo, I. K. Y.; Marchuk, L.; Hart, D. A.; Frank, C. B. *J. Orthop. Res.* **1998,** *16*, 421.

17. Guo, C.; Spector, M. In *Scaffolding in Tissue Engineering*, Ma, P. X.; Elisseeff, J., Eds.; Taylor & Francis: Boca Raton, 2006; pp. 385-411.

18. Fu, F. H.; Bennett, C. H.; Ma, C. B.; Menetrey, J.; Lattermann, C. *Am. J. Sports Med.* **2000,** *28*, 124.

19. Lin, V. S.; Lee, M. C.; O'Neal, S.; McKean, J.; Sung, K.-L. P. *Tissue Eng.* **1999,** *5*, 443.

20. Amiel, D.; Kuiper, S.; Newton, P. O.; Horibe, S.; Woo, S. L.-Y. In *Knee Ligaments: Structures, Function, Injury and Repair*, Daniel, D. M.; Akeson, W. H.; O'Connor, J. J., Eds.; Raven Press: New York, 1990; pp. 379-400.

21. Jackson, D. W.; Lemos, M. J.; Tolin, B. S.; Friedman, M. J.; Fu, F., H.; Jamison, J.; Simon, T. M.; McCarthy, D. M.; Schwendeman, L.; Woo, S. L.-Y. In *The Anterior Cruciate Ligament: Current and Future Concepts*, Jackson, D. W., Ed.; Raven Press: New York, 1993; pp. 291-356.

22. Thomas, N. P.; Turner, I. G.; Jones, C. B. *J. Bone Joint Surg.* **1987,** *69-B*, 312.

23. Chen, J.; Moreau, J.; Horan, R. L.; Collette, A.; Bramono, D.; Volloch, V.; Richmond, J.; Vunjak-Novakovic, G.; Kaplan, D. L.; Altman, G. H. In *Culture of Cells for Tissue Engineering*, Vunjak-Novakovic, G.; Freshney, R. I., Eds.; John Wiley & Sons, Inc.: Hoboken, 2006; pp. 191-211.

24. Freeman, J. W.; Kwansa, A. L. *Recent Patents Biomed. Eng.* **2008,** *1*, 23.

25. Friedman, M. J.; Sherman, O. H.; Fox, J. M.; Del Pizzo, W.; Snyder, S. J.; Ferkel, R. J. *Clin. Orthop. Relat. Res.* **1985,** *196*, 9.

26. Simonian, P. T.; Harrison, S. D.; Cooley, V. J.; Escabedo, E. M.; Deneka, D. A.; Larson, R. V. *Am. J. Knee Surg.* **1997,** *10*, 54.

27. Noyes, F. R.; Butler, D. L.; Grood, E. S.; Zernicke, R. F.; Hefzy, M. S. *J. Bone Joint Surg.* **1984,** *66*, 344.

28. Amiel, D.; Kleiner, J. B.; Roux, R. D.; Harwood, F. L.; Akeson, W. H. *J. Orthop. Res.* **1986,** *4*, 162.

29. Ballock, R. T.; Woo, S. L.-Y.; Lyon, R. M.; Hollis, J. M.; Akeson, W. H. *J. Orthop. Res.* **1989,** *7*, 474.

30. Laurencin, C. T.; Ambrosio, A. M. A.; Borden, M. D.; Cooper Jr., J. A. *Annu. Rev. Biomed. Eng.* **1999,** *1*, 19.

31. Ge, Z.; Yang, F.; Goh, J. C. H.; Ramakrishna, S.; Lee, E. H. *J. Biomed. Mater. Res.* **2006,** *77A*, 639.

32. Weitzel, P. P.; Richmond, J. C.; Altman, G. A.; Calabro, T.; Kaplan, D. L. *Orthop. Clin. North Am.* **2002,** *33*, 653.

33. Bell, E. *Tissue Eng.* **1995,** *1*, 163.

34. Shino, K.; Inoue, M.; Horibe, S.; Nagano, J.; Ono, K. *J. Bone Joint Surg.* **1988,** *70-B*, 556.

35. Jackson, D. W.; Grood, E. S.; Goldstein, J. D.; Rosen, M. A.; Kurzweil, P. A. *Am. J. Sports Med.* **1993,** *21*, 176.

36. Jackson, D. W.; Grood, E.; Arnoczky, S. P.; Butler, D.; Simon, T. M. *Am. J. Sports Med.* **1987,** *15*, 295.

37. Jackson, D. W.; Grood, E. S.; Arnoczky, S. P.; Butler, D. L.; Simon, T. M. *Am. J. Sports Med.* **1987,** *15*, 528.

38. Jackson, D. W.; Windler, G. E.; Simon, T. M. *Am. J. Sports Med.* **1990,** *18*, 1.

39. Scheffler, S. U.; Scherler, J.; Pruss, A.; Von Versen, R.; Weiler, A. *Cell Tissue Bank.* **2005,** *6*, 109.

40. Jackson, D. W.; Heinrich, J. T.; Simon, T. M. *Arthroscopy* **1994,** *10*, 442.

41. Markolf, K. L.; Pattee, G. A.; Strum, G. M.; Gallick, G. S.; Sherman, O. H.; Nuys, V.; Dorey, F. J. *J. Bone Joint Surg.* **1989,** *71*, 887.

42. Fischer, S. P.; Ferkel, R. D. *Prosthetic Ligament Reconstruction of the Knee*. W. B. Saunders Company: Philadelphia, 1988.

43. Silver, F. H.; Tria, A. J.; Zawadsky, J. P.; Dunn, M. G. *J. Long Term Eff. Med. Implants* **1991,** *1*, 135.

44. Fujikawa, K. In *Prosthetic Ligament Reconstruction of the Knee*, Friedman, M. J.; Ferkel, R. D., Eds.; W. B. Sanders Company: Philadelphia, 1988.

45. Bolton, C. W.; Bruchman, W. C. *Clin. Orthop. Relat. Res.* **1985,** *196*, 202.

46. Richmond, J. C.; Manseau, C.; Patz, R.; McConville, O. *Am. J. Sports Med.* **1992,** *20*, 24.

47. Fujikawa, K.; Iseki, F.; Seedhom, B. B. *J. Bone Joint Surg.* **1989,** *71-B*, 566.

48. Miller, R. H. In *Campbell's Operative Orthopaedics*, Canale, S. T., Ed.; CV Mosby: St. Louis, 2003; pp. 2274-2275.

49. McPherson, G. K.; Mendenhall, H. V.; Gibbons, D. F.; Plenk, H.; Rottmann, W.; Sanford, J. B.; Kennedy, J. C.; Roth, J. H. *Clin. Orthop. Relat. Res.* **1985,** *196*, 186.

50. Van Kampen, C. L. *Clin. Mater.* **1994,** *15*, 23.

51. Kumar, K.; Maffulli, N. *Arthroscopy* **1999,** *15*, 422.

52. Moyen, B. J.; Jenny, J. Y.; Mandrino, A. H.; Lerat, J. L. *J. Bone Joint Surg.* **1992,** *74*, 1313.

53. Lopez-Vazquez, E.; Juan, J. A.; Vila, E.; Debon, J. *J. Bone Joint Surg.* **1991,** *73*, 1294.

54. Murray, A. W.; Macnicol, M. F. *Knee* **2003,** *11*, 9.

55. Parsons, J. R.; Bhayani, S.; Alexander, H.; Weiss, A. B. *Clin. Orthop. Relat. Res.* **1985,** *196*, 69.

56. Olson, E. J.; Kang, J. D.; Fu, F. H.; Georgescu, H. I.; Mason, G. C.; Evans, C. H. *Am. J. Sports Med.* **1988,** *16*, 558.

57. Rose, F. R. A. J.; Oreffo, R. O. C. *Biochem. Biophys. Res. Commun.* **2002,** *292*, 1.

58. Kenley, R.; Yim, K.; Abrams, J.; Ron, E.; Turek, T.; Marden, L.; Hollinger, J. *Pharm. Res.* **1993,** *10*, 1393.

59. Bhatia, S. N.; Chen, C. S. *Biomed. Microdevices* **1999,** *2*, 131.

60. Neurath, M. *Acta Anatomica* **1993,** *145*, 387.

61. Amiel, D.; Frank, C.; Harwood, F.; Fronek, J.; Akeson, W. *J. Orthop. Res.* **1984,** *1*, 257.

62. Riechert, K.; Labs, K.; Lindenhayn, K.; Sinha, P. *J. Orthop. Sci.* **2001,** *6*, 68.

63. Frank, C. B. *J. Musculoskelet. Neuronal Interact.* **2004,** *4*, 199.

64. Chen, E. H.; Black, J. *J. Biomed. Mater. Res.* **1980,** *14*, 567.

65. Noyes, F. R.; Grood, E. S. *J. Bone Joint Surg.* **1976,** *58A*, 1074.

66. Woo, S. L.-Y.; Adams, D. J. In *Knee Ligaments: Structure, Function, Injury, and Repair*, Daniel, D.; Akeson, W. H.; O'Connor, J., Eds.; Raven Press: New York, 1990.

67. Woo, S. L.-Y.; Hollis, J. M.; Adams, D. J.; Lyon, R. M.; Takai, S. *Am. J. Sports Med.* **1991,** *19*, 217.

68. Martin, R. B.; Burr, D. B.; Sharkey, N. A. In *Skeletal Tissue Mechanics*, Springer-Verlag: New York, 1998; pp. 309-349.

69. Silver, F. H. *Biomaterials, Medical Devices, and Tissue Engineering: An Integrated Approach*. Chapman & Hill: London, 1994.

70. Diamant, J.; Keller, A.; Baer, E.; Litt, M.; Arridge, R. G. *Proc. R. Soc. Lond., Part B: Biol. Sci.* **1972,** *180*, 293.

71. Mosler, E.; Folkhard, W.; Knorzer, E.; Nemetschek-Gansler, H.; Nemetschek, T.; Koch, M. H. *J. Molec. Biol.* **1985,** *182*, 589.

72. McBride Jr., D. J.; Hahn, R. A.; Silver, F. H. *Int. J. Biol. Macromol.* **1988,** *7*, 71.

73. Chvapil, M.; Speer, D.; Holubec, H.; Chvapil, T.; King, D. *J. Biomed. Mater. Res.* **1993,** *27*, 313.

74. Dunn, M. G.; Liesch, J. B.; Tiku, M. L.; Zawadsky, J. P. *J. Biomed. Mater. Res.* **1995,** *29*, 1363.

75. Bellincampi, L. D.; Closkey, R. F.; Prasad, R.; Zawadsky, J. P.; Dunn, M. G. *J. Orthop. Res.* **1998,** *16*, 414.

76. Khor, E. *Biomaterials* **1997,** *18*, 95.

77. Law, J. K.; Parsons, J. R.; Silver, F. H.; Weiss, A. B. *J. Biomed. Mater. Res.* **1989,** *23*, 961.

78. Dunn, M. G.; Maxian, S. H.; Zawadsky, J. P. *J. Orthop. Res.* **1994,** *12*, 128.

79. Dunn, M. G.; Tria, A. J.; Kato, Y. P.; Bechler, J. R.; Ochner, R. S.; Zawadsky, J. P.; Silver, F. H. *Am. J. Sports Med.* **1992,** *20*, 507.

80. Dunn, M. G.; Bellincampi, L. D.; Tria, A. J.; Zawadsky, J. P. *J. Appl. Polym. Sci.* **1997,** *63*, 1423.

81. Koob, T. J.; Hernandez, D. J. *Biomaterials* **2002,** *23*, 203.

82. Caruso, A. B.; Dunn, M. G. *J. Biomed. Mater. Res.* **2004,** *69A*, 164.

83. Lee, C. H.; Singla, A.; Lee, Y. *Int. J. Pharm.* **2001,** *221*, 1.

84. Fan, H.; Liu, H.; Toh, S. L.; Goh, J. C. H. *Biomaterials* **2008,** *29*, 1017.

85. Liu, H.; Ge, Z.; Wang, Y.; Toh, S. L.; Sutthikhum, V.; Goh, J. C. H. *J. Biomed. Mater. Res., Part B: Appl. Biomater.* **2007,** *82*, 129.

86. Toh, S. L.; Teh, T. K. H.; Vallaya, S.; Goh, J. C. H. *Key Eng. Mater.* **2006,** *326-328*, 727.

87. Altman, G. H.; Diaz, F.; Jakuba, C.; Calabro, T.; Horan, R. L.; Chen, J.; Lu, H.; Richmond, J.; Kaplan, D. L. *Biomaterials* **2003,** *24*, 401.

88. Chen, X.; Qi, Y.-Y.; Wang, L.-L.; Yin, Z.; Yin, G.-L.; Zou, X.-H.; Ouyang, H.-W. *Biomaterials* **2008,** *29*, 3683.

89. Altman, G. H.; Horan, R. L.; Lu, H. H.; Moreau, J.; Martin, I.; Richmond, J.; Kaplan, D. L. *Biomaterials* **2002,** *23*, 4131.

90. Chen, J.; Altman, G. H.; Karageorgiou, V.; Horan, R. L.; Collette, A.; Volloch, V.; Colabro, T.; Kaplan, D. L. *J. Biomed. Mater. Res.* **2003,** *67A*, 559.

91. Funakoshi, T.; Majima, T.; Iwasaki, N.; Yamane, S.; Masuko, T.; Minami, A.; Harada, K.; Tamura, H.; Tokura, S.; Nishimura, S.-I. *J. Biomed. Mater. Res.* **2005,** *74A*, 338.

92. Majima, T.; Funakoshi, T.; Iwasaki, N.; Yamane, S.; Harada, K.; Nonaka, S.; Minami, A.; Nishimura, S.-I. *J. Orthop. Sci.* **2005,** *10*, 302.

93. Messenger, M. P.; Raif, E. M.; Seedhom, B.; Brookes, S. J. *Tissue Eng.* **2007,** *13*, 2041.

94. Bourke, S. L.; Kohn, J.; Dunn, M. G. *Tissue Eng.* **2004,** *10*, 43.

95. Buma, P.; Kok, H. J.; Blankevoort, L.; Kuijpers, W.; Huiskes, R.; Van Kampen, A. *Int. Orthop.* **2004,** *28*, 91.

96. Ge, Z.; Goh, J. C. H.; Wang, L.; Tan, E. P. S.; Lee, E. H. *J. Biomater. Sci. Polym. Ed.* **2005,** *16*, 1179.

97. Laitinen, O.; Alitalo, I.; Toivonen, T.; Vasenius, J.; Tormala, P.; Vainionpaa, S. *J. Mater. Sci. Mater. Med.* **1993,** *4*, 547.

98. Laitinen, O.; Pohjonen, T.; Tormala, P.; Saarelainen, K.; Vasenius, J.; Rokkanen, P.; Vainionpaa, S. *Arch. Orthop. Trauma Surg.* **1993,** *112*, 270.

99. Sahoo, S.; Goh, J. C. H.; Toh, S. L. *Biomed. Mater.* **2007,** *2*, 167.

100. Sahoo, S.; Ouyang, H.; Goh, J. C. H.; Tay, T. E.; Toh, S. L. *Tissue Eng.* **2006,** *12*, 91.

101. Shao, H.-J.; Chen, C. S.; Lee, I.-C.; Wang, J.-H.; Young, T.-H. *Artif. Organs* **2009,** *33*, 309.

102. Cooper Jr., J. A.; Lu, H. H.; Ko, F. K.; Freeman, J. W.; Laurencin, C. T. *Biomaterials* **2005,** *26*, 1523.

103. Lu, H. H.; Cooper Jr., J. A.; Manuel, S.; Freeman, J. W.; Attawia, M. A.; Ko, F. K.; Laurencin, C. T. *Biomaterials* **2005,** *26*, 4805.

104. Freeman, J. W.; Woods, M. D.; Laurencin, C. T. *J. Biomech.* **2007,** *40*, 2029.

105. Park, T. G. *Biomaterials* **1995,** *16*, 1123.

106. Lamba, N. M. K.; Woodhouse, K. A.; Cooper, S. L. *Polyurethanes in Biomedical Applications*. CRC Press LLC: Boca Raton, 1998.

107. Gogolewski, S. *Colloid. Polym. Sci.* **1989,** *267*, 757.

108. Guelcher, S. A. *Tissue Eng., Part B: Rev.* **2008,** *14*, 3.

109. Santerre, J. P.; Woodhouse, K. A.; Laroche, G.; Labow, R. S. *Biomaterials* **2005,** *26*, 7457.

110. *The Polyurethanes Book*. John Wiley & Sons, Ltd.: New York, 2002.

111. Oertel, G. *Polyurethane Handbook*. Hanser Gardner Publications, Inc.: Berlin, 1994.

112. Stokes, K.; McVenes, R. *J. Biomater. Appl.* **1995,** *9*, 321.

113. Szycher, M.; Reed, A. *Med. Device Technol.* **1992,** *3*, 42.

114. Lelah, M. D.; Cooper, S. L. *Polyurethanes in Medicine*. CRC Press, Inc.: Boca Raton, 1986.

115. Szycher, M. *Szycher's Handbook of Polyurethanes*. CRC Press, Inc.: Boca Raton, 1999.

116. Gogolewski, S. *Trends Polym. Sci.* **1991,** *1*, 47.

117. Legge, N.; Helden, G.; Schoeder, H. *Thermoplastic Elastomers: A Comprehensive Review*. Macmillan Publishing Company: New York, 1987.

118. Bonart, R.; Morbitzer, L.; Hentze, G. *J. Macromol. Sci., Part B: Phys.* **1969,** *3*, 337.

119. Bonart, R.; Morbitzer, L.; Muller, E. H. *J. Macromol. Sci., Part B: Phys.* **1974,** *9*, 447.

120. Christenson, E. M.; Anderson, J. M.; Hiltner, A.; Baer, E. *Polymer* **2005,** *46*, 11744.

121. Martin, D. J.; Meijs, G. F.; Gunatillake, P. A.; Yozghatlian, S. P.; Renwick, G. M. *J. Appl. Polym. Sci.* **1999,** *71*, 937.

122. Santerre, J.; Labow, R. *J. Biomed. Mater. Res.* **1997,** *36*, 223.

123. Chang, Y.-J. P.; Wilkes, G. L. *J. Polym. Sci., Part B: Polym. Phys.* **1975,** *13*, 455.

124. Zha, L.; Wu, M.; Yang, J. *J. Appl. Polym. Sci.* **1999,** *73*, 2895.

125. O'Sickey, M. J.; Lawrey, B. D.; Wilkes, G. L. *J. Appl. Polym. Sci.* **2002,** *84*, 229.

126. Skarja, G. A.; Woodhouse, K. A. *J. Appl. Polym. Sci.* **2000,** *75*, 1522.

127. Gisselfalt, K.; Helgee, B. *Macromol. Mater. Eng.* **2003,** *288*, 265.

128. Gisselfalt, K.; Edberg, B.; Flodin, P. *Biomacromolecules* **2002,** *3*, 951.

129. Coury, A. In *Biomaterials Science: An Introduction to Materials in Medicine*, Ratner, B.; Hoffman, A.; Schoen, F.; Lemons, J., Eds.; Elsevier Academic Press: Boston, 2004; pp. 411-430.

130. Mazzu, A. L.; Smith, C. P. *J. Biomed. Mater. Res.* **1984,** *18*, 961.

131. Szycher, M.; Siciliano, A. A. *J. Biomater. Appl.* **1991,** *5*, 323.

132. Guelcher, S.; Srinivasan, A.; Hafeman, A.; Gallagher, K. M.; Doctor, J. S.; Khetan, S.; McBride, S.; Hollinger, J. O. *Tissue Eng.* **2007,** *13*, 2321.

133. Saad, B.; Ciardelli, G.; Matter, S.; Welti, M.; Uhlschmid, G. K.; Neuenschwander, P.; Suter, U. *J. Biomed. Mater. Res.* **1998,** *39*, 594.

134. Saad, B.; Hirt, T. D.; Welti, M.; Uhlschmid, G. K.; Neuenschwander, P.; Suter, U. W. *J. Biomed. Mater. Res.* **1997,** *36*, 65.

135. Saad, B.; Kuboki, M.; Matter, S.; Welti, M.; Uhlschmid, G. K.; Neuenschwander, P.; Suter, U. *Artif. Organs* **2000,** *24*, 939.

136. Skarja, G. A.; Woodhouse, K. A. *J. Biomater. Sci. Polym. Ed.* **1998,** *9*, 271.

137. Skarja, G. A.; Woodhouse, K. A. *J. Biomater. Sci. Polym. Ed.* **2001,** *12*, 851.

138. Zhang, J.; Beckman, E.; Piesco, P.; Agarwal, A. *Biomaterials* **2000,** *21*, 1247.

139. Zhang, J. Y.; Beckman, E. J.; Hu, J.; Yang, G. G.; Agarwal, S.; Hollinger, J. O. *Tissue Eng.* **2002,** *8*, 771.

140. Zhang, J. Y.; Doll, B. A.; Beckman, E. J.; Hollinger, J. O. *J. Biomed. Mater. Res.* **2003,** *67A*, 389.

141. Guelcher, S.; Wilkes, G. *Acta Biomater.* **2005,** *1*, 471.

142. Guelcher, S. A.; Patel, V.; Gallagher, K. M.; Connolly, S.; Didier, J. E.; Doctor, J. S.; Hollinger, J. O. *Tissue Eng.* **2006,** *12*, 1247.

143. Bruin, P.; Veenstra, G. J.; Nijenhuis, A. J.; Pennings, A. J. *Makromol. Chem.-Rapid* **1988,** *9*, 589.

144. Gorna, K.; Gogolewski, S. *J. Biomed. Mater. Res.* **2002,** *60*, 592.

145. Guan, J.; Sacks, M. S.; Beckman, E. J.; Wagner, W. R. *Biomacromolecules* **2005,** *6*, 2833.

146. Asplund, B. J. O.; Bowden, T.; Mathisen, T.; Hilborn, J. *Biomacromolecules* **2007,** *8*, 905.

147. Gogolewski, S.; Gorna, K. *J. Biomed. Mater. Res.* **2007,** *80A*, 94.

148. Gogolewski, S.; Gorna, K.; Turner, A. S. *J. Biomed. Mater. Res.* **2006,** *77A*, 802.

149. Elliott, S. L.; Fromstein, J. D.; Santerre, J. P.; Woodhouse, K. A. *J. Biomater. Sci. Polym. Ed.* **2002,** *13*, 691.

150. Cohn, D.; Stern, T.; Gonzales, M.; Epstein, J. *J. Biomed. Mater. Res.* **2002,** *59*, 273.

151. Woo, G. L. Y.; Mittelman, M. W.; Santerre, J. P. *Biomaterials* **2000,** *21*, 1235.

152. Borkenhagen, M.; Stoll, R. C.; Neuenschwander, P.; Suter, U. W.; Aebischerl, P. *Biomaterials* **1998,** *19*, 2155.

153. Guan, J.; Sacks, M.; Beckman, E.; Wagner, W. *Biomaterials* **2004,** *25*, 85.

154. Cohn, D.; Hotovely-Salomon, A. *Polymer* **2005,** *46*, 2068.

155. Storey, R. F.; Wiggins, J. S.; Mauritz, K. A.; Puckett, A. D. *Polym. Composites* **1993,** *14*, 17.

156. Storey, R. F.; Wiggins, J. S.; Puckett, A. D. *J. Polym. Sci.* **1994,** *32*, 2345.

157. Liljensten, E.; Gisselfalt, K.; Edberg, B.; Bertilsson, H.; Flodin, P. *J. Mater. Sci. Mater. Med.* **2002,** *13*, 351.

158. Gorna, K.; Gogolewski, S. *J. Biomed. Mater. Res.* **2003,** *67A*, 813.

159. Sawhney, A. S.; Hubbell, J. A. *J. Biomed. Mater. Res.* **1990,** *24*, 1397.

160. Fromstein, J. D.; Woodhouse, K. A. *J. Biomater. Sci. Polym. Ed.* **2002,** *13*, 391.

161. Park, S. A.; Kim, I. A.; Lee, Y. J.; Shin, J. W.; Kim, C.-R.; Kim, J. K.; Yang, Y.-I.; Shin, J.-W. *J. Biosci. Bioeng.* **2006,** *102*, 402.

162. Zeichen, J.; Van Griensven, M.; Bosch, U. *Am. J. Sports Med.* **2000,** *28*, 888.

163. Yang, G.; Crawford, R. C.; Wang, J. H.-C. *J. Biomech.* **2004,** *37*, 1543.

164. Almekinders, L. C.; Banes, A. J.; Bracey, L. W. *Am. J. Sports Med.* **1995,** *23*, 119.

165. Miyaki, S.; Ushida, T.; Nemoto, K.; Shimojo, H.; Itabashi, A.; Ochiai, N.; Miyanaga, Y.; Tateishi, T. *Mater. Sci. Eng.* **2001,** *17*, 91.

166. Lee, C. H.; Shin, H. J.; Cho, I. H.; Kang, Y.-M.; Kim, I. A.; Park, K.-D.; Shin, J.-W. *Biomaterials* **2005,** *26*, 1261.

167. Toyoda, T.; Matsumoto, H.; Fujikawa, K.; Saito, S.; Inoue, K. *Clin. Orthop. Relat. Res.* **1998**, 247.

168. Hannafin, J. A.; Attia, E. A.; Henshaw, R.; Warren, R. F.; Bhargava, M. M. *J. Orthop. Res.* **2006,** *24*, 149.

169. Henshaw, D. R.; Attia, E.; Bhargava, M.; Hannafin, J. A. *J. Orthop. Res.* **2006,** *24*, 481.

170. Gilbert, T. W.; Stewart-Akers, A. M.; Sydeski, J.; Nguyen, T. D.; Badylak, S. F.; Woo, S. L.-Y. *Tissue Eng.* **2007,** *13*, 1313.

171. Wang, J. H.-C.; Jia, F.; Gilbert, T. W.; Woo, S. L.-Y. *J. Biomech.* **2003,** *36*, 97.

172. Wang, J. H.-C.; Yang, G.; Li, Z.; Shen, W. *Biomaterials* **2004,** *37*, 573.

173. Jones, B. F.; Banes, A. J.; Wall, M. E.; Carroll, R. L.; Washburn, S. *Mater. Res. Soc. Symp. Proc.* **2004,** *EXS*, 197.

174. Jones, B. F.; Wall, M. E.; Carroll, R. L.; Washburn, S.; Banes, A. J. *J. Biomech.* **2005,** *38*, 1653.

175. Kim, S.-G.; Akaike, T.; Sasagawa, T.; Atomi, Y.; Kurosawa, H. *Cell Struct. Funct.* **2002,** *27*, 139.

176. Hsieh, A. H.; Tsai, C. M.-H.; Ma, Q.-J.; Lin, T.; Banes, A. J.; Villareal, F. J.; Akeson, W. H.; Sung, K.-L. P. *J. Orthop. Res.* **2000,** *18*, 220.

177. Lee, C.-Y.; Liu, X.; Smith, C. L.; Zhang, X.; Hsu, H.-C.; Wang, D.-Y.; Luo, Z.-P. *Matrix Biol.* **2004,** *23*, 323.

178. Abousleiman, R. I.; Sikavitsas, V. I. *Adv. Exp. Med. Biol.* **2006,** *585*, 243.

179. Foos, M. J.; Hickox, J. R.; Mansour, P. G.; Slauterbeck, J. R.; Hardy, D. M. *J. Orthop. Res.* **2001,** *19*, 642.

180. Zhou, D.; Lee, H. S.; Villareal, F.; Teng, A.; Lu, E.; Reynolds, S.; Qin, C.; Smith, J.; Sung, K. L. P. *J. Orthop. Res.* **2005,** *23*, 949.

181. Kerkvliet, E. H. M.; Docherty, A. J. P.; Beersten, W.; Everts, V. *Matrix Biol.* **1999,** *18*, 373.

182. Bramono, D. S.; Richmond, J. C.; Weitzel, P. P.; Chernoff, H.; Martin, I.; Volloch, V.; Jakuba, C. M.; Diaz, F.; Gandhi, J. S.; Kaplan, D. L.; Altman, G. H. *Connect. Tissue Res.* **2005,** *46*, 53.

183. Sottrup-Jensen, L.; Birkedal-Hansen, H. *J. Biol. Chem.* **1989,** *264*, 393.

184. Welgus, H. G.; Jefferey, J. J.; Eisen, A. Z. *J. Biol. Chem.* **1981,** *256*, 9511.

185. Whitham, S. E.; Murphy, G.; Angel, P.; Rahmsdorf, H. J.; Smith, B.; Lyons, A.; Harris, R. J. R.; Reynolds, J. J.; Herrlich, P.; Docherty, A. J. *Biochem. J.* **1986,** *240*, 913.

186. Hermanson, G. T. *Bioconjugate Techniques*. Academic Press: San Diego, 1996.

187. Ma, X.; Mohammad, S. F.; Kim, S. W. *J. Biomed. Mater. Res.* **1993,** *27*, 357.

188. Hou, S.; McCauley, L.; Ma, P. *Macromol. Biosci.* **2007,** *7*, 620.

189. Fuke, I.; Hayashi, T.; Tabata, Y.; Ikada, Y. *J. Control. Release* **1994,** *30*, 27.

190. Xiong, F.; Li, J.; Wang, H.; Chen, Y.; Cheng, J.; Zhu, J. *Polymer* **2006,** *47*, 6636.

191. Weissleder, R.; Poss, K.; Wilkinson, R.; Zhou, C.; Bogdanov, A. J. *Antimicrob. Agents Chemother.* **1995,** *39*, 839.

192. Klotz, I. M. In *Methods in Enzymology*, Hirs, C. H. W., Ed.; Academic Press: New York, 1967.

193. Xu, S.; Held, I.; Kempf, B.; Mayr, H.; Steglich, W.; Zipse, H. *Chemistry* **2005,** *11*, 4751.

194. Ke, T.; Jeong, E.-K.; Wang, X.; Feng, Y.; Parker, D. L.; Lu, Z.-R. *Int. J. Nanomed.* **2007,** *2*, 191.

195. Sagara, K.; Kim, S. W. *J. Control. Release* **2002,** *79*, 271.

196. Lee, S.-H.; Moon, J. J.; Miller, J. S.; West, J. L. *Biomaterials* **2007,** *28*, 3163.

197. Jo, S.; Engel, P. S.; Mikos, A. G. *Polymer* **2000,** *41*, 7595.

198. Xu, H.; Kaar, J. L.; Russell, A. J.; Wagner, W. R. *Biomaterials* **2006,** *27*, 3125.

199. DeLong, S. A.; Moon, J. J.; West, J. L. *Biomaterials* **2005,** *26*, 3227.

200. Nojima, Y.; Iguchi, K.; Suzuki, Y.; Sato, A. *Biol. Pharm. Bull.* **2009,** *32*, 523.

201. Yamasaki, N.; Matsuo, A.; Isobe, H. *Agr. Biol. Chem.* **1988,** *52*, 2125.

202. Staros, J. V. *Biochemistry* **1982,** *21*, 3950.

203. Savva, M.; Duba, E.; Huang, L. *Int. J. Pharm.* **1999,** *184*, 45.

204. Chu, B. C. F.; Kramer, F. R.; Orgel, L. E. *Nucl. Acids Res.* **1986,** *14*, 5591.

205. Williams, A.; Ibrahim, I. A. *J. Am. Chem. Soc.* **1981,** *103*, 7090.

206. Lahiri, J.; Isaacs, L.; Tien, J.; Whitesides, G. M. *Anal. Chem.* **1999,** *71*, 777.

207. Williams, A.; Ibrahim, I. A. *Chem. Rev.* **1981,** *81*, 589.

208. Brinkley, M. *Bioconj. Chem.* **1992,** *3*, 2.

209. Park, C. H.; Kim, J. P.; Lee, S. W.; Jeon, N. L.; Yoo, P. J.; Sim, S. J. *Adv. Funct. Mater.* **2009,** *19*, 3703.

210. Ali, M.; Schiedt, B.; Healy, K.; Neumann, R.; Ensinger, W. *Nanotechnology* **2008,** *19*, 1.

211. Cline, G. W.; Hanna, S. B. *J. Am. Chem. Soc.* **1987,** *109*, 3087.

212. Susuki, Y.; Hojo, K.; Maeda, M.; Nomizu, M.; Okazaki, I.; Nishi, N.; Kamada, H.; Yamamoto, Y.; Nakagawa, S.; Mayumi, T.; Kawasaki, K. *Pept. Sci.* **2000,** *37*, 193.

213. Tosatti, S.; De Paul, S. M.; Askendal, A.; VandeVondele, S.; Hubbell, J. A.; Tengvall, P.; Textor, M. *Biomaterials* **2003,** *24*, 4949.

214. Jun, H.-W.; West, J. *J. Biomed. Mater. Res., Part B: Appl. Biomater.* **2004,** *72B*, 131.

215. Proks, V.; Ludka, M.; Popelka, S.; Rypacek, F. *Adv. Exp. Med. Biol.* **2003,** *534*, 191.

216. Lutolf, M. P.; Hubbell, J. A. *Biomacromolecules* **2003,** *4*, 713.

217. Grun, J.; Revell, J. D.; Conza, M.; Wennemers, H. *Bioorg. Med. Chem.* **2006,** *14*, 6197.

218. Deftereos, M.; Gunn, J.; Mann, B. K. In *Summer Bioengineering Conference*, Key Biscayne, 2003; pp. 1115-1116.

219. Lee, S. H.; Miller, J. S.; Moon, J. J.; West, J. L. *Biotechnol. Progr.* **2005,** *21*, 1736.

220. Kim, S.; Chung, E. H.; Gilbert, M.; Healy, K. E. *J. Biomed. Mater. Res.* **2005,** *75A*, 73.

221. Ehrbar, M.; Rizzi, S. C.; Schoenmakers, R. G.; Miguel, B. S.; Hubbell, J. A.; Weber, F. E.; Lutolf, M. P. *J. Am. Chem. Soc.* **2007,** *8*, 3000.

222. Lutolf, M. P.; Lauer-Fields, J. L.; Schmokel, H. G.; Metters, A. T.; Weber, F. E.; Fields, G. B.; Hubbell, J. A. *Proc. Natl. Acad. Sci. U. S. A.* **2003,** *100*, 5413.

223. Chen, C. P.; Park, Y.; Rice, K. G. *J. Pept. Res.* **2004,** *64*, 237.

224. Gobin, A. S.; West, J. L. *FASEB Journal* **2002**.

225. West, J. L.; Hubbell, J. A. *Macromolecules* **1999,** *32*, 241.

226. Terada, T.; Iwai, M.; Kawakami, S.; Yamashita, F.; Hashida, M. *J. Control. Release* **2006,** *111*, 333.

227. Vettakkorumakankav, N. A.; Ananthanarayanan, V. S. *B.B.A.-Protein Struct. M.* **1999,** *1432*, 356.

228. Netzel-Arnett, S.; Fields, G.; Birkedal-Hanseng, H.; Van Wart, H. E. *J. Biol. Chem.* **1991,** *266*, 6747.

229. Rizzi, S. C.; Hubbell, J. A. *Biomacromolecules* **2005,** *6*, 1226.

230. Zisch, A. H.; Lutolf, M. P.; Ehrbar, M.; Raeber, G. P.; Rizzi, S. C.; Davies, N.; Schmokel, H.; Bezuidenhout, D.; Djonov, V.; Zilla, P.; Hubbell, J. A. *FASEB Journal* **2003,** *17*, 2260.

231. Parks, W. C.; Mecham, R. P. In *Matrix Metalloproteinases*, Imper, V.; Van Wart, H. E., Eds.; Academic Press: San Diego, 1998; pp. 219-242.

232. Korley, L. T. J.; Pate, B. D.; Thomas, E. L.; Hammond, P. T. *Polymer* **2006,** *47*, 3073.

233. Bagheri, M.; Pourmoazzen, Z. *React. Funct. Polym.* **2008,** *68*, 507.

234. Simonovsky, F. I.; Porter, S. C.; Ratner, B. D. *J. Biomater. Sci. Polym. Ed.* **2005,** *16*, 267.

235. Heintz, A. M.; Duffy, D. J.; Hsu, S. L. *Macromolecules* **2003,** *36*, 2695.

236. Woo, G.; Mittelman, M.; Santerre, J. *Biomaterials* **2000,** *21*, 1235.

237. Yuan, J.; Mao, C.; Zhou, J.; Shen, J.; Lin, S. C.; Zhu, W.; Fang, J. L. *Polym. Int.* **2003,** *52*, 1869.

238. Chen, K.-Y.; Kuo, J.-F. *Macromol. Chem. Phys.* **2000,** *21*, 2676.

239. Sheth, J. P.; Unal, S.; Yilgor, E.; Yilgor, I.; Beyer, F. L.; Long, T. E.; Wilkes, G. L. *Polymer* **2005,** *46*, 10180.

240. Santerre, J. P.; Labow, R. S.; Adams, G. A. *J. Biomed. Mater. Res.* **1993,** *27*, 97.

241. Grand, A. D. L.; Vitale, G. G.; Grand, D. G. L. *Polym. Eng. Sci.* **1977,** *17*, 598.

242. Helfand, E.; Tagami, Y. *J. Polym. Sci., Part B: Polym. Phys.* **1971,** *B9*, 741.

243. Helfand, E.; Wasserman, Z. R. *Macromolecules* **1978,** *11*, 683.

244. Wang, L.-F.; Wei, Y.-H. *Colloids Surf., Part B: Biointer.* **2005,** *41*, 249.

245. Kojio, K.; Nakamura, S.; Furukawa, M. *Polymer* **2004,** *45*, 8147.

246. Yilgor, I.; Yilgor, E.; Guler, I. G.; Ward, T. C.; Wilkes, G. L. *Polymer* **2006,** *47*, 4105.

247. Gisselfalt, K.; Helgee, B. *Macromol. Mater. Eng.* **2003,** *288*, 265.

248. Saha, K.; Keung, A. J.; Irwin, E. F.; Li, Y.; Little, L.; Schaffer, D. V.; Healy, K. E. *Biophys. J.* **2008,** *95*, 4426.

249. Yeung, T.; Georges, P. C.; Flanagan, L. A.; Marg, B.; Ortiz, M.; Funaki, M.; Zahir, N.; Ming, W.; Weaver, V.; Janmey, P. A. *Cell Motil. Cytoskeleton* **2005,** *60*, 24.

250. Hersel, U.; Dahmen, C.; Kessler, H. *Biomaterials* **2003,** *24*, 4385.

251. Vijayasankaran, N.; Carlson, R.; Srienc, F. *Appl. Microbiol. Biotechnol.* **2005,** *68*, 737.

252. Andersen, D. C.; Krummen, L. *Curr. Opin. Biotechnol.* **2002,** *13*, 117.

253. Swartz, J. R. *Curr. Opin. Biotechnol.* **2001,** *12*, 195.

254. Izhak, L.; Wildbaum, G.; Zohar, Y.; Anunu, R.; Klapper, L.; Elkeles, A.; Seagal, J.; Yefenof, E.; Ayalon-Soffer, M.; Karin, N. *J. Immunol.* **2009**, 732.

255. Schmoldt, H.-U.; Wentzel, A.; Becker, S.; Kolmar, H. *Protein Expression Purif.* **2005,** *39*, 82.

256. Sousa, F.; Melo, A.; Almeida, S.; Paixao, P.; Queiroz, J. A.; Domingues, F. C. *Biotechnol. Lett.* **2006,** *28*, 73.

257. Wen, Q.; Ma, L.; Luo, W.; Zhou, M.-Q.; Wang, X.-N. *Biomed. Environ. Sci.* **2008,** *21*, 509.

258. Balmayor, E. R.; Tuzlakoglu, K.; Marques, A. P.; Azevedo, H. S.; Reis, R. L. *J. Mater. Sci. Mater. Med.* **2008,** *19*, 1617.

259. Vemula, P. K.; Cruikshank, G. A.; Karp, J. M.; John, G. *Biomaterials* **2009,** *30*, 383.

260. Dover, J. E.; Hwang, G. M.; Mullen, E. H.; Prorok, B. C.; Suh, S.-J. *J. Microbiol. Methods* **2009,** *78*, 10.

261. Enander, K.; Choulier, L.; Olsson, A. L.; Yushchenko, D. A.; Kanmert, D.; Klymchenko, A. S.; Demchenko, A. P.; Mely, Y.; Altschuh, D. *Bioconj. Chem.* **2008,** *19*, 1864.

APPENDIX

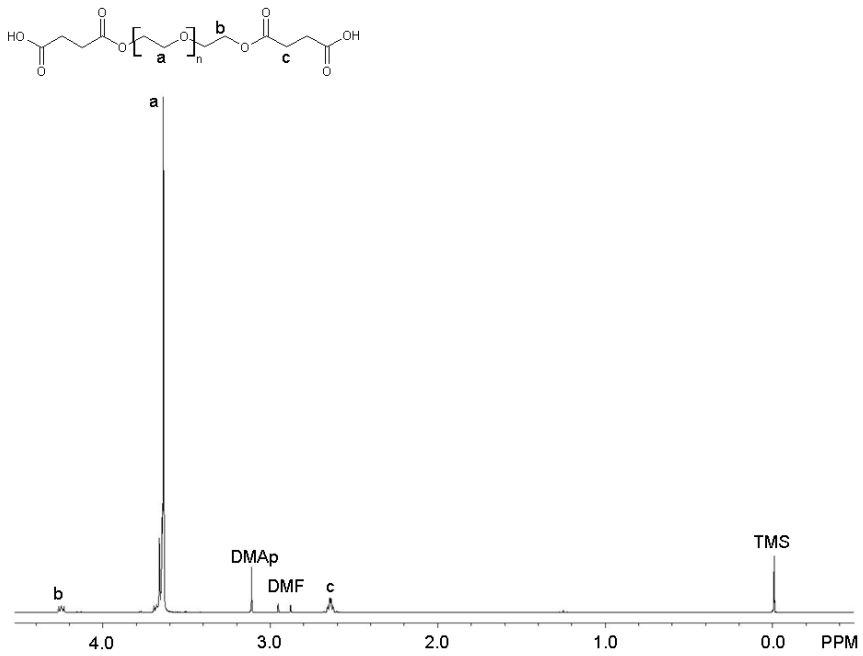

^{1}H-NMR spectrum of PEG (1000) diacid.

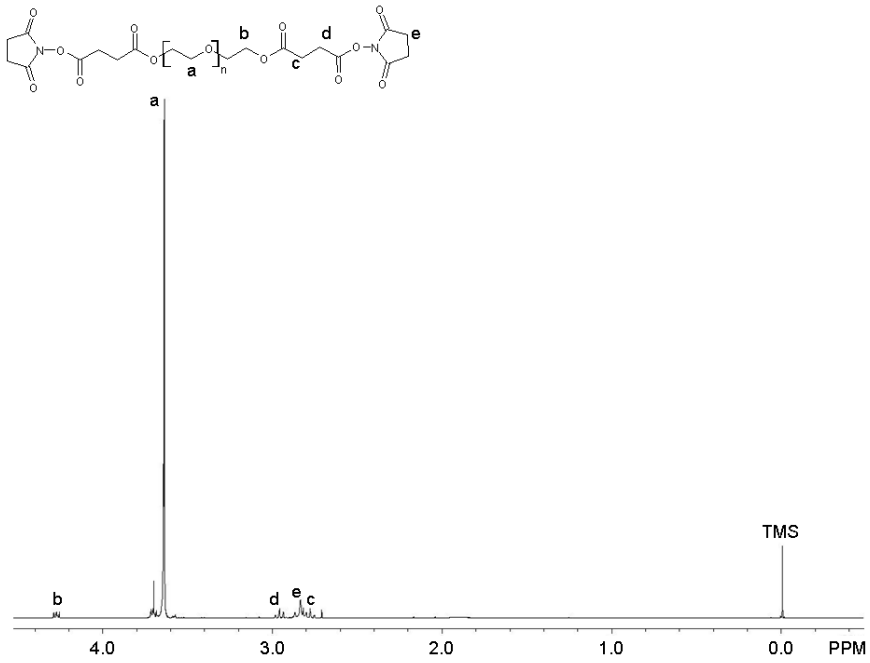

^{1}H-NMR spectrum of NHS-PEG (1000)-NHS.

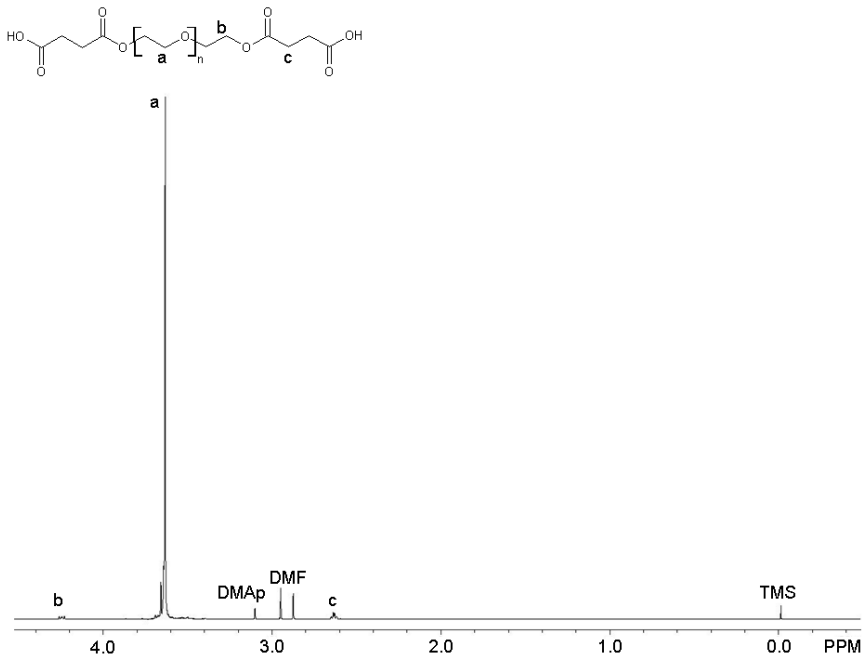

^{1}H-NMR spectrum of PEG (2000) diacid.

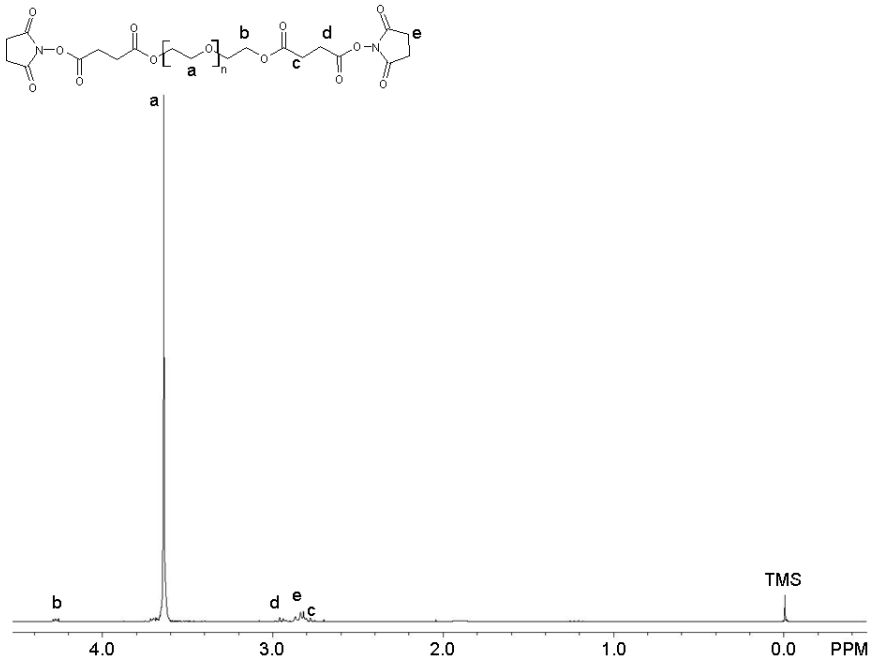

^{1}H-NMR spectrum of NHS-PEG (2000)-NHS.

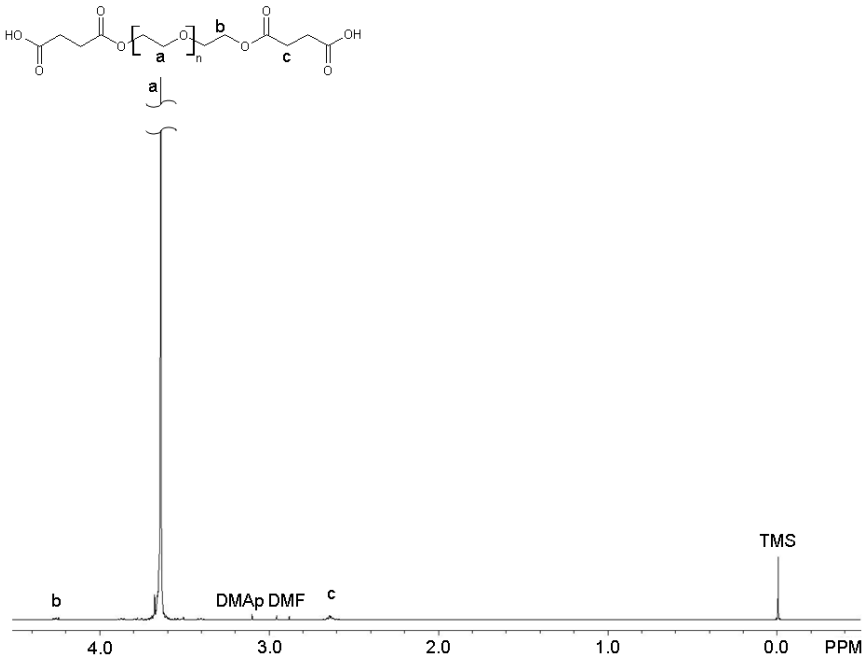

^{1}H-NMR spectrum of PEG (6000) diacid.

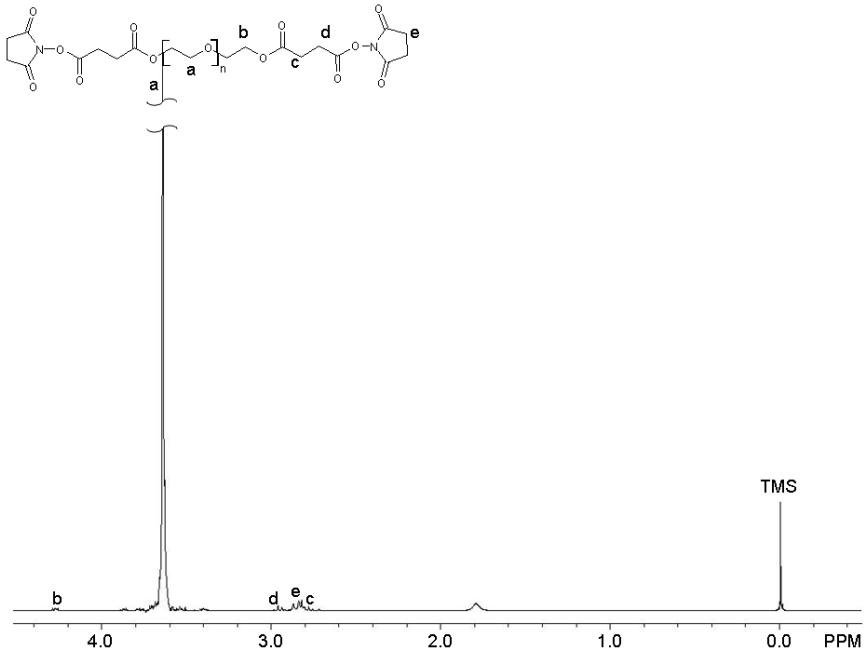

^{1}H-NMR spectrum of NHS-PEG (6000)-NHS.

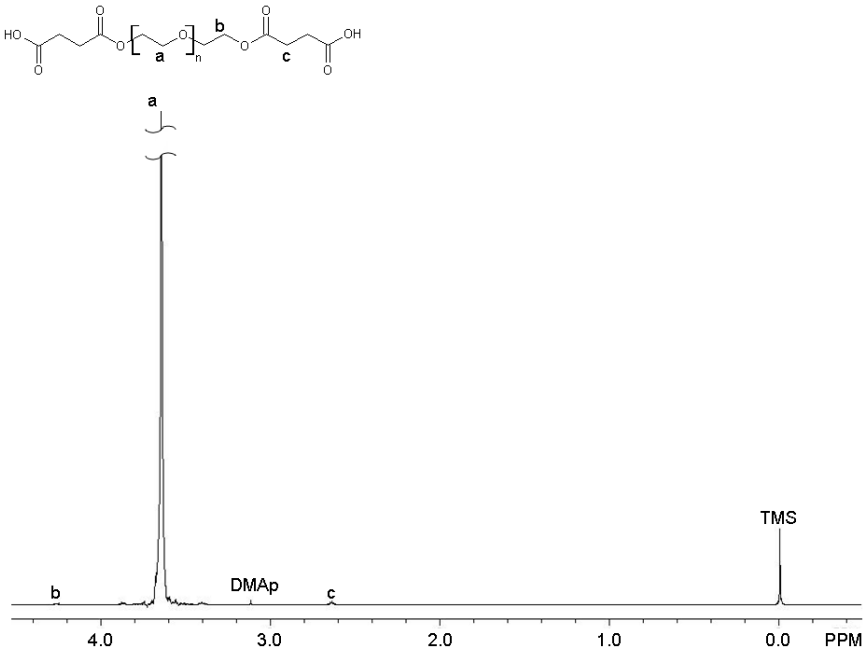

^{1}H-NMR spectrum of PEG (10000) diacid.

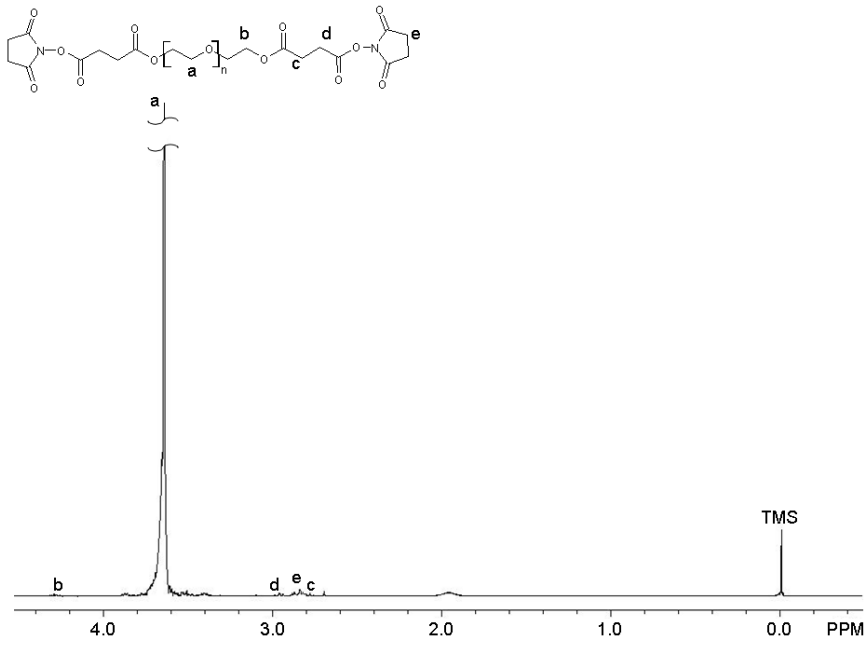

^{1}H-NMR spectrum of NHS-PEG (10000)-NHS.

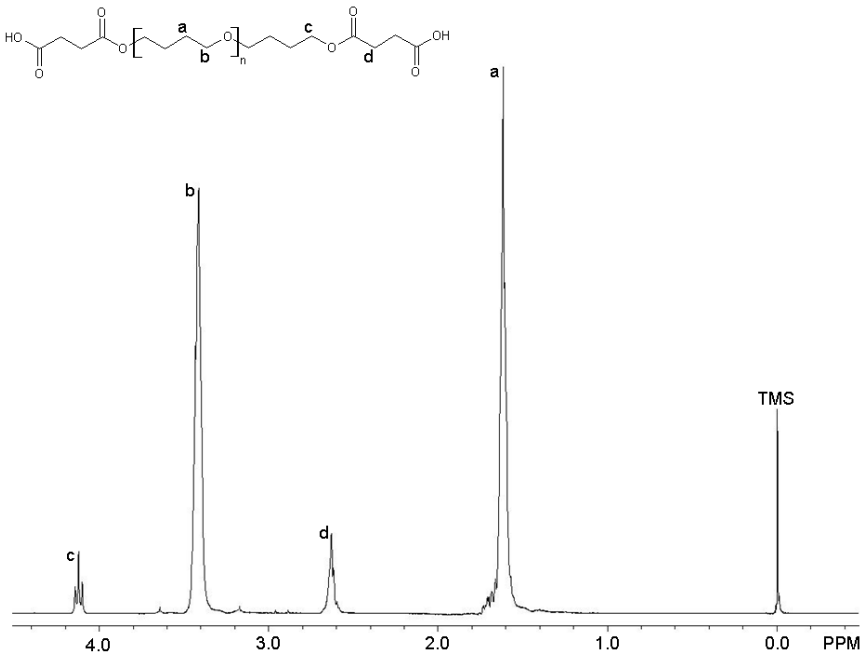

^{1}H-NMR spectrum of PTMG (1000) diacid.

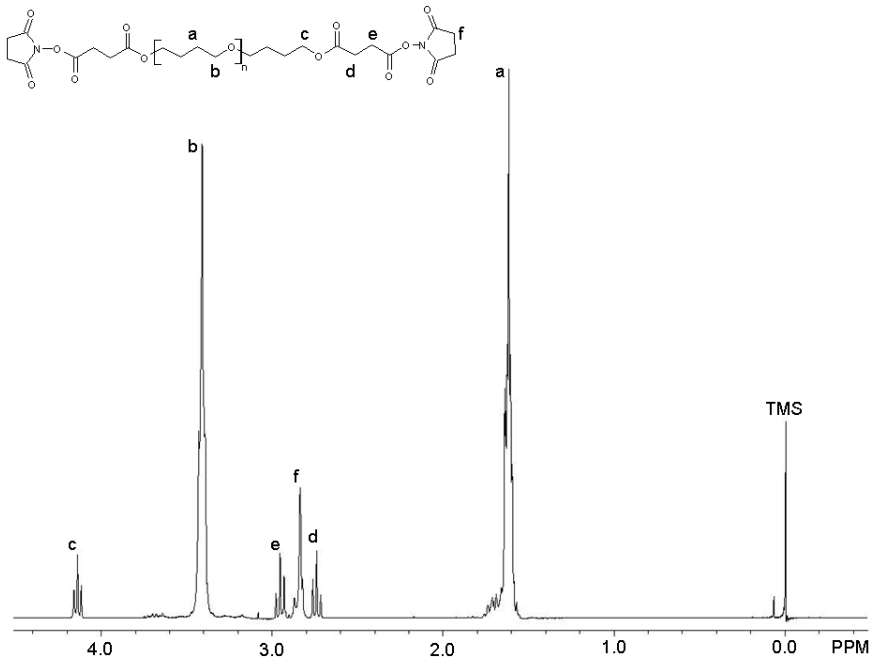

^{1}H-NMR spectrum of NHS-PTMG (1000)-NHS.

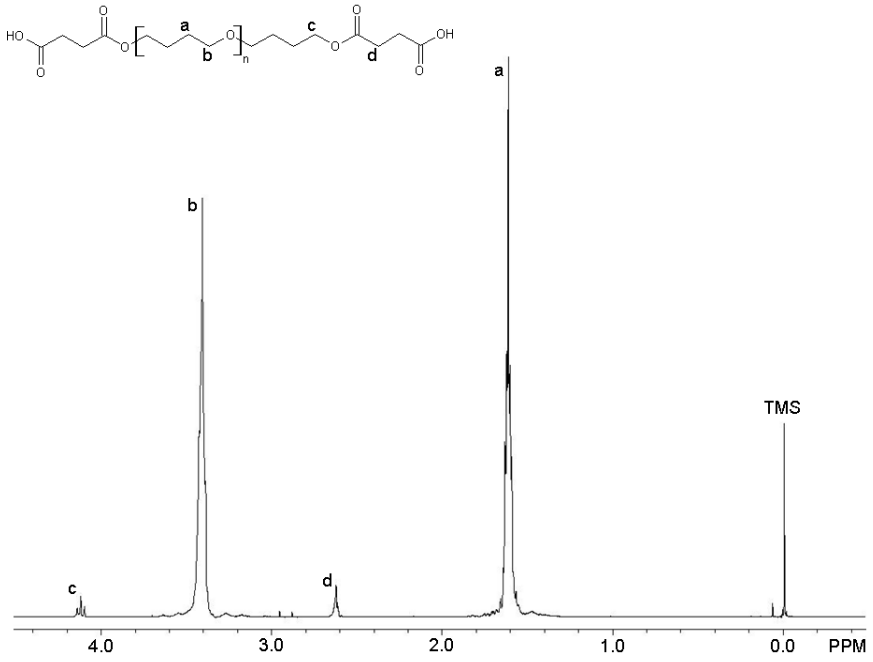

^{1}H-NMR spectrum of PTMG (2900) diacid.

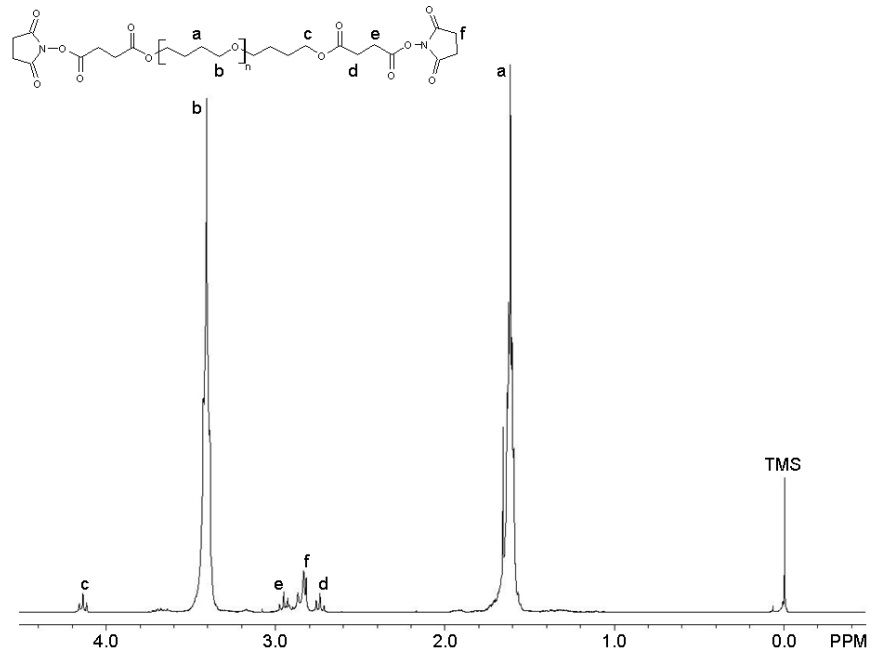

^{1}H-NMR spectrum of NHS-PTMG (2900)-NHS.

VITA

Hugh Adam Benhardt received his Bachelor of Science in mechanical engineering from the University of Missouri-Rolla in May 2006. He entered the biomedical engineering program at Texas A&M University in September 2007 and received his Master of Science in May 2010. His research interests include musculoskeletal tissue engineering and polymeric biomaterials, specifically polyurethane synthesis and characterization.

Mr. Benhardt may be contacted through Dr. Elizabeth Cosgriff-Hernandez at the Department of Biomedical Engineering, Texas A&M University, College Station, TX 77843-3120. His email address is hughbenhardt@hotmail.com.